August 2016

Sedimentology of the Mid-Carboniferous Basal Fill of the Olta Paleovalley, Eastern Paganzo Basin, Argentina

Levi Darwin Moxness
University of Wisconsin-Milwaukee

SEDIMENTOLOGY OF THE MID-CARBONIFEROUS BASAL FILL OF THE OLTA PALEOVALLEY, EASTERN PAGANZO BASIN, ARGENTINA

by

Levi Darwin Moxness

A Thesis Submitted in

Partial Fulfillment of the

Requirements for the Degree of

Master of Science

in Geosciences

at

The University of Wisconsin-Milwaukee

August 2016

ABSTRACT

SEDIMENTOLOGY OF THE MID-CARBONIFEROUS BASAL FILL OF THE OLTA PALEOVALLEY, EASTERN PAGANZO BASIN, ARGENTINA

by
Levi Darwin Moxness

The University of Wisconsin-Milwaukee, 2016
Under the Supervision of Professor John L. Isbell

As global climate transitioned from the icehouse of the Late Paleozoic Ice Age (LPIA) to greenhouse conditions of the Late Permian, glaciers vanished across Gondwana; however, not all ice centers responded synchronously. The Paganzo basin, northwestern Argentina, was geographically adjacent to significant mid-Carboniferous ice centers that disappeared notably earlier than ice over much of Gondwana. Confining the extent of glacial ice during the LPIA and resolving the timing of its disappearance is of particular interest as this dramatic climatic transition is the closest analogue in Earth history to late Cenozoic climate change, potentially aiding in anticipating the response of modern climate to similar drivers.

The majority of the late Paleozoic glacial record in the region is from paleofjord deposits in the Calingasta-Uspallata, Rio Blanco, and western Paganzo basins, but in the eastern Paganzo basin a paleovalley, only a few hundred meters wide, was cut into the predominantly granitic basement of the Sierra de los Llanos near Olta, in La Rioja Province. The basal fill of the valley was previously interpreted as glacigenic, with the valley carved by either local alpine glaciers or an outlet glacier draining westward from an ice sheet situated over the eastern part of the Paganzo Basin. This study tests the glacigenic setting for the paleovalley.

The strata are dominated by medium to thick-bedded, fine- to coarse-grained sandstones deposited by lacustrine wave activity and underflow currents, and by massive or weakly graded conglomerates deposited by stream and debris flows associated with prograding alluvial fans and fan deltas. Lacustrine sediments interfinger with distal alluvial fan conglomerates along the valley wall, suggesting water was impounded by transverse progradation of the fans across the valley. Bulleted clasts, glacial abrasion marks, diamictites with clast fabrics, and other diagnostic glacial features were not observed. Diamictites were rare and associated with landslide deposits along the valley wall, and soft sediment deformation beneath boulder-rich conglomerates and breccias can be attributed to mass-transport deposits and rock fall off of the steep valley walls. The basal fill of the Olta Paleovalley is interpreted here as a lacustrine depositional environment in a narrow mountain valley and contains no evidence for glacial ice in the eastern Paganzo basin.

TABLE OF CONTENTS

LIST OF FIGURES

Figure Page

LIST OF TABLES

Table Page

ACKNOWLEDGEMENTS

I would like to express the deepest appreciation to Dr. John Isbell for his patience, guidance, and support during this study. I will undoubtedly carry his significant contributions to my skills as a field geologist and scientific communicator throughout my career. I am also deeply grateful to Dr. Dyanna Czeck and Dr. J. Elmo Rawling for their generous investments of time, expertise, and insight on this project. I would like to thank Dr. Erik Gulbranson for his contributions to my understanding of this succession, both in the field and the classroom. This project would have been considerably more difficult without the scientific expertise, institutional knowledge, interpretive skills, and friendship of Kate N. Pauls.

I would like to express my gratitude for the generous financial support of the Geological Society of America, the Society for Sedimentary Geologists, the UWM Center for Latin American and Caribbean studies, the Wisconsin Geological Society, and the UWM Geosciences Department, whose contributions facilitated this research.

It would be remiss of me if I neglected to thank the many teachers who have invested their effort in my education over the course of my academic and work career, especially Dr. Allan Ashworth and Dr. Ken Lepper. This work is a product of your previous instruction, patience, and encouragement.

Finally, I would like to thank my mother, Heidi, for her unrelenting love and care, and father, Kevin, for the quiet example set of living by principle.

Introduction

Problem

The glaciation of Gondwana during the Late Paleozoic Ice Age (LPIA; ~372 to 259 million years ago) represents the longest duration glacial interval during the last 542 million years, and the warming of global climate during the Permian is the only example of a long-term transition from icehouse to hothouse conditions in Earth's history under conditions similar to those seen today (e.g., biologically complex Earth, transition from low atmospheric CO_2 levels to 10X pre-industrial concentrations; Gastaldo et al., 1996; Isbell et al., 2003, 2012; Soreghan, 2004; Montañez and Soreghan, 2006; Montañez et al., 2007; Fielding et al., 2008a, 2008b; Montañez and Paulsen, 2013). Traditional models of Gondwanan glaciation are characterized by an enormous ice sheet that fluctuated but persisted for up to 100 million years (Veevers and Powell, 1987; Frakes and Francis, 1988; Frakes et al., 1992; Ziegler et al., 1997; Hyde et al., 1999; Blakey, 2008; Buggisch et al., 2011). However, recent studies of late Paleozoic glacigenic deposits (López-Gamundí, 1997; Isbell et al., 2003, 2008a, 2008b, 2012; Fielding et al., 2008a, 2008b, Gulbranson et al., 2010), glacioeustacic fluctuations (Rygel et al., 2008; Heckel, 2008), and paleoclimate modeling (Horton et al., 2007, 2010, 2012; Horton and Poulsen, 2009) suggest a significantly more dynamic glacial history. This emerging view of the LPIA (Fig. 1) recognizes evidence for several glacial and nonglacial intervals, each lasting between 1-8 million years, where alpine and continental glaciations were separated by ice minimal or ice sheet-free periods, and estimates of global ice volume that are significantly reduced from previous models. Thus, in this view, ice was limited to numerous discrete ice centers rather than a supercontinent-scale ice sheet (Crowell and Frakes, 1970; Caputo and Crowell, 1985; Dickins, 1997; López-Gamundí, 1997; Isbell et al., 2003, 2008a, 2008b, 2012; 2016; Fielding et al., 2008a, 2008c; Gulbranson et

al., 2010; Montañez and Paulsen, 2013; Frank et al., 2015). Glaciation began in South America and northern Africa in the late Devonian (Caputo and Crowell, 1985; López-Gamundí, 1997; Isbell et al., 2003; Caputo et al., 2008) with the main phase of the LPIA commencing in western South America in the Mississippian (Visean) before spreading across Gondwana in the Pennsylvanian and Early Permian (Caputo et al., 2008; Pérez Loinaze et al., 2010; Limarino et al., 2014). The transition out of the LPIA into greenhouse/hothouse conditions was diachronous across Gondwana beginning in western South America in the Early Pennsylvanian and ending in eastern Australia during the early Late Permian (Caputo and Crowell, 1985; Veevers and Powell, 1987; Eyles, 1993; Fielding et al. 2008c; Isbell et al., 2012; Frank et al., 2015; Metcalfe et al., 2015). Numerous drivers have been proposed to have initiated, sustained and terminated the LPIA including: drift of Gondwana across the late Paleozoic South Pole, changes in atmospheric CO_2 levels, tectonically-induced changes in elevation, changing plate configurations and opening and closing of oceanic gateways, upwelling, and changing ocean currents (Caputo and Crowell, 1985; Eyles 1993, Isbell et al., 2003, 2012; Tabor and Poulsen 2008; Montañez and Poulsen, 2013). Confining the extent of glacial ice during the LPIA, resolving the timing of its disappearance, and understanding the mechanisms that drove this ice age and its demise is of particular interest as developing an understanding of the drivers of deep-time climate may aid in our understanding of similar drivers affecting modern climate.

Recent studies of sedimentary basins throughout central and southern South America (Fig. 2) have contributed greatly to our understanding of this important climatic event (Eyles et al., 1993; López-Gamundí et al., 1994, 2016; López-Gamundí, 1997; Limarino et al., 2002, 2006, 2014; Vesely, and Assine, 2006, 2014; Kneller et al., 2004; Dykstra et al., 2006; 2007; Limarino and Spalletti, 2006; Vesely et al., 2007, 2014; Rocha Campos et al., 2008; Gulbranson

et al., 2010, 2014; Caputo et al., 2008; Henry et al., 2008, 2010, 2012; Aquino et al., 2014, 2016). Basins in western Argentina (Rio Blanco, Callingasta-Uspallata, and western Paganzo basins) record the onset of the main stage of LPIA glaciation during the Visean (cf. López-Gamundí et al., 1994; López-Gamundí, 1997; Caputo et al. 2008; Henry et al., 2008), and were the first in Gondwana to be de-glaciated in the Early Pennsylvanian. In east central South America, the Sauce Grande (eastern Argentina), Chaco-Paraná (northeastern Argentina and Uruguay), and Paraná basins (Brazil), are reported as having undergone the glacial to post-glacial transition much later during the Late Pennsylvanian and Early Permian (Holz et al., 2008; Rocha Campos et al., 2008; Limarino et al., 2014), despite their location at essentially the same paleolatitude as the western Argentine basins. One area of particular interest is the eastern Paganzo Basin. Although this area was located between the two ice centers mentioned above (western Argentina and the Chaco-Paraná and Paraná basins), the presence and extent of ice in the eastern Paganzo Basin is highly controversial. However, this area is highly important in resolving the size, timing, and extent of glacial centers; when and where ice sheets formed, waxed and waned, and disappeared; and why glaciation ended in one area of South America while glaciers in adjacent areas at the same paleolatitude persisted. This paper focuses on the Olta paleovalley in the eastern Paganzo basin to help resolve the nature or absence of glaciation in this area.

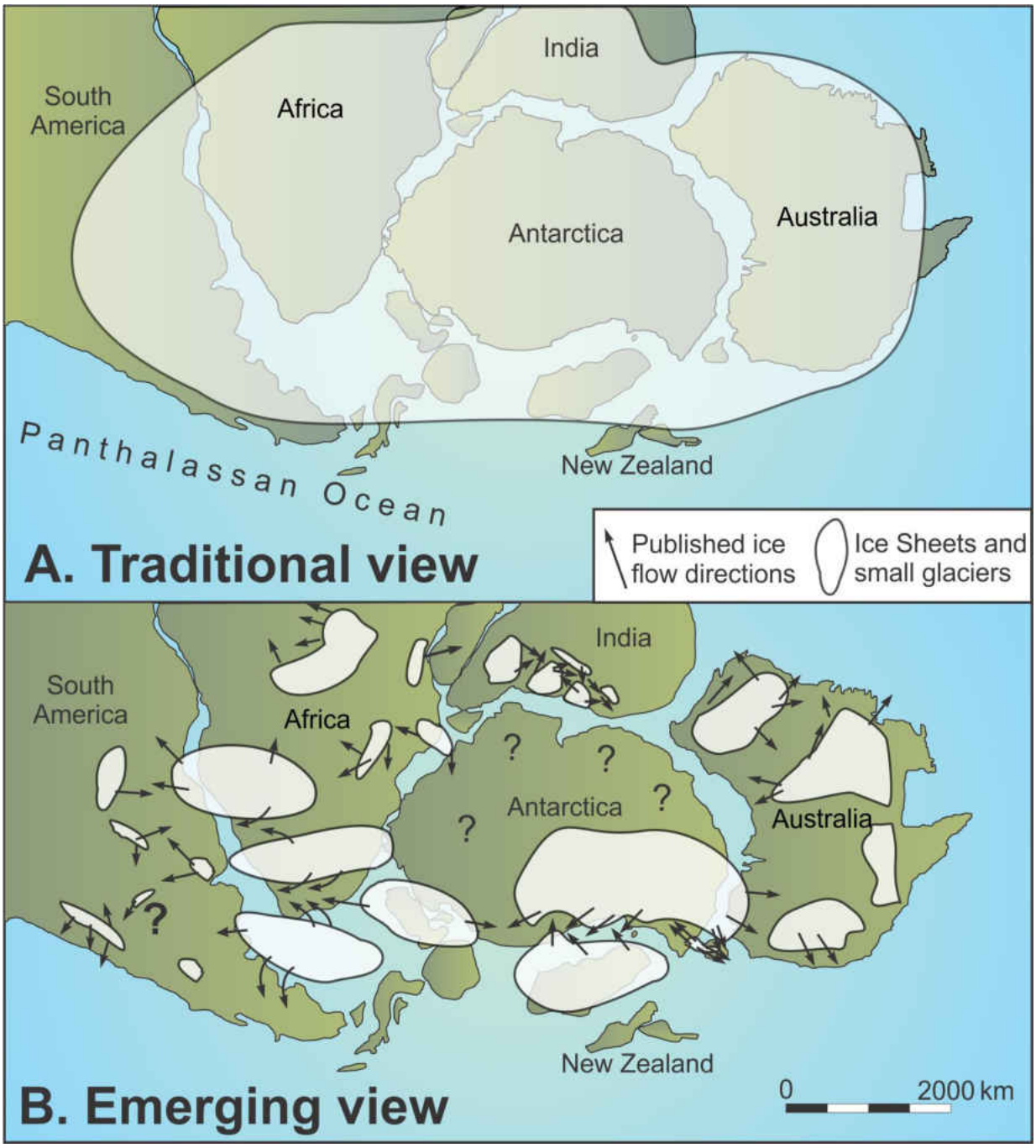

Figure 1. (A) Traditional view of ice extent during the LPIA characterized by a persistent, supercontinent-scale ice sheet, and (B) an emerging view that includes small ice sheets, ice caps, and alpine glaciers that waxed, waned, and disappeared for periods during the ice age (modified from Isbell et al., 2012).

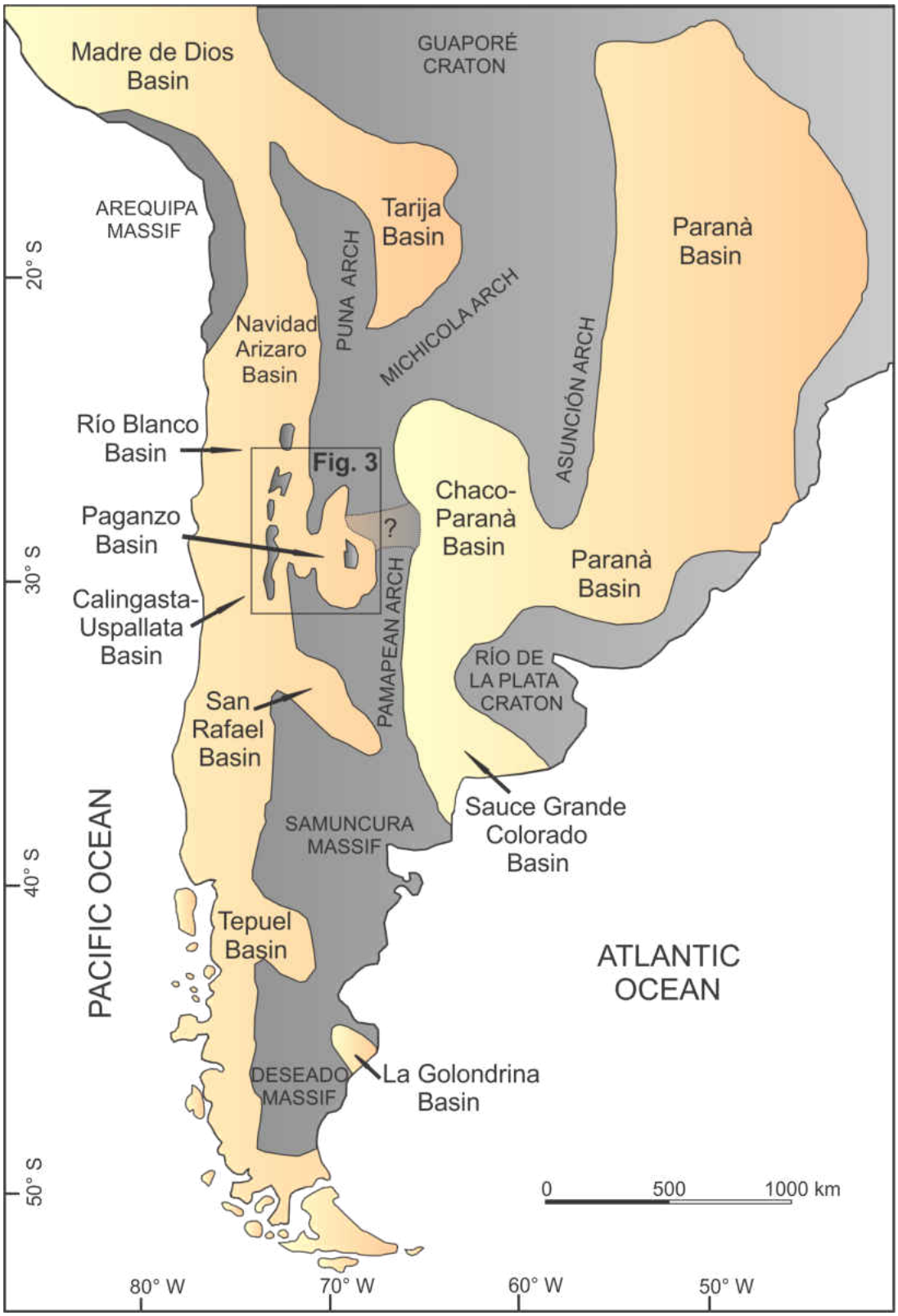

Figure 2. Late Paleozoic basins (yellow) and surrounding uplands (gray) of southern South America.

Geologic Setting

One of the earliest lines of evidence for glaciation associated with the main phase of the LPIA is recognized from the Protoprecordillera of western Argentina, where Middle Mississippian to Early Pennsylvanian (Viséan to early Bashkirian) glaciers carved an extensive network of fjords (López-Gamundí and Martínez, 2000; Kneller et al, 2004; Dykstra et al., 2006; Aquino et al., 2014). The Protoprecordillera was an ancient mountain range believed to have exhibited significant topographic relief as it developed into a fold thrust belt during later stages of the Chañic orogeny (Late Devonian to Mississippian) as the Chilenia terrane accreted to the western margin of Gondwana (Ramos et al., 1984, 1986; Limarino et al., 2006; Henry et al., 2008; Isbell et al., 2012). In this belt, glacigenic deposits occur in deeply-incised paleovalleys that drain radially from the Protoprecordillera into the adjacent Calingasta-Uspallata, Rio Blanco, and western Paganzo basins (Fig. 3B). Glaciers disappeared in the range during the Early Pennsylvanian; possibly associated with the collapse of the Protoprecordillera during the Pennsylvanian and Permian as the active margin of Gondwana shifted to the west and the region underwent back-arc extension (Fig. 3C) (Ramos, 1988; López-Gamundí et al., 1994; Limarino et al., 2002, 2006, 2014; Isbell et al., 2012).

Early stages of deposition in the Paganzo basin are characterized by late Mississippian glacial and glacilacustrine deposition in paleovalleys and a narrow foreland area along the Protoprecordillera, but also inland lacustrine deposition that occurred further to the east in small intermontane depocenters bounded by uplifted blocks of Pampean basement (López-Gamundí et al., 1994). As regional extension began in the early Pennsylvanian and the Paganzo basin became a more extensive back-arc basin, the collapse or breaching of the Protoprecordillera allowed

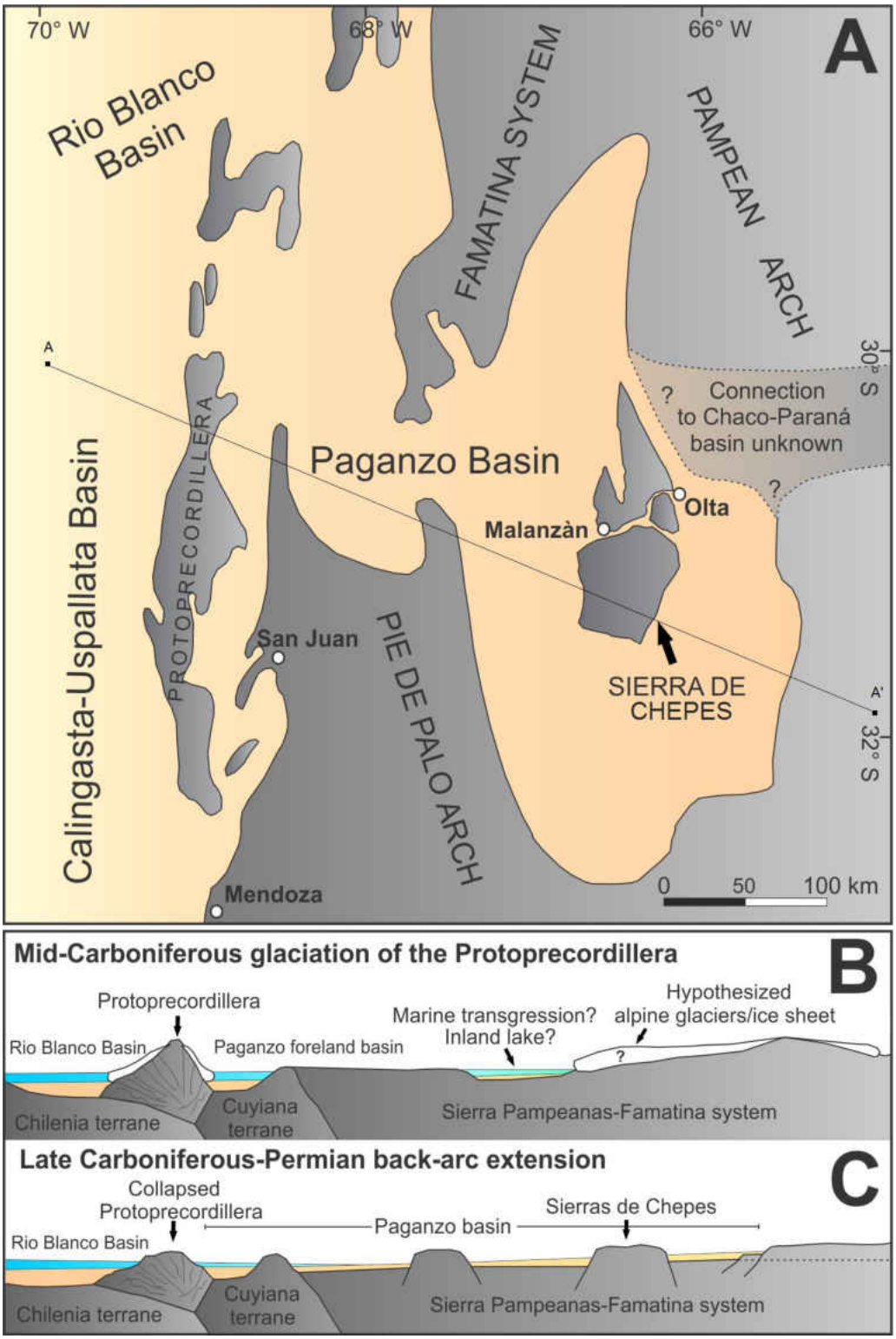

Figure 3. (A) Map and (B and C) schematic cross sections (A-A') of the Paganzo basin and its position east of the Protoprecordillera, a fold-thrust belt that housed glaciers in the mid-Carboniferous prior to its extensional collapse through the Pennsylvanian. (Modified after Limarino et al., 2006)

marine incursion (Namurian postglacial transgression; Limarino et al., 2002) to advance inland reaching as far as the eastern Paganzo basin. Widespread deltaic and fluvial deposition occurred across the basin for most of the late Carboniferous into the Permian (Net and Limarino, 2006).

The major granitic bodies that bound the eastern Paganzo Basin are also inferred to have been topographic highs during the late Paleozoic (López-Gamundí et al., 1994; Limarino and Spalletti, 2006; Enkelmann et al., 2014) and are noteworthy for their potential to host alpine glaciers as the Protoprecordillera did to the west. One block, containing the Sierra de los Llanos and neighboring Sierras de Chepes (Fig. 4), lies within the Paganzo basin nearly 200 km east of the Protoprecordillera. These ranges are composed primarily of Ordovician granite (Chepes Fm.) and schist (Olta Fm.). In the center of this basement block a narrow elongate depression, the Olta-Malanzán paleovalley, has been described as glacially carved; an interpretation which has important implications for estimations of mid-Carboniferous ice volumes, as the valley contains the only deposits in the eastern Paganzo basin for this interval that have been extensively described as possibly glacigenic (Buatois and Mángano, 1995; Sterren and Martinez, 1996; Socha et al., 2014), while other reports suggest that deposits in this valley were the result of lacustrine and alluvial fan activity (Bracaccini, 1946; Andreis and Bossi, 1981; Andreis et al., 1986).

The main axis of the paleovalley stretches approximately 40 km in the southern La Rioja Province, and narrows from its width of nearly 1500 m at the village of Malanzán in the west to less than 500 m near Olta on the eastern end of the valley (Fig. 4). In several places, the paleovalley is less than 250 m wide. It is especially narrow in an area where two modern valleys enter the Olta valley. These valleys are cut in Carboniferous sediment, which indicates that the

Figure 4. Simplified geologic map of the Olta-Malanzán paleovalley and surrounding ranges (modified from Net and Limarino, 1999).

current drainage is exhuming Carboniferous paleovalleys. Paleoslopes in the Olta-Malanzán paleovalley are interpreted to dip towards the west (Andreis et al., 1986; Sterren and Martinez, 1996). Late Paleozoic deposits preserved in the paleovalley are represented by at least four formations belonging to the Paganzo Group (Fig. 5). The basal fill is represented by the Malanzán Formation, which has been described in detail from exposed strata in the western portion of the valley system (Azcuy, 1975; Andreis et al., 1986; Buatois and Mángano, 1995) and includes the basal fill of the valley to the east near Olta (Bracaccini, 1948; Sterren and Martinez, 1996; Gutiérrez and Limarino, 2001; Net et al., 2002). Palynological assemblages have been used to correlate these outcrops with deposits of the lower Paganzo Group in western portions of the Paganzo basin, which are identified as Middle Carboniferous (Late Serpukhovian to Bashkirian) in age (López-Gamundí et al., 1994; Gutiérrez and Limarino, 2001; Limarino et al., 2006; Pérez Loinaze, 2009; Gulbranson et al., 2010). The Malanzán Formation was divided into four members by Andreis et al., (1986). The first member, which directly overlies basement, contains abundant conglomerates, breccias, and diamictites that intercalate with and deform lacustrine turbidites. The coarse clastics in this member have generally been interpreted to record deposition by alluvial fans and debris flows that impounded water in a narrow mountain valley (Andreis et al., 1986; Buatois and Mángano, 1995; Net and Limarino, 1999), but recently these deposits have been interpreted as evidence of subglacial deposition and deformation (Socha et al., 2014). Members 2 through 4 of the Malanzán Formation record a lacustrine transgression and suspension settling of fine-grained material in a deep lake environment, progradation of coarse Gilbert-type deltas, and a transition from deltaic to braided-fluvial systems, respectively (Andreis et al., 1986). Late Carboniferous and Permian braided-fluvial, alluvial fan, and aeolian deposits

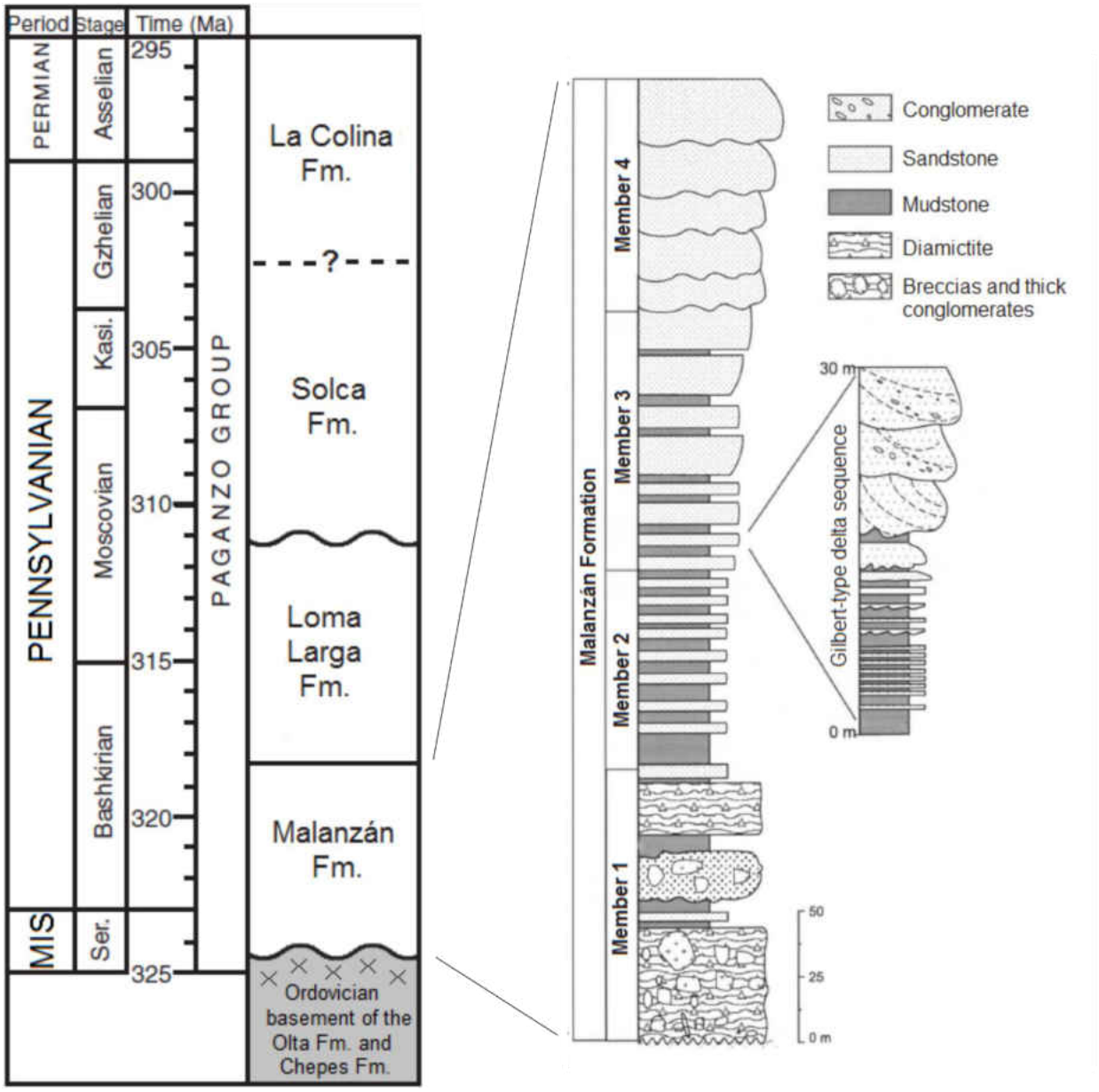

Figure 5. Stratigraphic chart for the Late Paleozoic units of the Olta-Malanzán paleovalley (modified from Gulbranson et al., 2010) with a generalized stratigraphic column showing the members of the Malanzán Formation modified from Gutiérrez and Limarino (2001). Ages are extrapolated from radiogenic dates of coeval deposits in the western Paganzo basin (Gulbranson et al., 2015).

of the overlying Loma Larga, Solca, and La Colina Formations record increasing aridification in the eastern Paganzo basin (Andreis et al., 1986; Gulbranson et al., 2015)

Speculation on the style and extent of glaciation in the eastern Paganzo basin includes both basin-wide and localized ice centers. Socha et al. (2014) interpreted the Olta–Malanzán paleovalley as having been carved by a valley glacier and reported hanging paleovalleys carved by tributary glaciers, suggesting alpine glaciation of the Sierra de Los Llanos similar to that of the Protoprecordillera in the western Paganzo basin. Other authors have also invoked alpine glaciation of topographic highs along the eastern and southern margins of the eastern Paganzo basin (Limarino et al., 2014). Aquino et al., (2014) hypothesized the paleovalley was carved by and outlet glacier from one of these possible eastern ice centers, while Astini et al., (2010) suggested the valley was carved by a receding ice sheet that covered much of the eastern Paganzo basin. The central postulate of these hypotheses is the existence of Carboniferous glacigenic deposits in the eastern Paganzo basin based primarily on interpretations of the Malanzán Fm. in the Olta-Malanzán paleovalley, but these deposits themselves are equivocal.

Project Goals

This study tests the glacigenic setting for the paleovalley near Olta, in La Rioja Province. The goals of the project are to document the presence or absence of diagnostic glacial features in the Olta paleovalley and accordingly confirm or reject evidence for late Paleozoic glaciation in the eastern Paganzo Basin. Evidence for glacial abrasion (striated and grooved surfaces, faceted and striated clasts), subglacial deposition (diamictites with imbricated boulders and sheared structures), and proximal glaciomarine deposition (pebbly dropstone shales) is common in Carboniferous paleovalleys in the western Paganzo Basin (López-Gamundí and Martínez, 2000;

Pazos, 2002; Dykstra et al., 2006; Aquino et al., 2014; López-Gamundí et al., 2016), and should be readily observable in the Olta paleovalley if it was a similar fjord environment.

Methods

Field work conducted in March of 2015 in the Olta paleovalley employed standard stratigraphic techniques utilizing a Jacob's staff, Abney level, and Brunton compass to measure 13 stratigraphic sections of the Malanzán Formation ranging from 5.4 to 35.4 meters thick (See Appendix). These measurements, in addition to observational field data, include the identification of: 1) grain/clast size, lithology, sorting, and roundness, 2) sedimentary structures, 3) lithostratigraphic unit thicknesses and the nature of unit contacts, and 4) paleocurrent directions. This information was manually recorded and photo documented for the construction of detailed stratigraphic columns, facilitating the identification of the physical processes and depositional environments necessary for facies analysis. Exposures of the bedrock walls and floor of the paleovalley were examined for striations, grooves, and other signs of glacial abrasion. Diamictite clasts were also examined for facets, striations, polish, and other evidence of subglacial abrasion and transport. The mud content, clast orientation, and overall stratal geometry of unsorted deposits was documented in order to distinguish potential subglacial diamictites from alluvial fan conglomerates and mass-transport deposits. The fold axis orientations and stratigraphic context of deformed sandstone beds were investigated to establish whether soft-sediment deformation was caused by an advancing valley glacier, mass transport off of the steep valley walls, or due to some other syndepostional mechanism.

Lithofacies Analysis

Studied strata of the Malanzán Formation in the eastern portion of the Olta paleovalley are composed of 8 lithofacies, which consist of: A) clast-rich sandy diamictite, B) sandy conglomerate, C) boulder breccia, D) horizontally-laminated sandstone, E) laminated mudstone, F) ripple cross-laminated sandstone, G) folded sandstone and mudstone, and H) sandy clinoforms. These lithofacies are summarized in Table 1 and described below. Although the base of the Malanzán Formation is considered to rest on basement rock, the contact was observed only in Section OLTA1 and OG2 (Fig. 6; Appendix A) where strata lapped onto the underlying basement along a high relief nonconformity. At OLTA1 the unconformity is cut on schist and dips at ~20^{o} to the WNW. At OG2 sandstone of the Malanzán abuts against a near vertical wall of granite. Outcrops are exposed by modern incision of the Rio Olta, which flows eastward through the study area. Stratigraphically, the lowest exposures occur in the eastern end of the valley while the western end of the valley exposes higher stratigraphic levels. The overall facies trends are characterized by basal clast-rich sandy diamictite and horizontally-laminated coarse sandstones overlying basement in the easternmost sections (OLTA1-OLTA3), fining upwards to ripple cross-laminated fine and medium-grained sandstones, which are folded beneath intercalated beds of sandy conglomerate (OC1-OC2) and continue to fine upwards until the succession is dominated by laminated mudstone. Outcrops in the central portion of the valley near the steep paleovalley wall contain boulder breccia (OG1), and horizontally laminated sandstones (OG2), but near a tributary paleovalley sections are dominated by interbedded sandy conglomerates that interfinger laterally with folded sandstone and mudstone (OG3-OG6). The uppermost sections in the western portion of the study area show a coarsening-upwards trend from laminated mudstones (OD1) to sandy clinoforms (OD2).

Lithofacies		Lithologies	Distinctive features and sedimentary structures	Bed thickness	Interpretation
A	Clast-rich sandy diamictite	Massive, matrix- to clast-supported diamictite with a muddy sand matrix	Body consisting of a clast-supported nose and matrix-supported tail with boulders protruding through top of unit	0-1.4 m	Debris flow into lake near moderately sloped valley walls
B	Sandy conglomerate	Massive to graded, matrix to clast-supported cobble-rich conglomerate with a sand matrix	Horizontal laminations, grading	0.2-32.7 m	Alluvial fan progradation across lake with coarse debris flows
C	Boulder breccia	Massive, clast-supported breccia with sandstone and mudstone between angular boulders	Heavily deformed sandstone and mudstone beds between boulders	8.2 m	Direct rockfall into lake near steep valley walls
D	Graded sandstone	Massive or graded gravelly coarse-grained sandstone to ripple cross-laminated fine sandstone with thin silt drapes	Horizontal laminations, asymmetrical ripples and ripple cross-laminations, dewatering structures, prod marks, load/flame structures, outsized clasts	0.1-0.6 m	Turbidity current-dominated deposition in proximal lake settings
E	Laminated mudstone	Thin horizontal laminations of mud with minor very fine sand and occasional outsized clasts	Outsized pebbles and cobbles	0.1-8.1 m	Suspension settling in distal lake settings with outsized clasts rafted by lake ice or vegetation
F	Ripple cross-laminated sandstone	Thin to very thin beds of symmetrically-rippled medium- to fine-grained sandstone, often overlain by horizontally-laminated siltstone	Symmetrical ripples, outsized clasts, unidirectional ripple cross-lamination	0.1-0.2 m	Wind-driven wave action in areas of the lake above wave-base level reworking sands of Facies D
G	Folded sandstone and mudstone	Coherent folded beds of sandstone and mudstone up to 1.5 m in thickness	Load/flame structures, convolute bedding, truncated beds	0.2-1.5m	Rapid loading of Facies D and E by cobble- and boulder-rich debris flows of Facies B. Seismic action and liquefaction possible
H	Sandy clinoforms	Massive to graded coarse- to fine-grained sandstone	Large-scale foreset and bottomset beds	0.1-2.3 m	Hyperpycnal flow of Gilbert-type delta progradation into freshwater

Table 1. Facies descriptions and interpretations for the Malanzán Formation in the Olta paleovalley.

Figure 6. Aerial photo of the Olta paleovalley with locations of measured stratigraphic columns.

#	Column	Height	Latitude	Longitude	Elevation	Facies Present
1	OLTA1	14.4 m	30° 37.926’ S	66° 18.629’ W	624 m	A, D, F
2	OLTA2	7.6 m	30° 37.936’ S	66° 18.664’ W	623 m	D
3	OLTA3	5.4 m	30° 37.934’ S	66° 18.746’ W	626 m	D
4	OC2	18.1 m	30° 37.966’ S	66° 18.930’ W	629 m	B, D, E, F, G
5	OC1	15.9 m	30° 37.870’ S	66° 19.103’ W	633 m	B, D, F, G
6	OG1	8.2 m	30° 38.330’ S	66° 20.453’ W	708 m	C
7	OG2	7.0 m	30° 38.364’ S	66° 20.464’ W	718 m	D
8	OG3	35.4 m	30° 38.446’ S	66° 20.609’ W	710 m	B, D, G
9	OG4	6.6 m	30° 38.456’ S	66° 20.635’ W	710 m	B, D, G
10	OG5	3.8 m	30° 38.483’ S	66° 20.704’ W	710 m	B, D, G
11	OG6	7.1 m	30° 38.506’ S	66° 20.742’ W	710 m	B, D, G
12	OD1	8.0 m	30° 38.609’ S	66° 21.464’ W	738 m	E
13	OD2	30.0 m	30° 38.651’ S	66° 21.697’ W	742 m	E, H

Table 2. Location of measured stratigraphic columns (Appendix). Number in left column corresponds to those on map in Figure 6. Facies are described in Table 1.

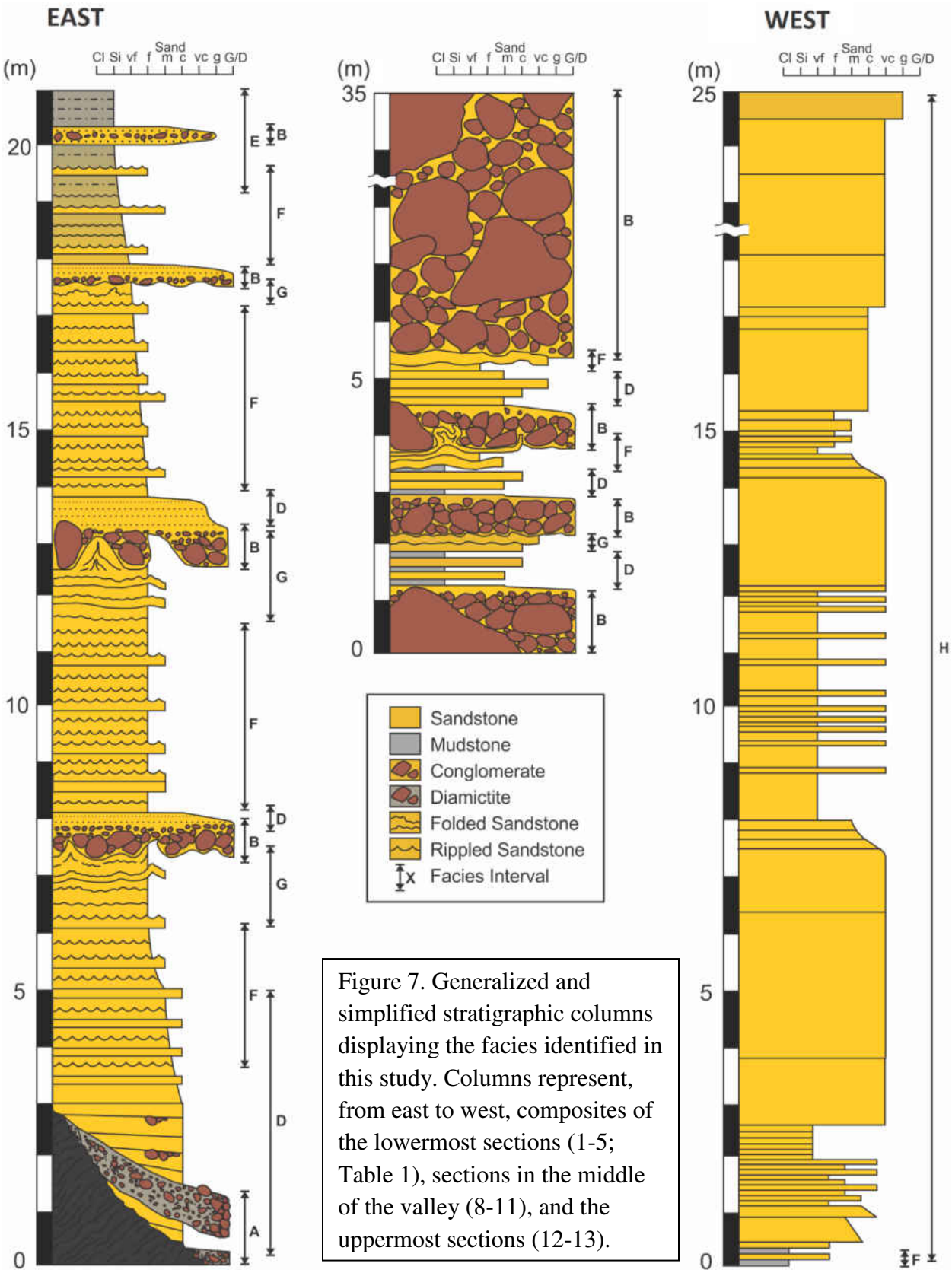

Figure 7. Generalized and simplified stratigraphic columns displaying the facies identified in this study. Columns represent, from east to west, composites of the lowermost sections (1-5; Table 1), sections in the middle of the valley (8-11), and the uppermost sections (12-13).

Facies A: Clast-rich sandy diamictites

Description:

The clast-rich sandy diamictite facies occurs in sections OLTA1 and consists of gray to tan colored, clast rich, intermediate to sandy (>10% mud), massive diamictite (cf. Hambrey and Glasser, 2012). At OLTA1, the diamictites rest on underlying schistose basement rocks, or are separated from the basement by up to 1 m of horizontally laminated or bedded, pebble-bearing, coarse-grained sandstone, which in turn downlaps onto the underlying basement rocks. The diamictite unit is wedge-shaped in cross-section (Fig. 8A) with one margin of the sediment body ending as clast-supported diamcitite in a steeply-dipping, rounded, "nose-like" margin (Fig. 8B), while the opposite margin ends as a matrix-supported diamictite that onlaps onto the underlying dipping nonconformity. Maximum bed thickness is 1.5 m near the downslope "nose" of the unit and thins upslope where the unit onlaps and pinches out against basement rocks. The facies predominantly contains subrounded pebbles and cobbles in a muddy, sand-rich matrix. However, subangular boulders up to 60 cm in diameter (long-axis) occur near the downslope portion of the body where boulders are common in the clast-supported "nose" (Fig. 8C). Clasts are mostly granitic in composition with minor schist and quartzite, and show no clear facets, polish, striations, or preferred orientation. Where this facies rests on horizontally-laminated, gravelly coarse sandstone of Facies D, the diamictites display sharp and erosional lower contacts and sharp upper contacts with boulders protruding from the top of the unit (Fig. 8A). Adjacent to the steeply-dipping "nose-like" margin of the deposit, gravelly stringers of sand (Facies D) onlap the diamictite. Laterally, these sands fine and thin away from the diamictite (Fig. 8D).

Interpretation:

Differentiation of glacial diamictites from nonglacial mass transport deposits is problematic (Visser, 1983), but at section OLTA1, the diamictite, which occurred adjacent to the valley wall, has several features associated with coarse-grained, cohesive subaqueous debris flows. These flows commonly develop a frontal concentration of large clasts resulting in a clast-supported flow snout and matrix-supported tail, "floating" boulders and cobbles that protrude through the top of the bed, and outrunner clasts carried beyond the nose of the bed by associated turbidity currents (Suwa et al., 1984; Postma et al., 1988; Mulder and Alexander, 2001, Sohn, 2002; Talling et al., 2012).

Resedimented glacial diamictites are reported from paleovalleys in the western Paganzo basin (Kneller et al., 2004; Dykstra et al., 2006; Henry et al., 2008; Limarino et al., 2014), but are associated with striated surfaces, true subglacial tillites, and faceted and striated clasts. The absence of these features in the Olta paleovalley suggests a non-glacial source for the remobilized sediment. Evidence of mass transport deposits are common in steep-walled mountain valleys (Van Steijn, 1996; Godt and Coe, 2007; Šilhán and Pánek, 2010) This facies is interpreted to be a debrite deposited by debris flows off the valley wall into a standing body of water that occupied the central portion of the valley.

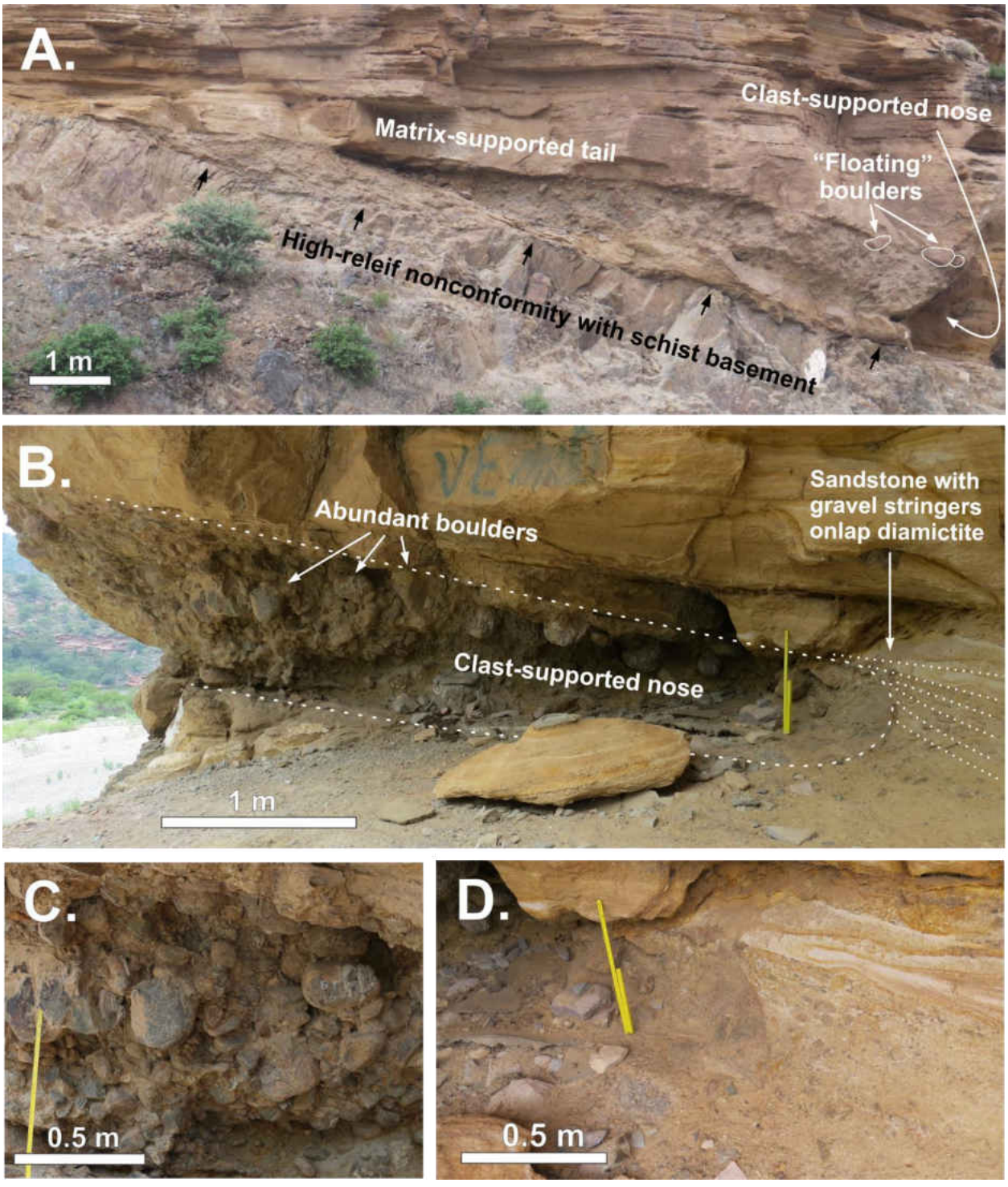

Figure 8. A clast-rich sandy diamictite bed exposed over schist basement at section OLTA1 with (A) a wedge-shaped profile and "floating" granite boulders protruding through the upper contact of the bed, (B) and (C) boulder-rich, clast-supported downslope "nose" of the unit, and (D) coarse-grained sandstone with gravel stringers onlapping the steeply-dipping margin of the diamictite.

Facies B: Sandy Conglomerate

Description:

The sandy conglomerate facies occurs in sections OC1-OC2 where isolated beds 0.2 to 1.7 m thick are separated by 5.0 to 6.1 m of sandstone and mudstone. In sections OG3-OG6 wedge-shaped sandy conglomerate beds can be traced laterally for over 200 m, originating from the mouth of a tributary paleovalley; thinning and fining westward where beds pinch out into laminated sandstones and mudstones (Fig. 9B-C) and thickening and coarsening eastward where beds merge and become indistinct in a boulder-dominated succession over 40 m thick (Fig. 9A). The bases of individual conglomerate beds rest on erosional, sharp and loaded bases. Loaded bases deform underlying sandstone and mudstone beds (Facies G) with sandstone flame structures extending upward as much as 60 cm into the overlying unit. In some cases, the flame structures pierce and are extruded through the conglomerate beds. Individual beds show normal grading near the tops of beds grading upward into horizontally-laminated sands of Facies D (Fig. 9F). The conglomerate is reddish-tan colored, massive to thickly-bedded with beds ranging from 0.2 to 32.9 m thick. The beds are generally internally massive. The conglomerate is typically clast-supported with sand filling the void spaces between the clasts (<10% mud) (cf. Hambrey and Glasser, 2012). Clasts are predominantly subrounded and granitic in composition, with common occurrences of quartzite and schist clasts. Clast size fractions vary from boulder-rich (with clasts up to 7.0 m diameter at section OG3) to cobble-rich with a coarse sand matrix filling the space between the gravel clasts.

Interpretation:

This facies represents deposition by streams and coarse debris flows associated with alluvial fans and fan deltas that interfinger laterally with lacustrine deposits of Facies D. Alluvial fans are common at the base of mountain valleys where steep-gradient, high-energy tributary streams rapidly deposit coarse-grained bedloads during an abrupt reduction in stream gradient upon reaching the main valley floor (Nilsen, 1982; Leeder, 1982). These fan- or cone-shaped deposits of alluvium are termed fan deltas where they terminate in a standing water body and deposition is mainly or entirely subaqueous (Holmes, 1965; Nemec and Steel, 1988), a setting that can occur in a narrow valley as fans prograde across the valley and impound drainage, forming a lake (Andreis et al., 1986; Colombo et al., 2009; Hutchinson, 1957; Hsu and Capart, 2008). Progradation is dominated by event sedimentation during high-discharge flood events and debris flows. Normal grading in upper portions of beds reflect the waning stages of discharge and transport by low-density fluids.

In the Olta paleovalley, thick deposits of conglomerate emanate from tributary paleovalleys and extend outward into the main paleovalley (Fig. 9A). The Olta paleovalley is less than 200 m wide in the area of these "paleo-tributaries." Therefore, progradation of these fans into and across the main paleovalley could easily impound drainage producing lakes as evidenced by lacustrine sediments that interfinger with distal alluvial fan conglomerates along the paleovalley wall (cf. Colombo et al., 2009). These conglomerates are similar to those described from Member 1 of the Malanzán Fm. by Andreis et al. (1986) from the Malanzán paleovalley where fan conglomerates represent the basal fill of that paleovalley. Socha (2007) and Socha et al. (2014) identified these deposits as diamictites with strongly-developed clast fabrics in the central portion of the valley (Fig. 9) and interpreted these deposits as subglacial

tillites. These authors noted the conspicuous absence of several diagnostic glacial features that were also not observed in this study including fine-grained matrix material and clasts exhibiting polish, striations, or facets. Clast fabrics can develop from streamflow and debris flows in alluvial fan deposits (Spearing, 1974; Nilsen, 1982). However, no clear preferred orientations of clasts were observed in this study.

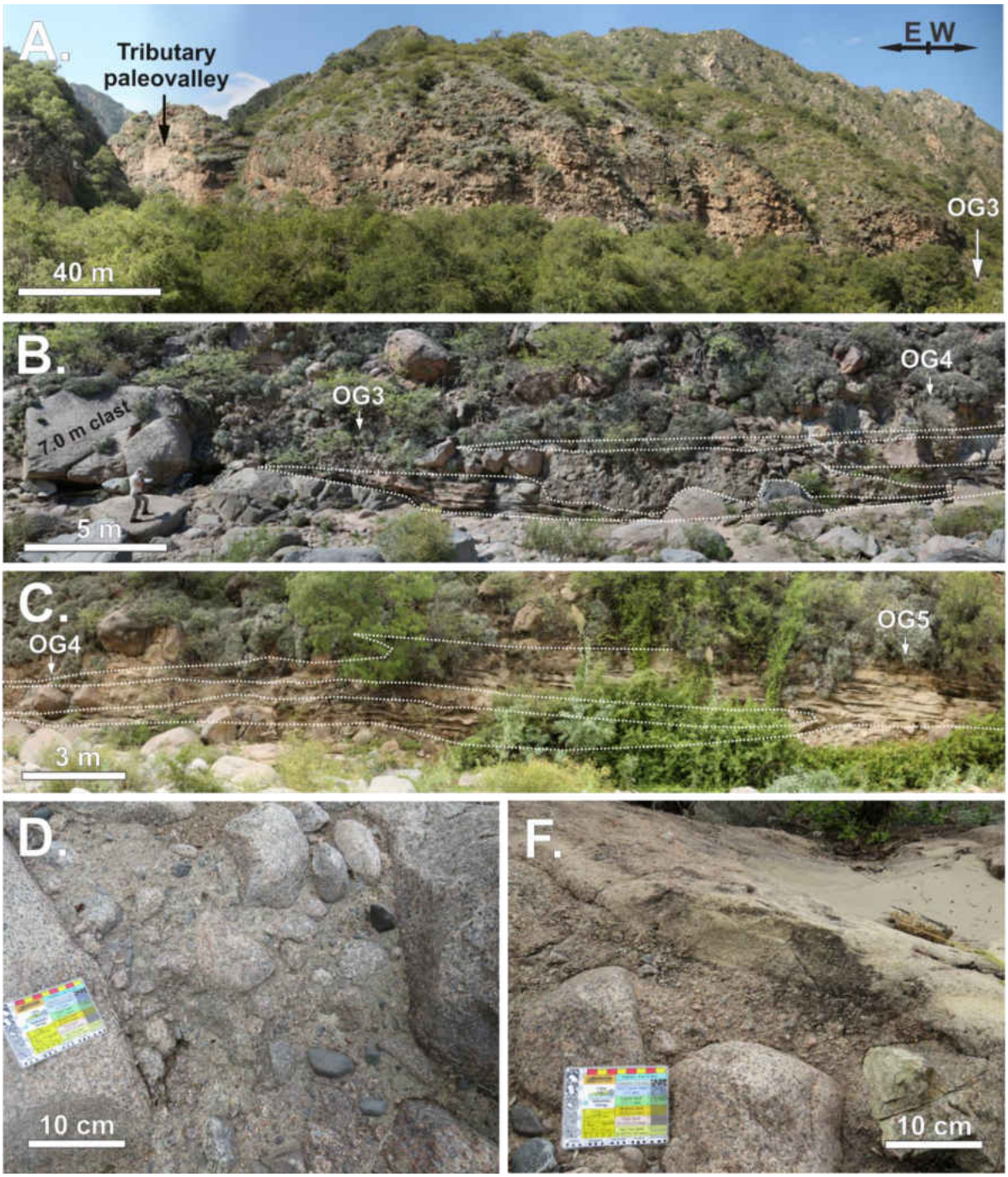

Figure 9. Sandy conglomerates of Facies B in the central portion of the Olta paleovalley where (A) a 40-m outcrop of sandy conglomerates is exposed at the mouth of a tributary paleovalley. (B) Wedge-shaped beds of conglomerate interfinger with horizontally-laminated sandstones of Facies D and pinch out to the west (C). Dashed line represents approximate contact between the facies. Locations of columns OG3-OG5 marked. (D) Conglomerate at the base of section OG3 consisting of subrounded granite clasts in a coarse sand matrix and (F) a normally-graded top.

Facies C: Boulder breccia

Description:

Clast-supported breccias were observed at section OG1, where angular granite boulders are chaotically stacked against a near-vertical granitic paleovalley wall. Upper, lower, and lateral contacts were not observed, but the matrix between boulders consists of very thin beds of heavily deformed, cohesive mudstone and fine sandstones (Fig. 10B) that include the trace fossil *Diplopodichnus biformis* (Fig. 10C), suggesting the unit overlies Facies G and laterally contacts Facies D. The 8.2 m+ thick unit lacks internal organization or stratification (Fig. 10A). Clasts are predominantly boulder-sized, including individual clasts up to 5 m in diameter, and typically the clasts display high angle (>20^{o}) to vertical orientations of their long axis.

Interpretation:

The boulder breccia observed at section OG1 is interpreted as direct rockfall off of valley walls into soft lake sediment. Exposures of the paleovalley walls possess slopes that commonly exceed 60° and approach vertical in many places. An exposed granite surface directly contacting lacustrine deposits less than 100 m laterally from the outcrop of breccia suggests this deposit rests against a steep portion of the wall. Clasts are largely angular and match the composition of the local bedrock, suggesting short transport distances. The arthropod grazing trace *Diplopodichnus biformis* (Brady, 1947) has been reported in deposits from multiple late Carboniferous water bodies, including fjord environments in the western Paganzo basin (Schatz et al., 2011) and glacial lakes in the Parana basin of Brazil (Netto et al., 2009). Its presence and soft-sediment deformation apparent in the lacustrine deposits between the clasts suggests rock avalanches occurred into an existing water body and the lake sediment was squeezed up into the voids between the clasts during the rock fall. Rockfall events are also catalysts for lake

development in narrow mountain valleys (Costa and Schuster, 1988; Ufimtsev et al., 1998; Wayne 1999; Sass et al., 2007).

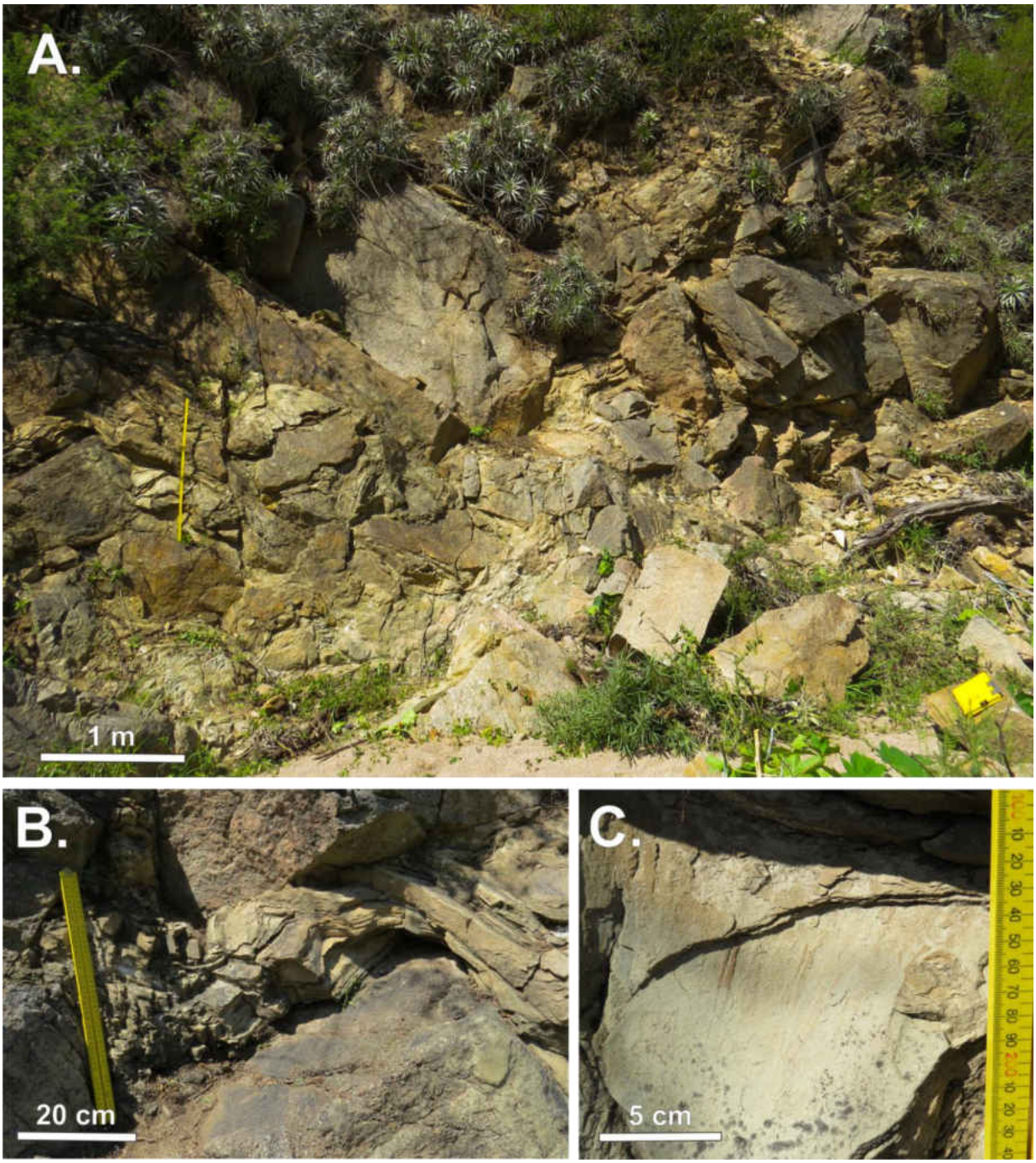

Figure 10. (A) An 8.2 m+ boulder breccia unit exposed at section OG1 that contains (B) highly deformed beds of sandstone and mudstone between angular granite boulders including (C) *Diplopodichnus biformis* traces exposed on a near vertical bedding plane.

Facies D: Graded sandstone

Description:

The graded sandstone facies consists of sandstone packages that may contain one or all of the following subunits: (Da) thin to medium beds of massive or graded, yellowish-gray colored, gravelly coarse-grained sandstone, (Db) thin beds of horizontally laminated, reddish-brown colored, coarse- to medium-grained sandstone, (Dc) thin beds of current ripple cross-laminated, yellow colored, medium- to fine-grained sandstone, and/or (Dd) medium laminations to thin beds of parallel-laminated, gray colored siltstone to very fine sandstone. Lower portions of sections OLTA 1-3 show repeating 15-40 cm thick Da/b packages of sandstone with abundant pebbles, cobbles, and occasional boulders. These lower units overlie bedrock or clast-rich sandy diamictites of Facies A with sharp or erosive contacts and onlap the nose of a wedge-shaped diamictite bed (Fig. 8D) Individual Da/b packages (Fig. 11A) are laterally continuous for distances for up to 25 m; slightly thickening and fining in the direction of paleoflow (~220). These beds transition upwards to 10-25 cm thick Db/c (Fig 11B) couplets that generally fine and thin upwards to 5-15 cm Db/c/d packages (Fig. 11C).

Sections OC1 and OC2 are dominated by 10-30 cm Db/c/d packages (Fig. 12A) except where 10-50 cm Da/b or Da/b/c/d beds (Fig. 12B) gradationally overlie massive sandy conglomerate beds (Facies B). Beds are laterally continuous over distances across exposures (up to 50 m). Upper portions of section OC2 show very thin beds of rippled fine sand (Dc) and very fine sand (Dd) grading into horizontally-laminated mudstone of Facies E. Upper portions of Sections OLTA1, OC1, and OC2 commonly show both asymmetric and symmetrical ripples (reworking to Facies G). The base of medium horizontally-laminated sandstones (Db) commonly show prod and bounce casts (Fig. 12D) where they overly siltstone (Dd), which occasionally

show small-scale (<5cm) load and flame structures (Fig. 12E) and dewatering pipes penetrating horizontal laminations (Fig. 12C). *Diplopodichnus biformis* trace fossils are common on rippled surfaces. Outsized pebbles and cobbles are common in coarse sandstones of this facies and are occasionally present in finer units.

Interpretation:

Together these subfacies record deposition by high and low density turbidity currents (divisions A/B/C/D of Bouma, 1962; $T_A/T_B/T_C/T_D$ of Talling et al., 2012; representing subfacies Da/Db/Dc/Dd), although sequential deposition of all four subfacies is rare. Graded or massive beds (Da) represent rapid settling from suspension of coarse-grained sand as the turbidity current begins to slow, followed by deposition of medium-grained sands (Db) that are horizontally-laminated by tractive upper flow regimes and cross-laminated fine sands (Dc) in lower flow regimes. Very fine-grained sand or silty upper parallel laminae (Dd) represent the final stages of tractive flow. As previously discussed, turbidity currents can be triggered from cohesive debris flows (Sohn, 2002; Talling et al., 2012), which is the interpretation for thick units belonging to this facies where the facies directly overlies or onlaps debrites in sections OLTA1 and OC1-2 (Fig. 12B). Lacustrine turbidites are more commonly triggered by hyperpycnal river discharge during flood events (Dadson et al., 2005; Talling, 2014) or prograding delta-front or delta-lip failures (Lambert and Giovanoli, 1988; Girardclos et al., 2007). The latter is considered the predominant triggering mechanism for turbidites observed in this facies that are not directly associated with coarse-grained cohesive debris flows, as hyperpycnal flows from river floods are thin (<2cm) and fine-grained with an inversely-graded base (see Facies F). The predominantly absent suspension settle out mud division (E of Bouma 1962; T_E of Talling et al., 2012, Facies E of this study) and common wave-influence observed in this facies in the eastern sections suggests

deposition in relatively shallow portions of the lake above storm wave base as fine-grained deposits are present negating deposition above normal wave base. A deepening of the lake through time likely occurred as coarse units dominate basal sections of the paleovalley and show a gradual fining and thinning of units upwards until the succession is dominated by suspension settling.

Similar turbidity current-dominated lacustrine deposits occur in the nearby Malanzán paleovalley (Andreis et al., 1986; Buatois and Mángano, 1995) and the western Paganzo basin (Limarino et al., 1984; Buatois and Mángano, 1994). The outsized clasts commonly observed in these deposits can be transported by the turbidity currents themselves (Postma et al., 1988) or by a variety of mechanisms including ice rafting (iceberg, lake ice, or anchor ice), rafting by vegetation, and as outrunner clast or clast left behind during sediment bypass of waning sediment gravity flows (see Facies E interpretation; Emery, 1955, 1965; Andreis and Bossi, 1981; Thomas and Connell, 1985; Woodborne et al., 1989; Gilbert, 1990; Dionne, 1993; Bennett et al., 1994; Kempema et al., 2001; Doublet and Garcia., 2004; Carto and Eyles, 2012). Bouncing clasts could also be projected lakeward during rockfall events off of the steep valley walls of this narrow paleovalley.

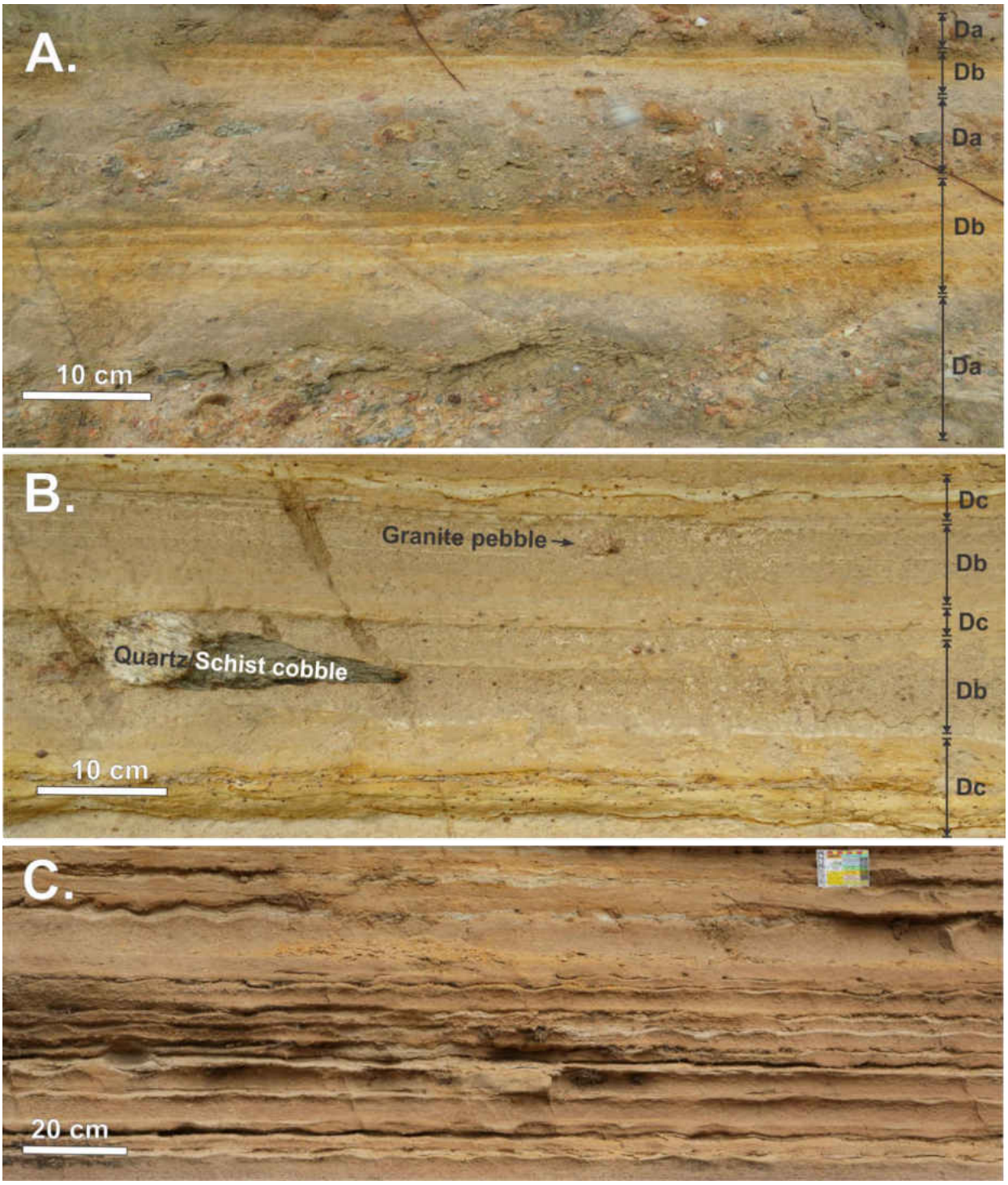

Figure 11. (A) Alternating beds of graded gravelly coarse-grained sandstone (Subfacies Da) and horizontally-laminated medium- to coarse-grained sandstone (Subfacies Db) at the base of section OLTA2. Upper portions of OLTA2 (B) are dominated by Subfacies Db interbedded with minor current ripple cross-laminated fine-grained sandstone (Subfacies Dc), which becomes the dominant subfacies represented in section OLTA3 (C).

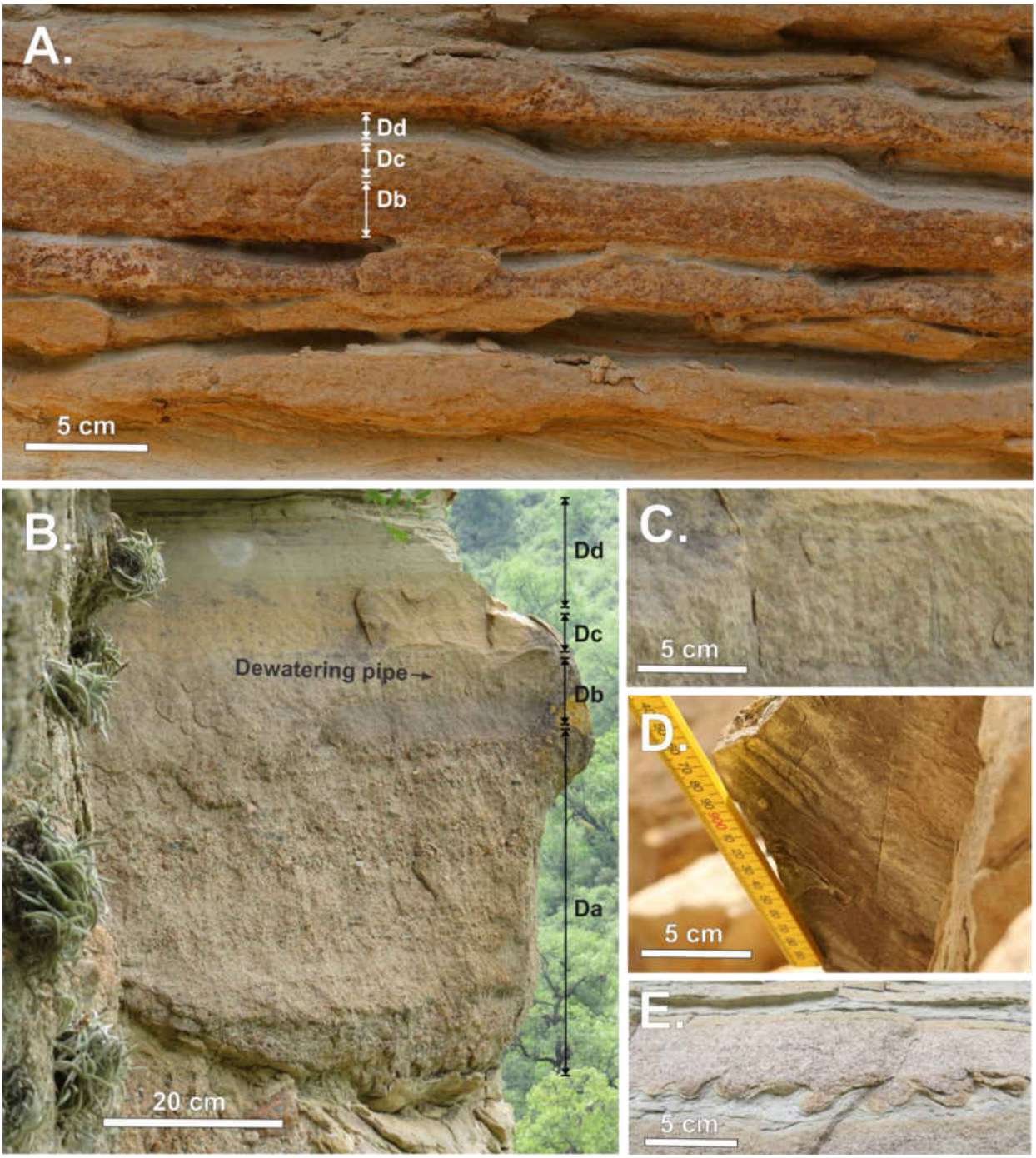

Figure 12. Graded sandstones from section OC2. Upper portions (A) show increasing thicknesses of parallel-laminated, very fine-grained sandstone and siltstones (Subfacies Dd) overlying current ripple cross-laminated, fine-grained sandstones (Subfacies Dc) and fewer, thinner beds of horizontally-laminated medium sandstones (Subfacies Db). (B) A fining-upwards sequence showing all four subfacies overlying a bed of sandy conglomerate (11 m in section OC2) which contains multiple graded laminae within the basal subdivision (Da) and dewatering pipes (C) immediately above it. Prod and bounce marks (D) and load and flame structures (E) commonly occur where Subfacies Db overlies Subfacies Dd.

Facies E: Laminated mudstone

Description:

The laminated mudstone facies consists of dark gray to tan colored, thin horizontal laminations of mud and silt. This facies occurs in beds up to 0.2 m thick in the uppermost portion of section OC2 (likely lower Member 2 of the Malanzán Fm.) where it is interbedded with fine sandstones of Facies D. In the western portion of the paleovalley the facies occurs in an interval at least 8.0 m thick (section OD1; upper Member 2 or lower Member 3 of the Malanzán Fm.; Fig. 13A), where occasional beds of horizontally-laminated very fine-grained sandstone up to 2 cm thick occur. In section OD2 (Member 3 of the Malanzán Fm.; Gutiérrez and Limarino, 2001) beds up to 0.2 m thick intercalate with sandy clinoforms of Facies H (Fig. 13E). Laminae are even and continuous, ranging from 1 to 5 mm in thickness and are occasionally disrupted by granule- to pebble-sized outsized clasts (Fig. 13D). Impressions of *Cordaites sp*. are commonly preserved on silty bedding planes (Fig. 13B).

Interpretation:

The fine-grained sediments of this facies record suspension settling in calm, deeper-water portions of the lake or in areas distal to the influx of coarse-grained clastics. Very thin beds of very fine sand observed in section OD1 are less than 400 m laterally from exposures of Gilbert delta bottomsets observed in section OD2 and likely represent deposition from distal hyperpycnal underflows (Lambert and Hsu, 1979; Lambert and Giovanoli, 1988; Crookshanks and Gilbert, 2008). Similar intervals of mudstone have been described in the Malanzán paleovalley (Andreis et al., 1986; Buatois and Mángano, 1995) where pebbles and cobbles are interpreted as dropstones and cited as the primary evidence for glacial influence in the valley; however, as discussed previously, multiple non-glacial processes can transport outsized clasts to

distal lake environments, including rafting by vegetation and lake ice. Sterren and Martinez (1996) suggested the diminutive flora that existed in the Olta paleovalley were incapable of rafting of large clasts, and reported the existence of clasts with extrabasinal lithologies that suggested glacial transport. However, Sterren and Martinez (1996) did not mention the lithologies of these exotic clast, and clasts representative of sources other than local basement rocks were not observed in this study. Andreis and Bossi (1981) and Andreis et al. (1985) considered outsized clasts as evidence for seasonally frozen lake surfaces which could accumulate sediment from tributaries and mass wasting off of the valley walls during the winter months and subsequently raft upon ice break-up. Section OD1 is located adjacent to the high relief nonconformity on the north valley wall, suggesting direct rock fall into the lake was also possible. The absence of glacial features on the clasts themselves (i.e., bullet shape, striations, and/or facets), including the absence of extrabasinal clast lithologies anywhere within the studied section, is consistent with non-glacial transport mechanisms for the outsized clasts.

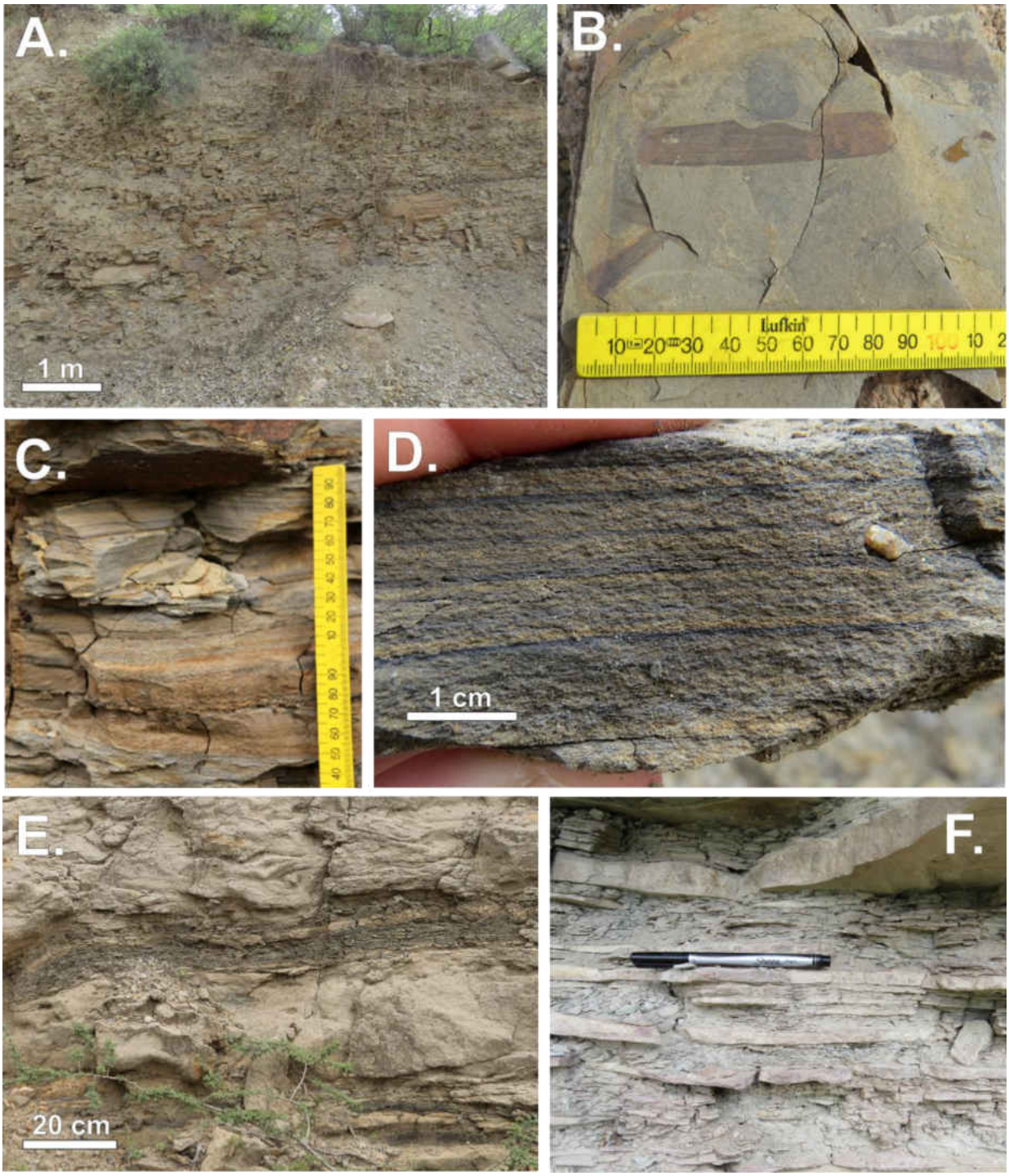

Figure 13. (A) An 8.0-m outcrop of laminated mudstone (Facies E) at section OD1 containing (B) *Cordaites sp.* exposed on silty bedding planes of very fine laminations (C) which are occasionally disrupted by pebble-sized clasts (D). Laminated mudstones interbedded with (E) sandy clinoforms (Facies H) at the base of section OD2 and (F) horizontally-laminated fine-grained sandstone (Facies D) in uppermost portions of section OC2.

Facies F: Ripple cross-laminated sandstone

Description:

Sequences of asymmetrically-rippled sandstones of Facies D are interrupted by intervals of variable thickness (0.1 to 5.2m) that show quasi-symmetric to symmetric ripples of this facies, which comprises the majority of upper portions of several sections (OLTA1, OC12, OG2). In these sections Facies F gradationally overlies horizontally-laminated coarse- to medium-grained sandstones of Facies D and is interbedded with sandy conglomerates of Facies B, beneath which it is folded to form Facies G. In more vertically extensive stratigraphic exposures (such as OC2), sandy units thin upward while silt drapes on top of rippled beds thicken, resulting in a gradual transition to Facies E. Individual beds show sharp upper and lower contacts and are laterally continuous over short distances (~5m) across exposures. This facies is superficially similar to fine-grained packages of Facies D in that these intervals are characterized by thin to thick beds of reddish-brown medium-grained sandstones that are horizontally-laminated and abruptly grade upward into yellow, fine-grained sandstones that are ripple cross-laminated. Rippled beds are commonly overlain with very thin beds of gray colored, parallel-laminated, very fine-grained sandstone and siltstone (Fig. 14A), but can be distinguished from Facies D by occurrence of symmetrical and weakly-asymmetrical ripples that are present at the top of medium-grained sandstone and throughout fine-grained sandstone beds. The symmetrical ripples typically rest on unidirectional cross-laminations that are anomalous to the profile of the overlying bedform. Occasional pebble-sized outsized clasts are present and *Diplopodichnus biformis* traces are common.

Interpretation:

Symmetrically-rippled sandstones represent wave-modification of sands deposited by turbidity currents in shallow areas of the lake. The internal structure of ripple laminae suggests unidirectional flow during deposition, as is apparent in turbidites of Facies D, but the symmetrical ripple profiles suggest reworking by bi-directional wave activity. Newton (1968) suggested symmetrical ripples with unidirectional foreset laminae form in nearshore environments where stronger incoming waves produce foreset laminae, and the proceeding back wave is strong enough to maintain ripple symmetry but not powerful enough to produce a corresponding bidirectional foreset. Buatois and Mángano (1995) suggested similar deposits from the Malanzán paleovalley represent post-depositional reworking of turbidites by storm waves, but the continuity of individual beds and lack of hummocky cross-stratification suggest minimal influence from high-energy storm events. Ripple Indices (after Tanner, 1967) are highly variable in this facies and suggest sedimentation under combined flow regimes where both unidirectional currents and wave activity are superimposed on the deposits, which is a syndepositional process that has been interpreted for wave-modified turbidites (Myrow et al., 2002). Hummocky cross-stratification can form in lakes (Eyles and Clark, 1986). However, the narrowness of the valley and potentially shallow water depths would have likely inhibited the formation of large amplitude waves within the depositional environment (cf. Syvitski et al, 1987; Boulton, 1990).

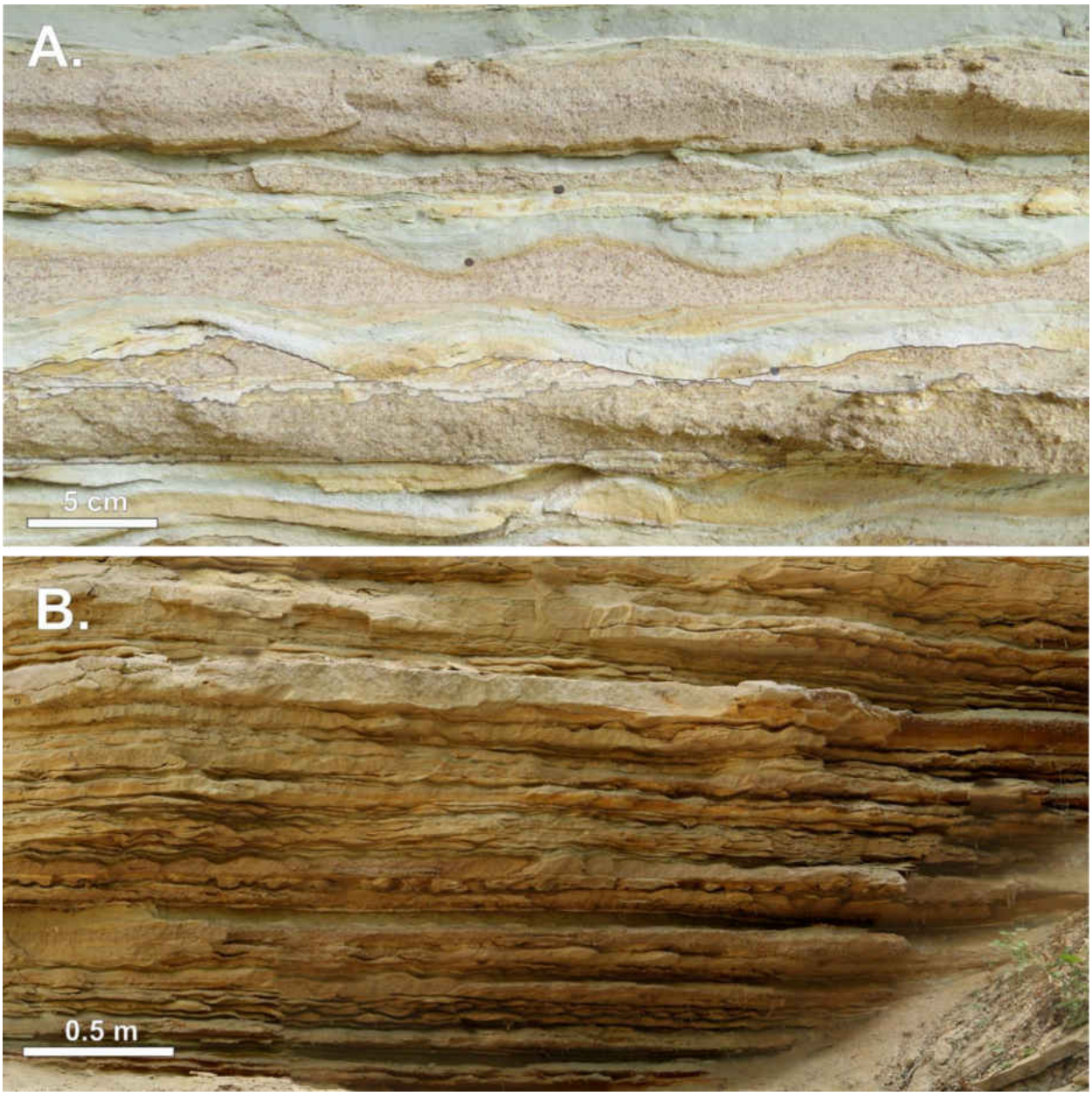

Figure 14. Symmetrical and weakly-asymmetrical rippled sandstones of Facies F observed in (A) section OC2, where cross-laminations in the reddish-brown medium-grained sandstone are unidirectional, and (B) the lower portion of section OC1.

Facies G: Folded sandstone and mudstone

Description:

This facies includes two distinct types of deformation consisting of 1) conglomerate load and associated sandstone and mudstone flame structures, and 2) localized decimeter to meter-scale folds that resemble dropstone ruck structures (cf. Thomas and Connell, 1985), which are associated with boulder-sized clasts.

Deformed sandstones and mudstones that occur below conglomeratic load structures within thin (0.1 to 0.7 m thick) horizons of Facies B represent laterally continuous deformation zones up to 1.8 m thick. They occur in association with granule to boulder conglomerate load structures. Deformed sandstone and mudstone rests on undeformed beds of the same composition (represented by Facies D and F). The base of the zone is only mildly deformed with cm to dm scale load structures and gentle open folds. Deformation increases gradually upward except at the top of the zone where finer-grained beds show tight sub-order folds and are brecciated in places, and extruded upward into the overlying conglomerate. These extruded beds form large flame structures that in some places penetrate the overlying conglomerate (Fig. 15C). In turn, the conglomerate occurs as a semi-continuous horizon of load structures 0.5 to 2 m wide and extending downward up to 0.5 m into the underlying sandstone. In a few places, the loads have detached from the conglomerate and form isolated pods of conglomerate in the underlying sandstone (Fig. 15D). In other places, individual clasts, including platy schist and phyllite clasts, extend downward into the underlying sandstone and/or are completely surrounded by deformed sandstone and mudstone (Fig. 15C). The load and flame structures form couplets that occur every 1- 4 m along the contact between the conglomerate and the underlying sandstone and mudstone. Sandstone and mudstone above the conglomerate beds are undeformed. At least three

different deformed horizons occur in the area that extends from section OC2 to section OC1. Orientations of apparent fold axes are highly variable, ranging from perpendicular to sub-parallel to the valley axis, depending on the orientation of the outcrop face. The thickness and severity of deformation is not proportional to the thickness of the overlying conglomerate. At the base of section OC1, sandstones are folded for over 1.2 m in thickness beneath a relatively thin (0.1 - 0.5 m) conglomerate bed with boulders that rarely exceed 0.4 m (Fig. 15A), but near the top of the section a thicker (0.3 – 0.7 m) and coarser (multiple boulders exceeding 1.0 m) conglomerate bed overlies a comparatively thin (0.3 - 0.6 m) zone of deformation (Fig. 15B).

At section OG4, sandstone and mudstone beds are locally penetrated, bent downward, and laterally deformed into decimeter to meter-scale folds that resemble large-scale dropstone related ruck structures (cf. Thomas and Connell, 1985) beneath and around the margins of m-scale boulders (Fig. 16A). These sandstone and mudstone beds interfinger with and are contained between matrix- and clast-supported boulder- and cobble-rich, sandy, massive to weakly normally graded boulder conglomerates of Facies B. Conglomerate beds thin laterally in sections OG5 and OG6, and the deformed intervals of sandstone and mudstone thin and overlie undeformed strata of the same composition (interbedded sandstone of Facies D and mudstone of Facies E). In places, these sandstones and mudstones are deformed below m-scale boulders and lenses of matrix-supported diamictites. Flame and/or ruck-like diapiric structures up to 0.8 m in height protrude upward along the margins of boulders, between boulders, and along the margins of the conglomerate lenses (Fig. 17B). Sandstone and mudstone beds are also truncated directly beneath the lenses. *Diplopodichnus biformis* and *Gordia marina* (Fig. 17C) trace fossils occur on the upper surface of the sandstone beds.

Interpretation:

Both types of deformed beds were interpreted by Socha (2007) and Socha et al. (2014) as the result of subglacial or proglacial deformation. The conglomerate and associated large-scale folds in the sandstone and mudstone it overlies at section OC1 were interpreted as either 1) a subglacial tillite overlying proglacial sediment folded by shear stress from the overriding ice, 2) a debrite originating off of an ice front which rapidly loaded sandy proglacial deposits, or 3) a combination of both; a debrite overridden by an advancing ice front. Socha et al. (2014) suggested the scale of folding exhibited by the sandstones were unlikely to have occurred strictly through gravitational settling, reporting fold axes perpendicular to the presumed ice-flow direction and the presence of shear fabric at the conglomerate base.

These conglomeratic loads and associated flamed and folded sandstones and mudstones are interpreted here as recording possible seismically-influenced, rapid loading of soft lake sediment (Facies D and F) by coarse-grained debris flows, with no evidence of glacial influence. The conglomerate contains minimal fine grained matrix material and boulders are commonly supported by granules or pebbles. Faceted clasts with striations or polished surfaces were not observed in this or other deposits in the paleovalley, suggesting the material was not glacially-sourced. Shear fabrics reported by Socha et al. (2014) at the base of conglomeratic loads were not observed. The contact between the deformed sandstones and conglomerates is largely not erosive. An erosive contact would be expected if the surface were overridden by a glacier prior to deposition of a "tillite." Fold axes of the folds are apparent and biased transverse to the valley axis (and therefore presumed glacial flow) due to modern fluvial exhumation and the orientation of outcrops parallel to the valley axis, and although some folds were observed sub-parallel to the valley axis, folds perpendicular to the axis were also observed.

Beds of dramatically-folded sandstones and mudstones in sections OC1 and OC2 meet the criteria for soft-sediment deformation structures induced by seismic liquefaction and/or fluidization put forth by Moretti and van Loon (2014) in that they 1) occur in laterally continuous, recurring horizons, separated by undeformed beds, 2) show differing severity of deformation reflecting differential earthquake strength or lateral distance from the epicenter, 3) occur in a basin that was tectonically active, and 4) show morphological features comparative to known seismites. Deformation zones are laterally continuous over the length of their exposures (>100 m) and correlate closely between sections OC1 and OC2 (a distance of approximately 300 m). The thickness of individual deformed zones is independent of the thickness of the overlying load, suggesting variable intensities of liquefaction. The position of the Paganzo basin along the active margin of Gondwana and the rapid uplift experienced by the Sierras de Los Llanos through the Carboniferous (Enkelmann et al., 2014) suggests the area was an active tectonic setting. Local depocenters were fault-bounded (elongated graben; Andreis et al., 1986), and deposition in the Olta paleovalley is believed to have been initiated due to differential subsidence (Net and Limarino, 1999) between the paleovalley and surrounding mountain ranges. Similar large-scale, semi-regularly spaced load structures in lacustrine sandstone and mudstone have been attributed to seismic liquefaction (Moretti and Sabato, 2007; Alfaro et al., 2010; Üner et al., 2014). Subglacial deformation is dominated by simple or pure shear structures and asymmetric folding ,suggesting these features were not produced beneath glacial ice, but vertical deformation structures characterized by load casts and open folds commonly occur in glaciolacustrine settings near the ice front associated with rapid loading (Eyles et al., 1987; McCarroll & Rijsdijk 2003). Moretti (2000) and Moretti and Sabato (2007) suggested deformation from seismic liquefaction can be distinguished from deformation caused purely by overloading where deformation zones

exhibit thicknesses 70% or greater of the thickness of the overlying load. Deformed zones in sections OC1 and OC2 meet this criteria.

Socha et al., (2014) interpreted the folded fine-grained sediments between conglomerates at sections OG3-OG6 as the result of subglacial deformation and/or dewatering of over-pressurized sediment being overridden by an advancing glacier. Sandstone beds were interpreted to have been deposited either as proglacial lacustrine sediment frozen onto the base of the glacier or due to fine sediment deposited in cavities within the ice. Coarse clastics were interpreted to be subglacial tills, recording a grounded ice advance down the valley. The authors noted fold axes perpendicular to the assumed ice-flow direction.

Folded lacustrine sediments are laterally traceable where they intercalate with wedges of fan conglomerates (see Facies B) in these sections. Alluvial fans and fan deltas prograde episodically during flood events as stream and debris flows transport coarse material to distal portions of the fan (Harvey, 1990; Blair and McPherson, 1994), causing rapid loading and deformation in the underlying soft sediment. An examination of specific folds identified as glacial shove by Socha et al., (2014) in a wider context suggest they are ruck structures, as these folds occur on both sides of large boulders in section OG4, which occurs in a bed that can be traced laterally to the large conglomeratic alluvial fan deposit emanating from a tributary paleovalley. These deformational structures may also have been caused by rock fall directly from the immediately adjacent southern paleovalley wall. The association of these boulders and deformation structures with the nearby alluvial fan and valley wall suggests mass transport off of steep slopes into soft lake sediment, causing truncation, bending, and rucking of lacustrine sediment. Folds have an apparent axis perpendicular to that of the valley due to modern fluvial incision and the orientation of the outcrops down the axis of the main valley.

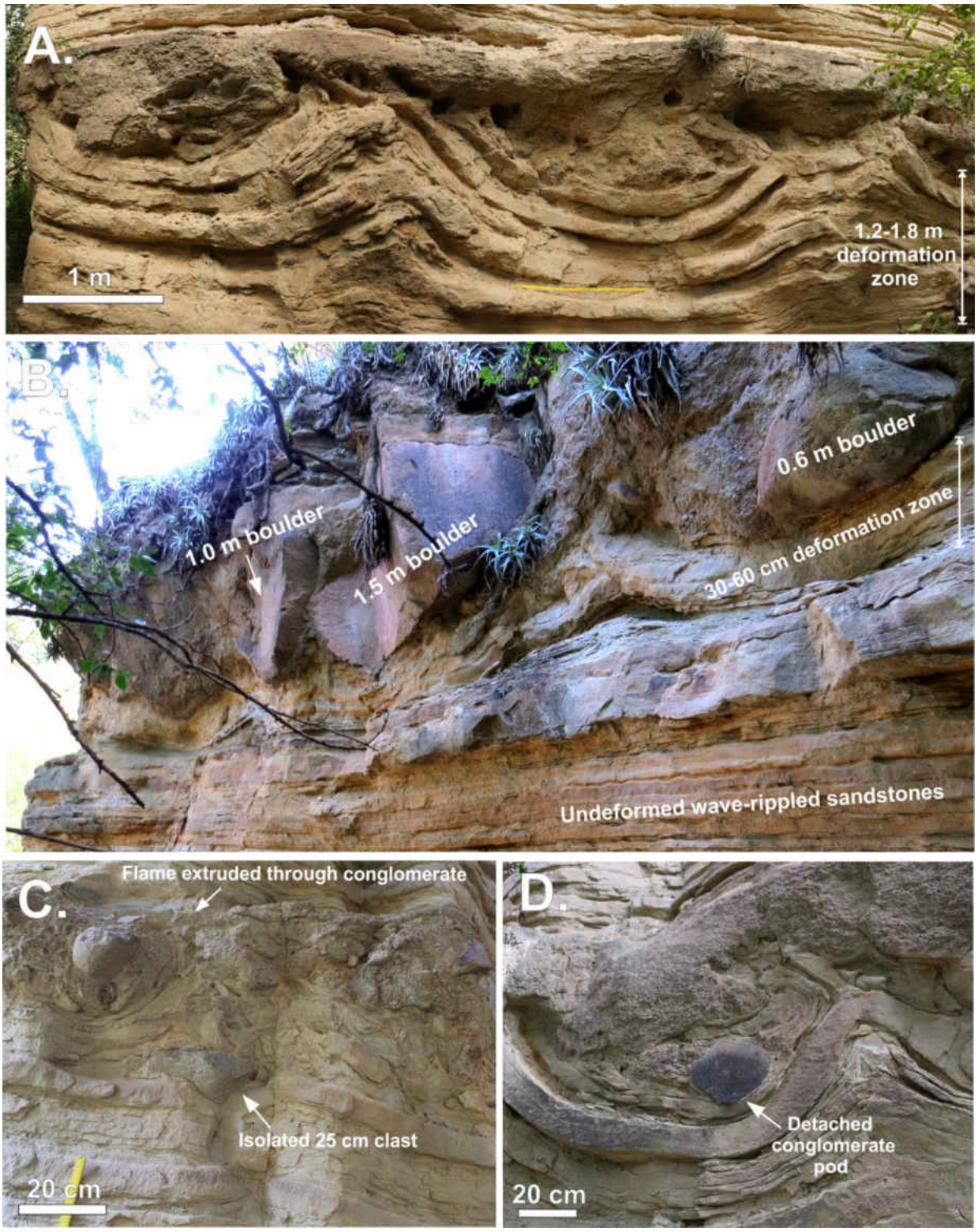

Figure 15. Deformed sandstones and mudstones that occur below conglomeratic load structures at (A) the base and (B) upper portions of section OC1. (C) Isolated clasts and (D) conglomerate pods are occasionally detached from the overlying conglomerate.

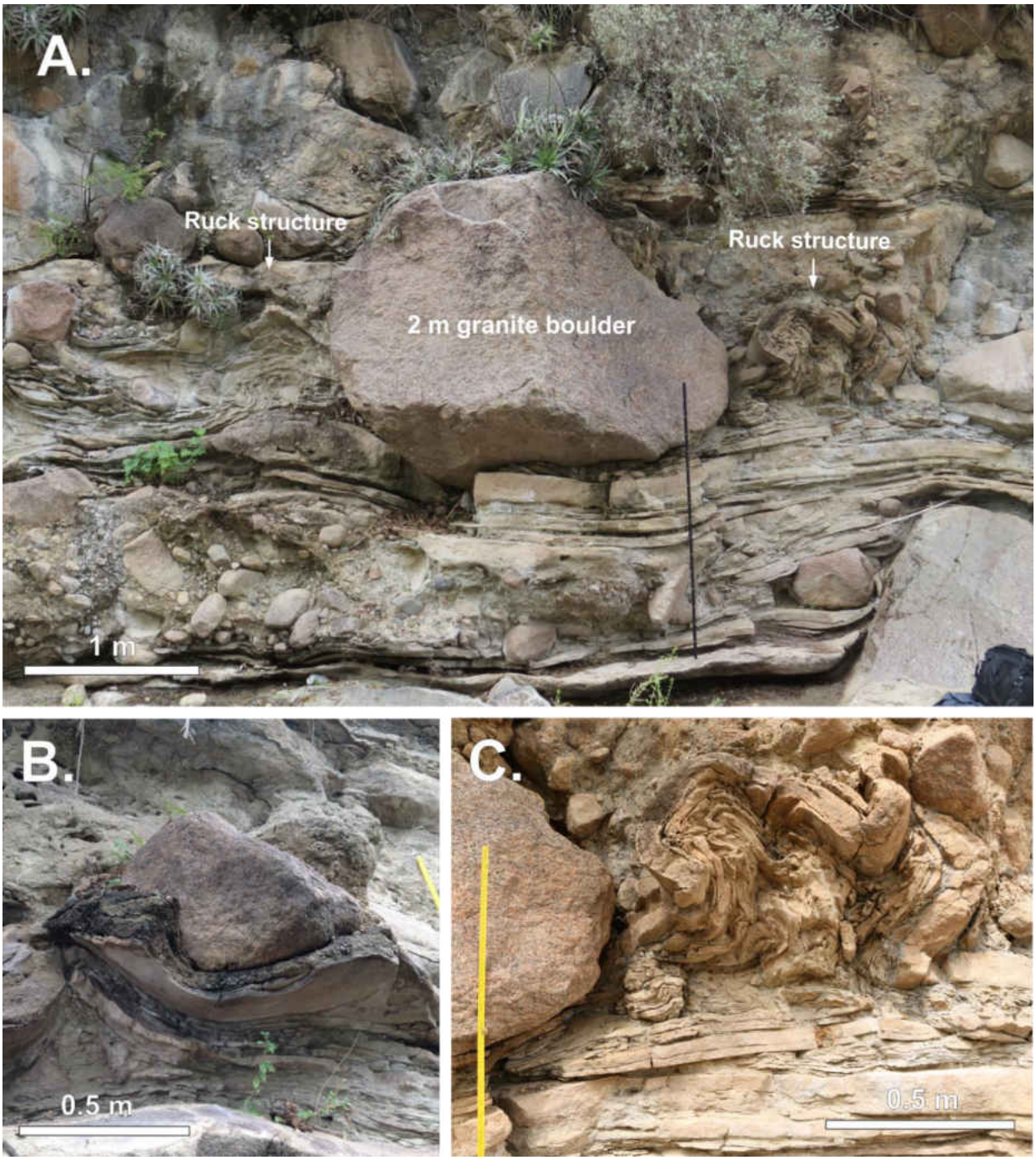

Figure 16. (A) A granite boulder with associated sandstone and mudstone ruck structures on either side at section OG4. Sandy diamictites and conglomerates may represent debris flows. (B) A granite boulder overlying bent sandstone beds. (C) Detailed view of the ruck structure at the right of A exhibiting highly-contorted fine-grained sandstone and siltstone beds.

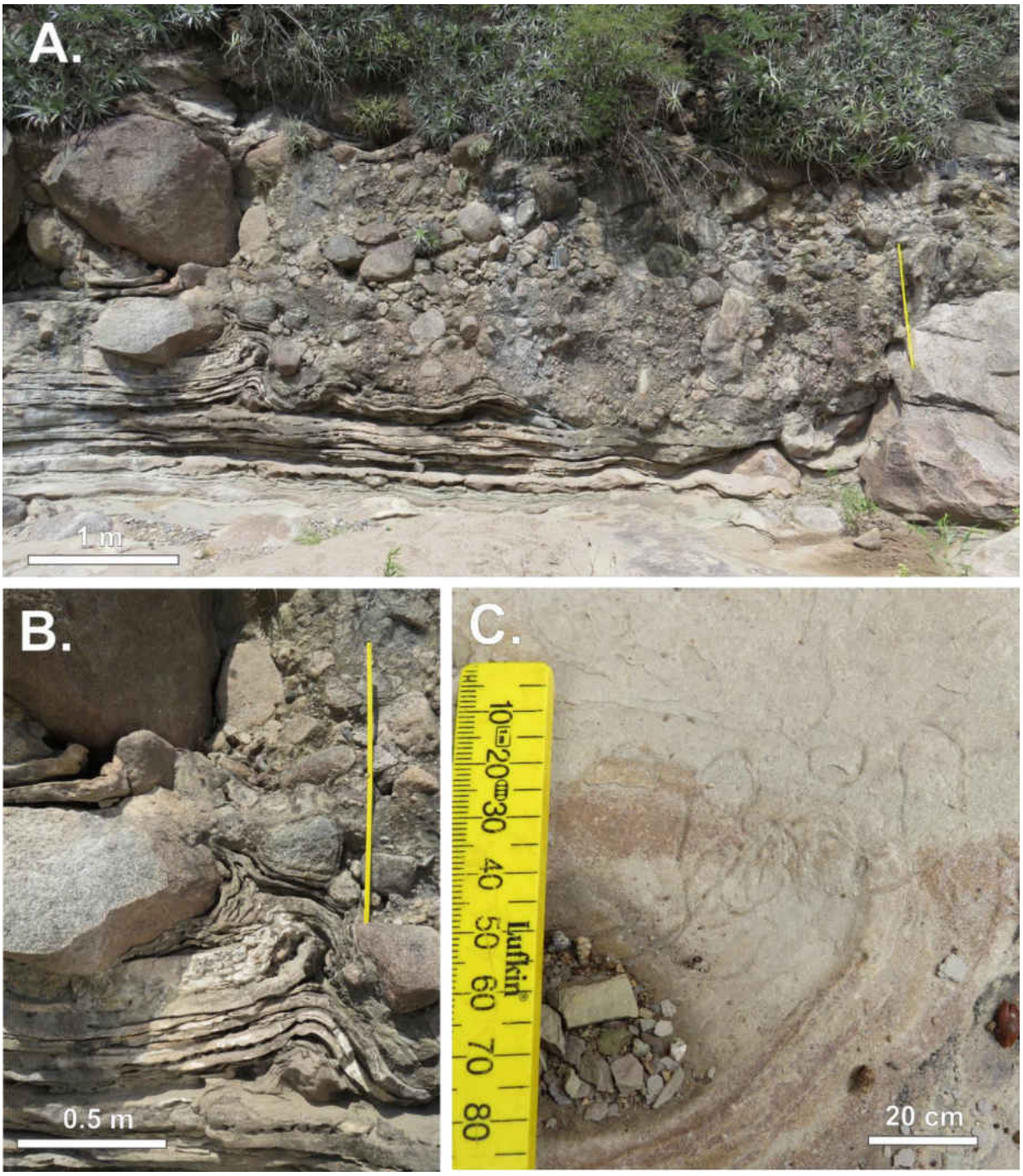

Figure 17. (A) Folded and truncated sandstone and mudstone beds at section OG3 beneath a bed of sandy diamictite. (B) Detailed view of the ruck structure at the left of A. (C) Trace fossils of cf. *Gordia marina* on a sandstone bedding plane.

Facies H: Sandy Clinoform

Description:

The sandy clinoform facies occurs in the highest stratigraphic position (Member 3 of the Malanzán Fm.; Gutiérrez and Limarino, 2001) in the westernmost portion of the study area. At section OD2 (Fig. 18A), a 38-m outcrop contains gently-dipping (~0-10°) bottomset beds (Fig. 18B) that are extensive over distances of over 50 m (and even further in other outcrops observed in the valley; Fig. 18D). Beds in this section coarsen, thicken, and steepen upwards to steeply-dipping (~10-35°) foreset beds (Fig. 18C). Basal portions of section OD2 contain 2-10 cm beds of very fine-grained sandstone and are variably intercalated with 1-20 cm beds of horizontally-laminated mudstone of Facies E (Fig. 13E). These beds are overlain by foreset beds comprised of very coarse-grained sandstone ranging from 0.2 to 2.3 m in thickness that are typically massive or parallel-bedded with normal grading in the upper portions of beds. The 30-m measured section at OD2 shows an overall coarsening-upwards succession from bottomset beds of muds and very fine-grained sands to gravelly upper foreset beds.

Interpretation:

The sandy clinoform of this facies represent progradation of Gilbert-type deltas and sedimentation by associated high-gradient streams into proximal lake environments. Clinoforms with coarse-grained, steeply-dipping forest beds imply rapid mixing of stream and basin waters resulting in rapid deposition of the bedload, while laterally extensive, fine-grained bottomset beds suggest underflows from sediment-laden streams. This type of combined deposition by homopycnal and hyperpycnal flows is characteristic of Gilbert-type deltas and requires the density of water in the basin to be approximately equal or lower to that of the inflowing steam, thus these deposits are common where high-relief streams terminate into fresh water bodies such

as mountain lakes (Gilbert, 1890; Bates, 1953; Stanley and Surdam, 1978). These deposits can occur in marine settings in tectonically active areas with high relief where the inflowing stream has a high suspended load (Colella et al., 1987; Falk and Dorsey, 1998) or the temperature of the stream is notably lower than the seawater (e.g., fjords; Prior and Bornhold, 1988; Corner et al., 1990), but the long distance spanned by bottomset beds suggest water in the basin was considerably lower in density than inflowing water and was likely fresh.

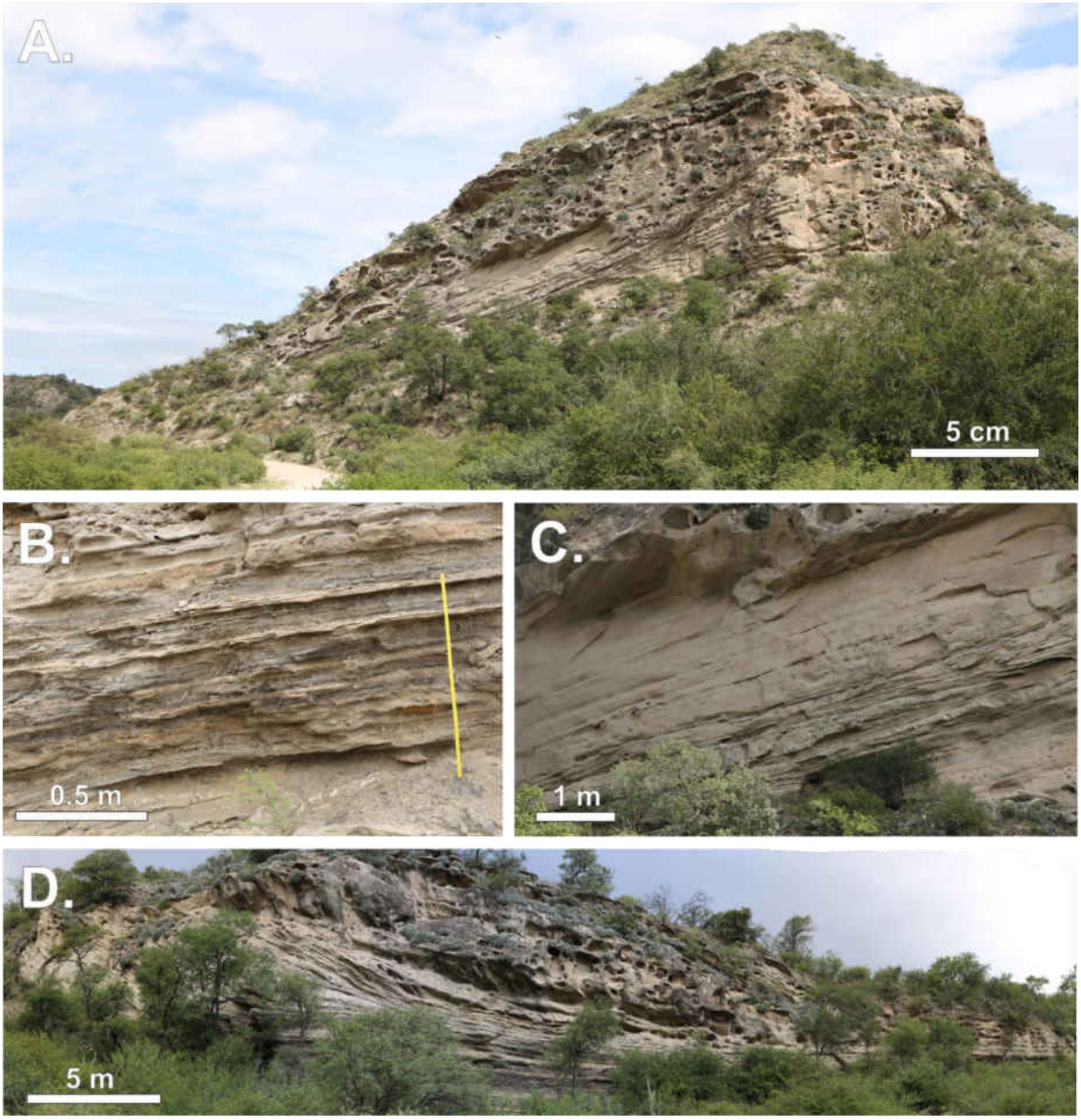

Figure 18. (A) A 38 m outcrop of sandy clinoforms (Facies G) exposed in section OD2 in the western Olta paleovalley containing (B) thin, low-angle (5-10°) bottomset beds of very fine-grained sandstone that coarsen upwards to (C) thick, steeply-dipping (10-35°) foreset beds of coarse-grained sandstone that become gravelly near the top of the section. (D) Nearby outcrops contain very low angle (<5°) bottomset beds extending over 100 m laterally.

Discussion

Valley Origin

Deposition of the Malanzán Formation in the Olta paleovalley began in the mid-Carboniferous across a high-relief erosional surface cut into granitic and metasedimentary Ordovician basement. Limited exposures of this surface within the valley prohibit a detailed characterization of the paleovalley floor, but nevertheless a primary line of evidence for the interpretation of the Olta paleovalley as an ancient fjord is its "U"-shaped profile (Sterren and Martinez, 1995; Socha et al., 2014). Alpine valleys carved by glaciers commonly have a flat floor, as opposed to the "V"-shaped profile of fluvially-incised valleys (Harbor, 2002). The Olta-Malanzán paleovalley is filled by up to 877 m of late Paleozoic and Cenozoic strata (Andreis et al., 1986), thus the true profile of the paleovalley cannot be observed. The deepest incisions by the Rio Olta in the central portion of the Olta paleovalley show granitic valley walls less than 250 m apart (Fig. 19). Andreis et al., (1986) did not consider the Malanzán paleovalley to be glacially carved, but that it formed as a narrow graben oriented perpendicular to the axis of the uplifted basement block. Net and Limarino (1999) suggested that the location and orientation of the Olta and Malanzán paleovalleys were controlled by a major northwest-southeast trending lineament and that these paleovalleys experienced high rates of subsidence relative to the surrounding ranges during early stages of deposition. The hypothesis that the surrounding ranges experienced alpine glaciation in the mid-Carboniferous and preserve a glacial geomorphic expression is not supported by the topography in the surrounding Sierra de Los Llanos and Sierra de Los Lujan ranges, which exhibit structurally-controlled fluvial erosion patterns. Tributary paleovalleys, including those in the Sierra de Malanzán and Sierra de Chepes ranges, do not show the steep headwalls of cirques that are characteristic of glaciated mountain ranges (Barr and Spagnolo, 2015). The paleovalley has also been hypothesized to have possibly been carved

by an outlet glacier that drained a possible ice sheet to the west (Aquino et al., 2014), but the variable width of the valley is inconsistent with that interpretation, as the Olta paleovalley narrows in its central portion and then rapidly widens to the west over distances of a few kilometers without significant tributary paleovalleys that could potentially possess tributary glaciers. The narrowest portions of the Olta paleovalley also occur where two tributary paleovalleys enter the trunk valley. Such an arrangement is inconsistent with an interpretation of these valleys as glacial in origin as an increase in ice volume down glacier from the confluent with a tributary glacier would be expected to have resulted in greater erosion and therefore a greater width for the valley rather than a narrowing of the valley.

Figure 19. Google Earth image of the Olta paleovalley (modern Rio Olta valley). View to WSW.

Exposures of the paleovalley wall directly contacting the Malanzán Formation were observed in two sections during this study. At OLTA1, schist basement of the Olta Formation is overlain by coarse-grained sandstone and sandy diamictite (Fig. 20A). The bedrock surface is jagged and uneven, with thin slabs of schist that project into the overlying diamictite (Fig. 20C). This is in contrast to comparatively smooth or polished surfaces observed on glacially-abraded floors and walls of paleovalleys along the Protoprecordillera (López-Gamundí and Martinez, 2000; Rocha-Campos et al., 2008; Colombo et al., 2014). Granitic subcrop of the Chepes Formation observed beneath coarse sandstones at section OG2, while planar, showed no striations or polish (Fig. 20D). Socha et al., (2014) suggested the absence of these features on bedrock surfaces and clasts was due to intense weathering and reported heavily-weathered granite clasts from the western Olta paleovalley, but the reddish conglomerates that outcrop in this area are part of the lower Solca Formation, which is late Carboniferous to Permian in age and overlies the middle to late Carboniferous Loma Larga Formation (Net and Limarino, 1999; Gulbranson et al., 2010). Weathering rinds on clasts severe enough to remove surficial abrasion features are present in the Malanzán Formation, but largely unweathered clasts predominate, as observed in this study and by Andreis et al., (1986), who reported a high degree of lithoclast "freshness."

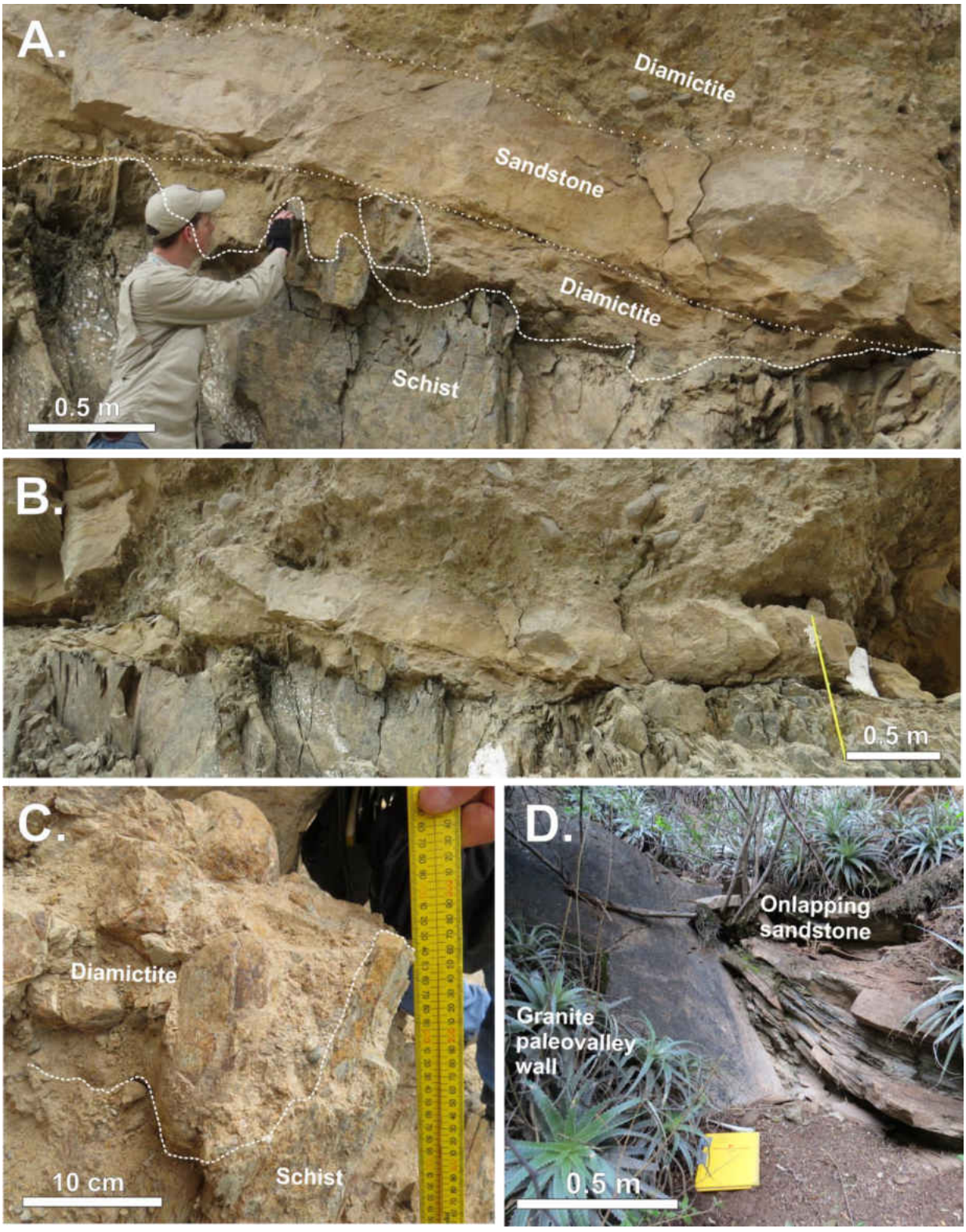

Figure 20. (A and B) The high-relief nonconformity between clast-rich sandy diamictite and schist basement at section OLTA1, which exhibits (C) thin slabs that protrude into the overlying diamictite, and (D) sandstones onlapping the steep (~65°), unstriated granite paleovalley wall.

Alluvial Fan Progradation

Filling of the valley began with alluvial fan progradation. In the central portion of the Olta paleovalley, wedges of sandy boulder conglomerate emanating from a paleotributary extend further down the main paleovalley (250+m) than the distance to bedrock on the opposite granite wall (<200 m) in this portion of the paleovalley. These conglomerate beds downlap onto and interfinger with lacustrine sandstones near the base of the outcrop, but the succession becomes exclusively conglomerate upward, suggesting coarse alluvial fans (and later, fan deltas) prograding transversely across the valley impounded drainage and initiated lake development (cf. Colombo et al., 2009). Lake sediments represented by high- and low-density turbidity deposits interfinger with fan conglomerates down-paleovalley, suggesting that a series of alluvial fans and associated impounded water bodies may have occurred throughout the paleovalley. Net and Limarino (1999) also noted the close association of alluvial fans and lacustrine deposits in the basal fill of the Olta paleovalley, which is consistent with interpretations for the initiation of lake development in the neighboring Malanzán paleovalley by Andreis et al. (1986), who assigned basal fanglomerates to Member 1 of the Malanzán Formation.

Socha et al. (2014) interpreted poorly-sorted, boulder-rich deposits in the Olta paleovalley as basal tillites, with the thick sequence of diamictite (sandy conglomerate, this study) in the central portion of the valley possibly representing a moraine. Socha et al. (2014) reported apparent clast fabric, uniform appearance, and the presence of stringers of sorted sediment in the matrix. In this study, these conglomerates are interpreted as non-glacial due to their: (1) wedge-shaped bed geometries that downlap onto and interfinger with sandstone of Facies D in their distal reaches and, where in more proximal positions, individual beds separated by fine-grained lacustrine sediments thicken, steepen, and merge into a thick succession of conglomerate at the mouth of a paleo-tributary; (2) lateral sorting, which contain abundant

boulders near the paleo-tributary that become rare distally; (3) predominantly sharp, non-erosive lower contacts and normally-graded upper contacts; (4) local clast lithologies; (5) absence of striations or facets on clast surfaces; and (6) lack of fine-grained matrix material between clasts. Clast fabrics and sand lenses within these deposits reported by Socha et al. (2014) are also common products of alluvial fans. These "sandstone stringers" may also represent laterally-traceable lacustrine sediments observed in this study. The lack of striations, polish, and fine-grained matrix material was hypothesized by Socha et al. (2014) to be due to the local glacial incorporation of highly weathered, coarse-grained granitic source material. While conglomerates in the westernmost Olta paleovalley contain abundant friable granitic clasts (Bracaccini, 1946; Socha et al., 2014), these deposits are stratigraphically, temporally, and paleoclimatically distinct (Solca Formation, latest Carboniferous-Permian; Net and Limarino, 1999; Gulbranson et al., 2010) from the Malanzán Fm., which predominantly contains clasts with low degrees of weathering (Andreis et al., 1986; this study).

Mass Transport into lake

These coarse-grained alluvial fans and fan deltas are here interpreted to have advanced episodically into the paleovalley during high-volume streamflow events and debris flows, as evidenced by steep fan slopes and rapid loading of lake sediments beneath conglomerates at distal portions of the fans. Large mass transport events from the valley wall into the lake include rockfalls, represented by boulder breccia chaotically stacked against a steep portions of the paleovalley wall containing a matrix of highly-deformed lake sediment, and clast-rich sandy diamictites overlying basement that exhibit clast-supported flow snouts, floating boulders, and associated graded-sandstone and conglomeratic beds of Facies D are indicative of subaqueous debris flows and linked high-density turbidity currents. Boulders contained within conglomeratic

wedges deform underlying beds of mudstone and sandstone in ruck-like structures that extrude upward on either side of boulders into the overlying conglomerate also suggest possible rock fall events. Some of these events may have been triggered by earthquake activity, as laterally-continuous zones up to 1.8 m thick of deformed lake sediment occur beneath comparatively thin beds of conglomerate displaying load structures in the eastern portion of the valley.

Socha et al., (2014) suggested that the folding of soft lake sediments was likely due to subglacial deformation, but several features of these beds and the overlying conglomeratic load structures are not consistent with a glacigenic interpretation, including: 1) a lack of glacial abrasion features on clasts in the overlying deposit or elsewhere in the paleovalley, 2) the absence of shear structures that dominate glacially-overridden soft sediment, 3) the symmetrical nature of the loading, which exhibited a repeating wavelength of a few meters between loads/flame structures along the length of the exposures, and 4) the prevalence of symmetrical folds with axes sub-parallel, and occasionally perpendicular, to presumed ice-flow direction. If not subglacially deformed, the formation of such large-scale folds requires intense liquefaction that, in the context of the relatively thin overlying conglomerate, did not occur solely through overloading. These laterally continuous, recurring horizons of folded sandstone and mudstone are separated by undeformed beds, show deformation intensities independent of load thickness, and occur in a basin that was tectonically active at the time of deposition (Andreis et al., 1986; Net and Limarino, 1999; Enkelmann et al., 2014). These features characterize deformation induced by possible seismic liquefaction (Moretti and van Loon, 2014). Other smaller, tightly-folded beds of sandstone and mudstone interpreted as glacial shove by Socha et al. (2014) occur on both sides of individual boulders and are thus interpreted here as ruck structures (Fig. 16A). Isolated stringers of sorted sediment within beds of tillite reported by Socha et al., (2014) are

deformed but laterally traceable and represent lacustrine sediments interfingering with wedges of alluvial fan conglomerate (Figs. 9B-C).

Lake Development

A lake-filling event is recorded in the eastern Olta paleovalley, approximately 3 km up-paleovalley from exposures of alluvial fan conglomerates impounding drainage. Incipient deposition by high-density turbidity currents is recorded by massive and graded beds of gravelly coarse-grained sandstones onlapping basement. Moving upwards stratigraphically, these beds thin through the basal portion of the section and become paired with horizontally-laminated, coarse- to medium-grained sandstones of Facies D deposited by low-density turbidity currents. Deposition by high-density turbidity currents is largely restricted to the basal portion of the section, as higher portions become dominated by cross-laminated fine-grained sandstones and eventually parallel-laminated, very fine-grained sandstone and siltstone. The fining-upwards eastern sections exhibit a transition from proximal to distal turbidites, which likely represents progressive deepening of the lake. The lake likely stayed fairly shallow through most of this early stage, as evidenced by wave activity indicated by the occurrence of symmetrical ripples throughout the middle portion of these eastern sections. Evidence of a deeper lake phase is recorded in the western Olta paleovalley, where distal underflows deposited very fine sandstone in a calm water setting dominated by laminated mudstones deposited from suspension settling. The lake was at least 40 m deep, as evidenced by the thickness of foreset beds in Gilbert-type deltas that do not preserve uppermost foreset or topset beds.

The outsized clasts that are present throughout the fine-grained members (2 and 3 of the Malanzán Fm, Andreis et al., 1986) have been the primary lines of evidence suggesting a glacial influence in the Malanzán Formation. While Buatois and Mángano (1995), Sterren and Martinez (1996), and Net and Limarino (1999) interpreted a glaciolacustrine depositional environment

based on these dropstones, none of these studies, which extensively characterized these deposits, reported signs of glacial abrasion on the clasts or surfaces in the valley, or direct glacial deposits such as tillites. Sterren and Martinez (1996) alluded to the presence of exotic dropstone lithologies, which were not recognized in this study or reported in other extensive investigations of the paleovalley. Andreis and Bossi (1981) and Andreis et al., (1986) reported a non-glacial climate based on the absence of these glacial features, cold and humid paleobotanical assemblages and fan types, and the wide distribution of outsized clasts throughout the formation from which they inferred evidence for seasonally-frozen lake surfaces. This study identified extensive evidence of mass transport off of the steep paleovalley walls into the lake, and high-gradient tributary streams that deposited coarse-grained material in distal portions of fan deltas. Deposition of this type during cold winter months would have occurred onto lake ice, and clasts could be subsequently rafted upon ice-breakup. Rockfall and bouncing clast off of walls within a narrow paleovalley would also produce dropstones and dropstone-like ruck structures.

While the fine-grained members of the Malanzán Fm. have traditionally been interpreted as exclusively lacustrine (Bracaccini, 1946; Andreis et al., 1986; Limarino and Césari, 1988; Buatois et al., 1994; Buatois and Mángano, 1995; Sterren and Martínez, 1996), they have recently been associated with the highstand of a postglacial marine transgression in the early Pennsylvanian (Limarino et al., 2002; 2006) from the identification of brackish water acritarchs (Gutiérrez and Limarino, 2001; Pérez Loinaze, 2009). These microfloras from the Malanzàan and Olta paleovalleys roughly correlate with those found in transgressive marine deposits of the Guandacol, Jejenes, and Lagares Formations in the western Paganzo basin (Net et al., 2002; Pazos, 2002; Kneller et al., 2004; Dykstra et al., 2006), although Pérez Loinaze (2009) noted "very scarce" marine elements and algal species. Net et al., (2002) identified a 45 meter interval

of marine influence based on the abundance of chlorite in clay mineral assemblages from middle portions of the Malanzán Formation, although these authors also attributed the occurrence of chlorite in non-marine, basal portions of the valley fill to abundant mica-schist and migmatite in the local basement. While no evidence directly supporting or contradicting this interpretation was identified in this study, the suggestion that the Olta paleovalley was at sea level in the mid-Carboniferous lies in contrast to previous ideas for its setting as a mountain valley located a considerable distance inland (Andreis et al., 1986; Buatois and Mángano, 1995).

Late stages of deposition within the Malanzán Formation exposed outside the study area record a shift from fluvio-deltaic (Member 4 of Andreis et al., 1986) to the braided-fluvial environments of the Loma Larga Formation. The valley continued to fill through the latest Carboniferous and early Permian as evidenced in the predominantly fluvial red-bed conglomerates and sandstones of the Solca, Arroyo Totoral, and La Colina Formations, which show increasing aridification into the Permian (Andreis et al., 1986; Net and Limarino, 1999; Gulbranson et al., 2010). Present day exhumation of the paleovalley is associated with the uplift of the surrounding ranges from flat-slab subduction that initiated in the Miocene (Enkelmann et al., 2014).

Implications for mid-Carboniferous ice volume in the eastern Paganzo basin

The lack of abundant temporal and geographic constraints on presumptive late Paleozoic glacial deposits in the eastern Paganzo basin, largely a product of limited exposures of late Paleozoic strata, precludes detailed reconstructions of possible surrounding ice centers, and this is evidenced by various interpretations of the scale and style of glaciation in the eastern Paganzo basin. Astini (2010) hypothesized the existence of a Mississippian elevated “ice cap-like glaciated plateau” in the eastern Paganzo basin, with valley glaciers then presumably eroding

into the peneplain as the ice cap receded. This hypothesis complicated by the occurrence of Serpukhovian floras in western Argentina that indicate warm-temperate conditions occurred between older Visean glaciation and younger Bashkirian glaciation (Balseiro et al, 2009; Limarino et al., 2014). A similar warm period is suggested by studies of fossil macrofloras in Peru, Bolivia and Brazil (Iannuzzi and Pfefferkorn, 2002; Grader et al., 2007). Such floras do not support hypotheses involving glacial conditions throughout the early Carboniferous. A similar interpretation proposed by Aquino et al. (2014) interpreted the Olta-Malanzán paleovalley as carved by an outlet glacier draining a hypothetical eastern ice sheet positioned over the eastern Paganzo basin and Sierras Pampeanas. Other authors have argued the surface of basement rocks surrounding the eastern Paganzo basin is not a preserved Gondwanan peneplain, but a product of Mesozoic and Cenezoic erosion, and therefore only preserves a late Paleozoic geomorphic expression where overlain by temporally equivalent strata (Carignano et al., 1999; Enkelmann et al., 2014). Although scenarios involving a stable ice cap or an outlet glacier draining an ice center situated to the east would explain the lack of alpine glacial geomorphic features observed in the Sierra de los Llanos and the immediately surrounding ranges, this study did not identify glacigenic deposits within the mid-Carboniferous strata or glacial abrasion features on late Paleozoic bedrock surfaces.

While the non-glacial interpretation for the Malanzán Formation near Olta presented in this study confines the extent of mid-Carboniferous ice in the Paganzo basin, additional temporal and spatial constraints on potential ice centers are needed in order to provide a more complete understanding of the drivers of glaciation in the region. Do other mid-Carboniferous paleovalleys within the eastern Paganzo basin, such as those to the south of the Sierra de Chepes (Sterren and Martinez, 1996) show a similar absence of diagnostic glacial features? Were uplands of the

Sierras Pampeanas along the margin of the eastern Paganzo basin also ice-free? If so, what specific drivers of glaciation in the western Paganzo basin did not affect eastern portions of the basin? The Sierra de los Llanos and surrounding ranges may not have been uplifted to the same extent as the Protoprecordillera, which was a major fold thrust belt, and therefore may not have attained the elevation necessary for glacier formation. It is also possible that the Protoprecordillera was a moisture barrier between inland areas and the Panthalassan Ocean, limiting the potential for tice accumulation in the eastern Paganzo basin. The identification of these underlying drivers may shed light on regional questions involving the diachronous nature of glacial deposits across central South America, including why similar paleolatitudes to the east, including the Sauce Grande, Chaco-Paraná, and Paraná basins, experienced glaciation into the Early Permian, far later than the Early Pennsylvanian deglaciation in the Rio Blanco, Callingasta-Uspallata, and western Paganzo basins (López-Gamundí, 1997; Henry et al., 2008; Rocha Campos et al., 2008; Limarino et al., 2014). However, data from this study suggests that the Olta-Malanzán valley was not of glacial origin, which in turn raises questions as to whether glaciers occurred in the eastern portions of the Paganzo Basin during the late Paleozoic Ice Age.

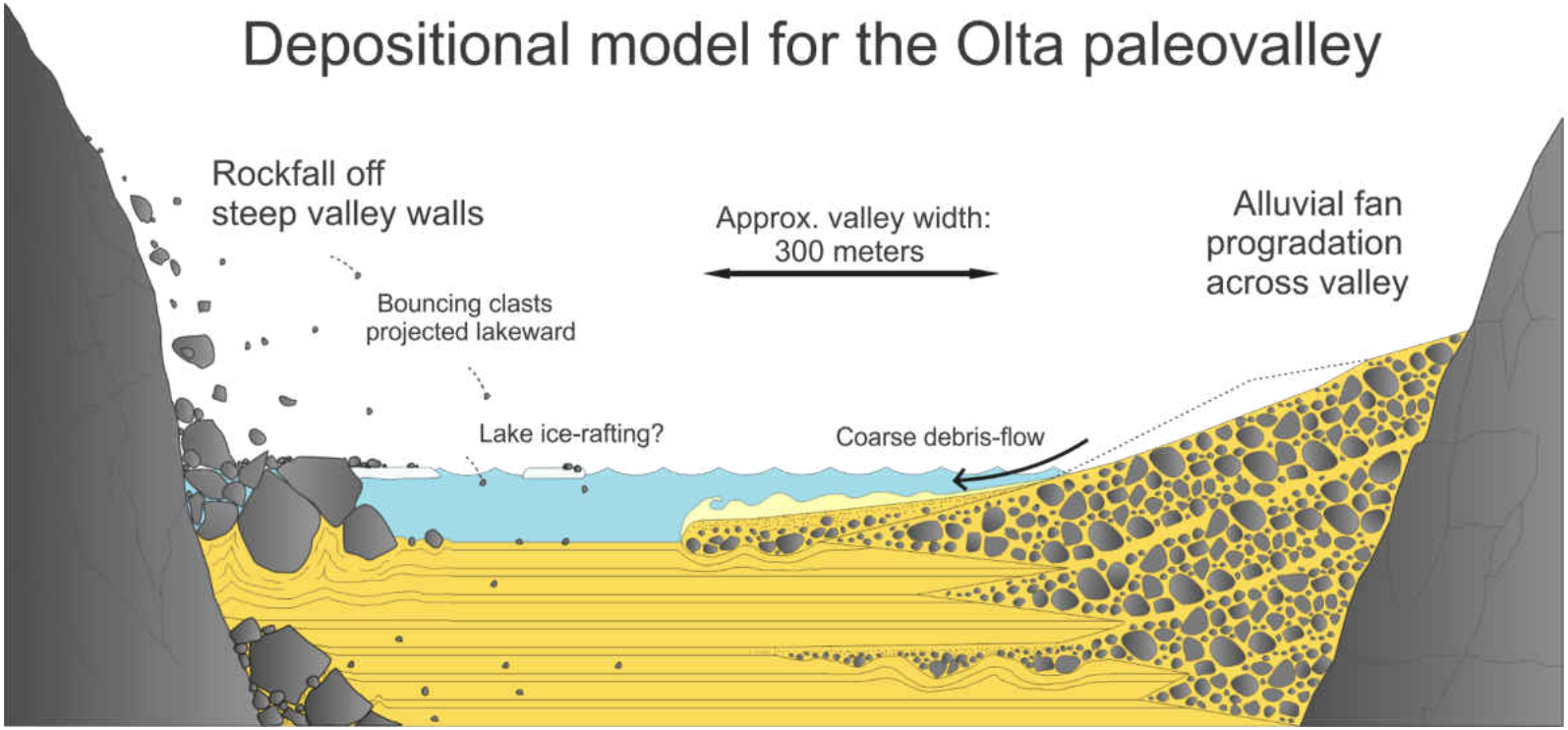

Figure 21. Model for deposition in the lower portion of the Malanzán Formation in the Olta paleovalley.

Conclusions

The sedimentology of the Malanzán Formation in the Olta paleovalley suggests non-glacial deposition in the mid-Carboniferous. Lake environments developed as drainage was impounded by the progradation of coarse-grained alluvial fans and fan deltas across a narrow mountain valley. A transgressive lacustrine event is recorded by a fining-upwards sequence from sandy turbidites to laminated mudstones in the eastern portion of the Olta paleovalley, while western portions record the later transition to fluvio-deltaic deposition. Rock avalanches and debris flows occurred off of the steep valley walls and fan deltas into the lake, deforming soft sediment. Some of these events were likely triggered by earthquakes, as evidence of liquefaction from large-scale folds in lake sediment suggesting that the area was seismically active. Outsized pebbles and cobbles within sandy lacustrine turbidites indicate rafting by lake ice, anchor ice, or vegetation, projection of clasts during rockfalls, or outrunner clasts carried by the turbidity currents. Bedrock surfaces also showed no evidence of glacial abrasion, and the geomorphology of the valley and surrounding ranges is not interpreted here as preserving a glacial signature.

The argument that glacial conditions existed in the eastern Paganzo basin during the mid-Carboniferous hinges almost exclusively on the interpretation of outsized clasts in fine-grained lacustrine sediments as glacial ice-rafted dropstones. This interpretation and the resulting implications for the presence of glacial ice is problematic in light of the many non-glacial mechanisms by which cobbles and pebbles can be transported to distal portions of a narrow mountain water body. Outsized clasts are thus not a reliable indicator of glacial transport without signs of abrasion or the presence of exotic lithologies, neither of which were identified in this study. Lake ice, specifically, seems a likely transport agent. While the lack of classical glacial abrasion features suggests a non-glacial climate for the paleovalley, conditions were cold during

the mid-Carboniferous, as evidenced by nearby glacial deposits in the western Paganzo basin. Sediment deposited on frozen lake surfaces by tributary streams and mass transport off of the valley walls during winter could be rafted in the spring. Rock fall is also a likely candidate for transport of debris including dropstones into lake waters.

This study reexamines many of the deposits mentioned in the only report of tillites and subglacial soft-sediment deformation (Socha et al., 2014) in the Malanzán Formation, which are reinterpreted here to be the product of debris flows and rock avalanches off of alluvial fans and valley walls into soft lake sediment. Diamictites and conglomerates in the paleovalley are commonly wedge-shaped, associated with slopes along the paleovalley wall or alluvial fans, and exhibited no facets, striations, or strong fabric. Heavily-deformed soft sediment is found closely associated with boulders within rockfall deposits and do not show evidence of being overridden by a valley glacier. Large-scale folded sandstones that were interpreted to be the product of several ice advances down the paleovalley show features more consistent with deformation from seismic activity.

The eastern Paganzo basin warrants further study not only because of the equivocal nature of its depositional history, but for its potential to elucidate the drivers of late Paleozoic glaciation, or in this case, the absence of glacial ice during a glacial interval. Additional investigations of coeval strata across the region are needed to make substantial conclusions about the nature of glaciation beyond the Olta-Malanzán paleovalley, but this work reinterprets the primary evidence necessitating the existence of mid-Carboniferous glacial ice in the eastern Paganzo basin, an interpretation with significant implications for reductions in our understanding of the volume and extent of late Paleozoic ice.

References

Alfaro, P., Gibert, L. Moretti, M., García-Tortosa, F.J., Sanz de Galdeano, C., Jesús Galindo-Zaldívar, J., López-Garrido, A.C., 2010. The significance of giant seismites in the Plio-Pleistocene Baza palaeo-lake (South Spain). Terra Nova 22, 172–179.

Andreis, R.R., Bossi, G.E., 1981. Algunos ciclos lacustres en la Formación Malanzán (Carbónico superior) en la región de Malanzán, sierra de Los Llanos, provincia de La Rioja [artículos de libros]. Publicado en: 8o. Congreso Geológico Argentino. San Luis. Actas 4, 639-655.

Andreis, R.R., Archangelsky, S., Leguizamón, R.R., 1986. El paleovalle de Malanzán: nuevos criterios para la estratigrafía del Neopaleozoico de la sierra de Los Llanos, La Rioja, República Argentina. Boletín de la Academia Nacional de Ciencias (Córdoba) 57, 1-119

Aquino, C.D., Milana, J.P., Faccini, U.F., 2014. New glacial evidences at the Talacasto paleofjord (Paganzo basin, W-Argentina) and its implications for the paleogeography of the Gondwana margin. Journal of South American Earth Sciences 56, 278-300.

Aquino, C.D., Buso, V.V., Faccini, U.F., Milana, J.P., Paim, P.S.G., 2016. Facies and depositional architecture according to a jet efflux model of a late Paleozoic tidewater grounding-line system from the Itararé Group (Paraná Basin), southern Brazil: Journal of South American Earth Sciences 67, 180-200.

Astini, R., 2010. Linked basins and sedimentary products across an accretionary margin: the case for the late history of the peri-Gondwanan Terra Australis orogen through the stratigraphic record of the Paganzo Basin. In: del Papa, C. & Astini, R. (Eds.), Field Excursion Guidebook, 18thInternational Sedimentological Congress, Mendoza, Argentina, FE-A1, pp. 1- 58.

Azcuy, C.A., 1975. Miosporas sel Namuriano y Westfaliano de la comarca de Malanzán-Loma Larga, provincial de La Rioja, Argentina. II. Descripciones sistemáticas y significado estratigráfico de las microfloras. Ameghiniana 12, 113-163.

Balseiro, D., Rustán, J. J., Ezpeleta, M., and Vaccari, N. E., 2009, A new Serpukhovian (Mississippian) fossil flora from western Argentina: Paleoclimatic, paleobiogeographic and stratigraphic implications: Palaeogeography, Palaeoclimatology, Palaeoecology 280, 517-531.

Barr, I., Spagnolo, M., 2015. Glacial cirques as palaeoenvironmental indicators: their potential and limitations. Earth-Science Reviews 151, 48-78.

Bates, C.C., 1953. Rational theory of delta formation. AAPG Bulletin, 37, 2119–2162.

Bennett, M.R., Doyle, P., Mather, A.E., Woodfin, J., 1994. Testing the climatic significance of dropstones: an example from the Miocene of the Sorbas Basin, south east Spain. Geol. Mag., 131, 845-848.

Blair, T.C., McPherson, J.G., 1994. Alluvial fans and their natural distinction from rivers based on morphology, hydraulic processes, sedimentary processes, and facies. Journal of Sedimentary Research A64: 451-190.

Blakey, R.C., 2008. Gondwana paleogeography from assembly to breakup—a 500m.y. odyssey. In: Fielding, C.R., Frank, T.D., Isbell, J.L. (Eds.), Resolving the Late Paleozoic Ice Age in Time and Space: Geological Society of America Special Paper 441, pp. 1–28.

Boulton, G.S., 1990, Sedimentary and sea level changes during glacial cycles and their control on glacimarine facies architecture, in Dowdeswell, J.A., Scourse, J.D., eds., Glaciomarine Environments: Processes and Sediments, v. 53. Geological Society of London, Special Publications, pp. 15-52

Bracaccini, I.O., 1948. Los Estratos de Paganzo y sus niveles plantiferos en la sierra de los Llanos (provincial de La Rioja). Revista de la Asociación Geológica Argentina 1, 19-61.

Brady, L.F., 1947. Invertebrate tracks from the Coconino sandstone of northern Arizona. Journal of Paleontology 21, 466-472.

Buatois, L.A., Mángano, M.G., 1994. Lithofacies and depositional processes from a Carboniferous lake, Sierra de Narvfiez, Northwest Argentina Sedimentary Geology 93, 25-49.

Buatois, L.A., Mángano, M.G., 1995. Post glacial lacustrine event sedimentation in an ancient mountain setting: Carboniferous Lake Malanzán (western Argentina). Journal of Paleolimnology 14, 1–22.

Buggisch, W., Wang, X., Alekseev, A.S., Joachimski, M.M., 2011. Carboniferous–Permian carbon isotope stratigraphy of successions from China (Yangtze platform), USA (Kansas) and Russia (Moscow Basin and Urals). Palaeogeography, Palaeoclimatology, Palaeoecology 301, 18–38.

Carto, S., Eyles, N., 2012. Sedimentology of the Neoproterozoic (c. 580 Ma) Squantum 'Tillite', Boston Basin USA: mass flow deposition in a non-glacial deep water arc basin. Sedimentary Geology 269, 1-14.

Caputo, M.V., Crowell, J.C., 1985. Migration of glacial centers across Gondwana during Paleozoic Era. Geological Society of America Bulletin 96, 1020–1036.

Caputo, M. V., de Melo, J. H. G., Streel, M., Isbell, J. L., 2008. Late Devonian and Early Carboniferous glacial records of South America, in Fielding, C. R., Frank, T. D., and Isbell, J. L., eds., Resolving the Late Paleozoic Ice Age in Time and Space: Boulder, CO, Geological Society of America Special Publication., p. 161-173.

Carignano, C., Cioccale, M., Rabassa, J., 1999. Landscape antiquity of the central-eastern Sierras Pampeanas (Argentina): Geomorphological evolution since Gondwanic times: Zeitschrift für Geomorphologie Neue Folge 118, 245–268.

Colella, A., De Boer, P.L., Nio, S.D., 1987. Sedimentology of a marine intermontane Pleistocene Gilbert-type fan-delta complex in the Crati Basin, Calabria, southern Italy. Sedimentology 34, 721-736.

Colombo, F., Limarino, C.O., Spalletti, L.A., Busquets, P., Cardó, R., Méndez-Bedia, I., Heredia, N., 2014. Late Palaeozoic lithostratigraphy of the Andean Precordillera revisited (San Juan Province, Argentina) Journal of Iberian Geology 40 (2), 241-259.

Corner, G.D., Nordahl, E., Munch-Ellingsen, K., Robertsen, K.R., 1990. Morphology and sedimentology of an emergent fjord-head Gilbert-type delta: Alta delta, Norway. In: Coarse-Grained Deltas (Ed. by A. Colella and D. B. Prior), Special Publication of the International Association of Sedimentologists 10: 155-168.

Costa, J.E., Schuster, R.L., 1988. The formation and failure of natural dams. Geological Society of America Bulletin 100, 1054–1068.

Crookshanks, S., Gilbert, R., 2008. Continuous, diurnally fluctuating turbidity currents in Kluane Lake, Yukon Territory. Canadian Journal of Earth Science 45, 1123–1138.

Crowell, J.C., Frakes, L.A., 1970. Phanerozoic glaciation and the causes of ice ages. American Journal of Science 268, 193–224.

Dadson, S., Hovius, N., Pegg, S., Dade, W.B., Horng, M.J., Chen, H., 2005. Hyperpycnal river flows from an active mountain belt. Journal of Geophysical Research 110, 04-16,

Dickins, J.M., 1997. Some problems of the Permian (Asselian) glaciation and the subsequent climate in the Permian. In: Martini, I.P. (Ed.), Late Glacial and Postglacial Environmental Changes: Quaternary, Carboniferous–Permian, and Proterozoic. U.K., Oxford University Press, Oxford, pp. 243–245.

Dionne, J.C., 1993. Sediment load of shore ice and ice rafting potential, Upper St. Lawrence Estuary, Quebec, Canada. Journal of Coastal Research 9, 628-646.

Doublet, S., Garcia, J.P., 2004. The significance of dropstones in tropical lacustrine setting, eastern Cameros Basin (Late Jurassic–Early Cretaceous, Spain). Sedimentary Geology 163, 293–309.

Dykstra, M., Kneller, B., Milana, J.P., 2006. Deglacial and postglacial sedimentary architecture in a deeply incised paleovalley–paleofjord — the Pennsylvanian (late Carboniferous) Jejenes Formation, San Juan, Argentina. Geological Society of America Bulletin 118, 913–937.

Dykstra, M., Kneller, B., Milana, J.P., 2007. A high-resolution record of deep-water processes in a confined paleofjord, quebrada de Las Lajas, Argentina. In: Nilsen, T.H., Shew, R.D., Steffens, G.S., Studlick, J.R.J. (Eds.), Atlas of Deep-Water Outcrops: AAPG Studies in Geology 56, CD-ROM, 19 p.

Emery, K.O., 1955. Transportation of rocks by driftwood. Journal of Sedimentary Petrology 25, 51-57.

Emery, K.O., 1965. Organic transportation of marine sediments. In: M.N. Hill (Editor), The Sea. Wiley, New York, pp. 776 793.

Enkelmann, E., Ridgway, K.D., Carignano, C., Linnemann, U., 2014. A thermochronometric view into an ancient landscape: tectonic setting, development, and inversion of the Paleozoic eastern Paganzo basin, Argentina. Lithosphere 6, 93-107.

Eyles, N., and Clark, B.M., 1986, Significance of hummocky and swaley cross-stratification in late Pleistocene lacustrine sediments of the Ontario Basin, Canada: Geology 14 (8), 679-682.

Eyles, N., Clark, B.M., Clague, J.J., 1987. Coarse grained sediment gravity flow facies in a large supraglacial lake. Sedimentology 34, 193–216.

Eyles, N., 1993. Earth's glacial record and its tectonic setting. Earth-Science Reviews 35, 1–248.

Falk, P., Dorsey, R.J., 1998. Rapid development of gravelly high-density turbidity currents in marine Gilbert-type fan deltas, Loreto basin, Baja California Sur, Mexico. Sedimentology 45, 331-349.

Fielding, C.R., Frank, T.D., Birgenheier, L.P., Rygel, M.C., Jones, A.T., Roberts, J., 2008a. Stratigraphic imprint of the Late Paleozoic Ice Age in eastern Australia: a record of alternating glacial and nonglacial climate regime. Journal of the Geological Society of London 165, 129–140.

Fielding, C.R., Frank, T.D., Isbell, J.L., 2008b. The late Paleozoic ice age — a review of current understanding and synthesis of global climate patterns. In: Fielding, C.R.,Frank, T.D., Isbell, J.L. (Eds.), Resolving the Late Paleozoic Ice Age in Time and Space: Geological Society of America Special Paper 441, 343–354.

Fielding, C.R., Frank, T.D., Birgenheier, L.P., Rygel, M.C., Jones, A.T., Roberts, J., 2008c. Stratigraphic record and facies associations of the late Paleozoic ice age in Eastern Australia (New South Wales and Queensland). In: Fielding, C.R., Frank, T.D., Isbell, J.L. (Eds.), Resolving the Late Paleozoic Ice Age in Time and Space: Geological Society of America Special Paper 441, 41–57.

Frakes, L.A., Francis, J.E., 1988. A guide to Phanerozoic cold polar climates from highlatitude ice-rafting in the Cretaceous. Nature 333, 547–549.

Frakes, L.A., Francis, J.E., Syktus, J.I., 1992. Climate Modes of the Phanerozoic. Cambridge University Press, Cambridge. 274 p.

Frank, T. D., Shultis, A. I., Fielding, C. R., 2015, Acme and demise of the late Palaeozoic ice age: A view from the southeastern margin of Gondwana: Palaeogeography Palaeoclimatology Palaeoecology 418, 176-192.

Gastaldo, R., DiMichele, W., Pfefferkorn, H., 1996. Out of the icehouse into the greenhouse: a late Paleozoic analogue for modern global vegetational change. GSA Today 10, 1–7.

Gilbert, R., 1990. Rafting in glacimarine environments. In: J.A. Dowdeswell and J.D. Scourse (Editors), Glacimarine Environments: Processes and Sediments. Geological Society London Special Publications 53, 105-120.

Gilbert, G.K., 1885, The topographic features of lake shores: U. S. Geological Survey Annual Report 5, 69–123.

Girardclos, S., Schmidt, O.T., Sturm, M., Ariztegui, D., Pugin, A., Anselmetti, F.S., 2007. The 1996 AD delta collapse and large turbidite in Lake Brienz. Marine Geology 241, 137-154.

Godt, J.W., Coe, J.A., 2007. Alpine debris flows triggered by a 28 July 1999 thunderstorm in the central Front Range, Colorado. Geomorphology 84, 80–97.

Grader, G.W., Díaz-Martínez, E., Davydov, V., Montañez, I., Tait, J., Isaacson, P., 2007. Late Paleozoic stratigraphic framework in Bolivia: constraints from the warm water Cuevo Megasequence. In: Díaz-Martínez, E., Rábano, I. (Eds.), 4th European Meeting on the Palaeontology and Stratigraphy of Latin America: Cuadernos del Museo Geominero 8, 181–188.

Gulbranson, E.L., Montañez, I.P., Schmitz, M.D., Limarino, C.O., Isbell, J.L., Marenssi, S.A., Crowley, J.L., 2010. High-precision U–Pb calibration of Carboniferous glaciation and climate history, Paganzo Group, NW Argentina. GSA Bulletin 122, 1480–1498.

Gutiérrez, P.R., Limarino, C.O., 2001. Palinología de la Formación Malanzán (Carbonifero Superior), La Rioja, Argentina: Nuevos datos y consideraciones paleoambientales. Ameghiniana 38, 99–118.

Hambrey, M.J., Glasser, N.F., 2012. Discriminating glacier thermal and dynamic regimes in the sedimentary record. Sedimentary Geology 251–252, 1–33.

Harvey, A.M., 1990. Factors influencing Quaternary alluvial fan development in southeast Spain. In: Rachocki, A.H. & Church, M. (eds) Alluvial Fans: A Field Approach. Wiley, Chichester, 247-269.

Heckel, P.H., 2008. Pennsylvanian cyclothems in midcontinent North America as far-field effects of waxing and waning of Gondwana ice sheets. In: Fielding, C.R., Frank, T., Isbell, J.L. (Eds.), Resolving the Late Paleozoic Ice Age in Time and Space: Geological Society of America Special Paper 441, 275–289.

Henry, L.C., Isbell, J.L., Limarino, C.O., 2008. Carboniferous glacigenic deposits of the Protoprecordillera of west central Argentina. In: Fielding, C.R., Frank, T.D., Isbell, J.L. (Eds.), Resolving the Late Paleozoic Ice Age in Time and Space: Geological Society of America Special Paper, 441, pp. 131–142.

Henry, L.C., Isbell, J.L., Limarino, C.O., McHenry, L.J., Fraiser, M.L., 2010. Mid-Carboniferous deglaciation of the Protoprecordillera, Argentina recorded in the Agua de Jagüel palaeovalley. Palaeogeography, Palaeoclimatology, Palaeoecology 298, 112–129.

Henry, L.C., Isbell, J.L., Fielding, C.R., Domack, E.W., Frank, T.D., Fraiser, M.L., 2012. Proglacial deposition and deformation in the Pennsylvanian to Lower Permian Wynyard Formation, Tasmania: a process analysis. Palaeogeography, Palaeoclimatology, Palaeoecology 315- 316, 142-157.

Holz, M., Souza, P.A., Iannuzzi, R., 2008. In: Fielding, C.R., Frank, T.D., Isbell, J.L. (Eds.), Sequence stratigraphy and biostratigraphy of the Late Carboniferous to Early Permian glacial succession (Itararé Subgroup) at the eastern-southeastern margin of the Paraná Basin, Brazil: Geological Society of America Special Paper 441, 115–129.

Horton, D.E., Poulsen, C.J., Pollard, D., 2007. Orbital and CO2 forcing of late Paleozoic continental ice sheets. Geophys. Res. Lett. 34, 1–6.

Horton, D.E., and Poulsen, C.J., 2009. Paradox of late Paleozoic glacioeustacy: Geology, v. 37, no. 8, p. 715-718.

Horton, D.E., Poulsen, C.J., Pollard, D., 2010. Influence of high-latitude vegetation feedbacks on late Paleozoic glacial cycles. Nat. Geosci. 3, 572–577.

Holmes, A., 1965. Principles of Physical Geology. Thomas Nelson & Sons Ltd. London. 1288 pp.

Horton, D.E., Poulsen, C.J., Montañez, I.P., DiMichele, W.A., 2012. Eccentricity-paced late Paleozoic climate change. Palaeogeography, Palaeoclimatology, Palaeoecology 331-332, 150–161.

Hsu, J.P.C., Capart, H., 2008. Onset and Growth of Tributary Dammed Lakes. Water Resource Research 44 (11), 6.

Hutchinson, G.E., 1957. A Treatise on Limnology. Vol. I. Geography, Physics and Chemistry. John Wiley & Sons, New York.

Hyde, W.T., Crowley, T.J., Tarasov, L., Paltier, W.R., 1999. The Pangean ice age: studies with a coupled climate-ice sheet model. Climate Dynamics 15, 619–629.

Iannuzzi, R., Pfefferkorn, H. W., 2002. A Pre-Glacial, Warm-Temperate Floral Belt in Gondwana (Late Visean, Early Carboniferous): PALAIOS 17, 571-590.

Isbell, J.L., Miller, M.F., Wolfe, K.L., Lenaker, P.A., 2003. Timing of late Paleozoic glaciation in Gondwana: was glaciation responsible for the development of northern hemisphere cyclothems? In: Chan, M.A., Archer, A.W. (Eds.), Extreme depositional environments: mega end members in geologic time: Geological Society of America Special Paper 370, 5–24.

Isbell, J.L., Fraiser, M.L., Henry, L.C., 2008a. Examining the complexity of environmental change during the late Paleozoic and early Mesozoic. Palaios 23, 267–269.

Isbell, J.L., Cole, D.I., Catunaenu, O., 2008b. Carboniferous–Permian glaciation in the main Karoo Basin, South Africa: stratigraphy, depositional controls, and glacial dynamics. In: Fielding, C.R., Frank, T.D., Isbell, J.L. (Eds.), Resolving the late Paleozoic ice age in time and space: Geological Society of America Special Paper 441, 71–82.

Isbell, J.L., Henry, L.C., Gulbranson, E.L., Limarino, C.O., Fraiser, M.L., Koch, Z.J., Ciccioli, P.L., Dineen, A.A., 2012. Glacial paradoxes during the late Paleozoic ice age: evaluating the equilibrium line altitude as a control on glaciation. Gondwana Research 22, 1–19.

Isbell, J.L., Biakov, A.S., Vedernikov, I.L., Davydov, V.I., Gulbranson, E.L., Fedorchuk, N.D., 2016. Permian diamictites in northeastern Asia: Their significance concerning the bipolarity of the late Paleozoic ice age. Earth-Science Reviews 154, 279-300.

Kempema, E.W., Reimnitz, E., Barnes, P.W., 2001. Anchor-ice formation and ice rafting in southwestern Lake Michigan, U.S.A. Journal of Sedimentary Research 71, 346–354.

Kneller, B., Milana, J.P., Buckee, C., Al Ja'aidi, O.S., 2004. A depositional record of deglaciation in a paleofjord (Late Carboniferous [Pennsylvanian] of San Juan Province, Argentina): the role of catastrophic sedimentation. Geological Society of America Bulletin 116, 348–367.

Lambert, A., Hsu, K.J., 1979. Non-annual cycles of varve-like sedimentation in Walensee, Switzerland. Sedimentology 26, 453–461.

Lambert, A., Giovanoli, F., 1988. Records of riverborne turbidity currents and indications of slope failures in the Rhone Delta of Lake Geneva. Limnology and Oceanography 33, 458–468.

Limarino, C.O., Gutiérrez, P., Cesari, S.N., 1984. Facies lacustre de la Formaci6n Agua Colorada (Paleozoico superior): aspectos sedimentologicos y contenido paleofloristico. Actos IX Congreso Geológico Argentino 5, 324-341.

Limarino, C.O., Césari, S.N., Net, L.I., Marenssi, S.A., Gutiérrez, P.R., Tripaldi, A., 2002. The Upper Carboniferous postglacial transgression in the Paganzo and Río Blanco Basins (northwestern Argentina): facies and stratigraphic significance. Journal of South American Earth Sciences 15, 445–460.

Limarino, C.O., Spalletti, L.A., 2006. Paleogeography of the Upper Paleozoic basins of southern South America: an overview. Journal of South American Earth Sciences 22, 134–155.

Limarino, C.O., Tripaldi, A., Marenssi, S., Fauqué, L., 2006. Tectonic, sea level, and climatic controls on late Paleozoic sedimentation in the western basins of Argentina. Journal of South American Earth Sciences 33, 205–226.

Limarino, C.O., Cesari, S.N., Spalletti, L.A., Taboada, A.C., Isbell, J.L., Geuna, S., Gulbranson, E.L., 2014. A paleoclimatic review of southern South America during the late Paleozoic: a record from icehouse to extreme greenhouse conditions. Gondwana Research 25, 1396-1421.

López-Gamundí, O.R., Espejo, I.S., Conaghan, P.J., Powell, C.McA., Veevers, J.J., 1994. Southern South America. In: Veevers, J.J., Powell, C.McA. (Eds.), Permian–Triassic Pangean basins and foldbelts along the Panthalassan margin of Gondwanaland. Boulder, Colorado: Geological Society of America Memoir 184, 281–329.

López-Gamundí, O.R., 1997. Glacial–postglacial transition in the late Paleozoic basins of Southern South America. In: Martini, I.P. (Ed.), Late Glacial and Postglacial Environmental Changes: Quaternary Carboniferous–Permian, and Proterozoic. Oxford University Press, Oxford U.K., pp. 147–168.

López-Gamundí, O.R., Martínez, M., 2000. Evidence of glacial abrasion in the Calingasta–Uspallata and western Paganzo Basins, mid-Carboniferous of western Argentina. Palaeogeography, Palaeoclimatology, Palaeoecology 159, 145–165.

López-Gamundí, O.R., Sterren, A.F., Cisterna, G.A., 2016. Inter- and Intratill Boulder Pavements in the Carboniferous Hoyada Verde Forma-tion of West Argentina: An insight on glacial advance/retreat fluctuations in South-western Gondwana. Palaeogeography, Palaeoclimatology, Palaeoecology 447, 29-41.

McCarroll D, Rijsdijk KF. 2003. Deformation styles as a key for interpreting glacial depositional environments. Journal of Quaternary Science 18, 473–489.

Metcalfe, I., Crowley, J. L., Nicoll, R. S., and Schmitz, M., 2015. High-precision U-Pb CA-TIMS calibration of Middle Permian to Lower Triassic sequences, mass extinction and extreme climate-change in eastern Australian Gondwana: Gondwana Research 28, 61-81.

Montañez, I., Soreghan, G.S., 2006. Earth's fickle climate. Geotimes 51, 24–27.

Montañez, I.P., Tabor, N.J., Niemeier, D., DiMichele, W.A., Frank, T.D., Fielding, C.R., Isbell, J.L., Birgenheier, L.P., Rygel, M.C., 2007. CO2-forced climate and vegetative instability during late Paleozoic deglaciation. Science 315, 87–91.

Montañez, I.P., Poulsen, C.J., 2013. The late Paleozoic ice age: an evolving paradigm. Annu. Rev. Earth Planet. Sci. 41, 24.1–24.28.

Moretti, M., Pieri, P., Tropeano M., 2002. Late Pleistocene soft-sediment deformation structures interpreted as seismites in paralic deposits in the City of Bari (Apulian foreland, southern Italy) Geological Society of America Special Paper 359, 75–85.

Moretti, M, Sabato, L., 2007. Recognition of trigger mechanisms for soft-sediment deformation in the Pleistocene lacustrine deposits of the Sant'Arcangelo Basin (Southern Italy): seismic shock vs. overloading. Sedimentary Geology 196, 31–45.

Moretti, M., Van Loon, A.J., 2014. Restrictions to the application of 'diagnostic' criteria for recognizing ancient seismites. Journal of Palaeogeography 3, 162–173.

Mulder, T., Alexander, J., 2001. The physical character of subaqueous sedimentary density flows and their deposits. Sedimentology 48, 269–299.

Myrow, P.M., Fischer, W., Goodge, J.W., 2002, Wave-modified turbidites: combined-flow shoreline and shelf deposits, Cambrian, Central Transantarctic Mountains: Journal of Sedimentary Research 72, 641-656.

Nemec, W., Steel, R.J., 1988. What is a fan delta and how do we recognize it? In: Nemec, W. and Steel, R.J. (eds.), Fan Deltas: Sedimentology and Tectonic Settings. Blackie, Glasgow and London, p. 2–13

Net, L.I., Limarino, C.O., 1999. Paleogeografía y correlación estratigrá fi ca del Paleozoico Tardío de la Sierra de Los Llanos, Provincia de la Rioja, Argentina. Revista de la Asociación Geológica Argentina 54, 229-239.

Net, L.I., Alonso, M.S., Limarino, C.O., 2002. Source rock and environmental control on clay mineral associations, lower section of Paganzo group (Carboniferous), northwest Argentina. Sedimentary Geology 152, 183–199.

Net, L.I., Limarino, C.O., 2006. Applying sandstone petrofacies to unravel the Upper Carboniferous evolution of the Paganzo Basin, northwest Argentina. Journal of South American Earth Sciences 22, 239–254.

Netto, R.G., Balistieri, P.R.M.N., Lavina, E.L.C., Silveira, D.M., 2009. Ichnological signatures of shallow freshwater lakes in the glacial Itarare Group (Mafra Formation, Upper Carboniferous-Lower Permian of Parana Basin, S Brazil). Palaeogeography, Palaeoclimatology, Palaeoecology 272, 240-255.

Newton, R.S., 1968. Internal structure of wave-formed ripple marks in the nearshore zone. Sedimentology 11, 275-292.

Nilsen, T.H., 1982. Alluvial fan deposits. In: Scholle P, Spearing D (eds.) Sandstone depositional environments. American Association of Petroleum Geologists Memoir 31, 49-86.

Pazos, P.J., 2002. The Late Carboniferous glacial to postglacial transition: facies and sequence stratigraphy, western Paganzo Basin, Argentina. Gondwana Research 5, 467–487.

Pérez Loinaze, V.P., 2009. New palynological data from the Malanzán Formation (Carboniferous), La Rioja Province, Argentina. Ameghiniana, 46: 495–512.

Pérez Loinaze, V.S., Limarino, C.O., Césari, S.N., 2010. Glacial events in Carboniferous sequences from Paganzo and Río Blanco Basins (Northwest Argentina): palynology and depositional setting. Geologica Acta 8, 399–418.

Postma, G., Nemec, W., Kleinspehn, K.L., 1988. Large floating clasts in turbidites: a mechanism for their emplacement. Sedimentary Geology 58, 47-61.

Prior, D.B., Bornhold, B.D., 1988. Submarine morphology and processes of fjord fan deltas and related high-gradient systems: modern examples from Britich Colombia. In: Fan Deltas: Sedimentology and Tectonic Settings (Ed. by W. Nemec and R. J. Steel), pp. 126–143. Blackie and Son, Ltd. Glasgow.

Ramos, V., Jordan, T., Allmendinger, R., Kay, S., Cortés, J., Palma, M., 1984. Chilenia: un terreno alóctono en la evolución paleozoica de los Andes Centrales. 10° Congr. Geol. Argentino, Actas 2, 84-106.

Ramos, V., Jordan, T., Allmendinger, R., Mpodozis, C., Kay, S., Cortés, J., Palma, M., 1986. Paleozoic terranes of the central Argentine-Chilean Andes. Tectonics, v. 5, 855-888.

Ramos, V.A., 1988. Tectonics of the Late Proterozoic–Early Paleozoic: a collisional history of Southern South America. Episodes 11, 168–174.

Rocha Campos, A. C., dos Santos, P. R., and Canuto, J. R., 2008, Late Paleozoic glacial deposits of Brasil: Paraná Basin, in Fielding, C. R., Frank, T. D., and Isbell, J. L., eds., Resolving the late Paleozoic Ice Age in time and space, Geological Society of America Special Paper 441, p. 97-114.

Rygel, M.C., Fielding, C.R., Frank, T.D., and Birgenheier, L.P., 2008, The magnitude of late Paleozoic glacioeustatic fluctuations: A synthesis: Journal of Sedimentary Research, v. 78, p. 500–511.

Sass, O., Krautblatter, M., Morche, D., 2007. Rapid lake infill following bergsturz events revealed by GPR measurements (Reintal, German Alps). The Holocene 17 (7), 965-976.

Schatz, E.R., Mángano, M.G., Buatois, L.A., and Limarino, C.O., 2011. Life in the late Paleozoic ice age: trace fossils from glacially influenced deposits in a late Carboniferous fjord of western Argentina. Journal of Paleontology 85, 502-518.

Šilhán, K., Pánek, T., 2010.Fossil and recent debrisflows in medium-high mountains (Moravskoslezské Beskydy Mts, Czech Republic). Geomorphology 124, 238–249.

Socha, B.J., Carignano, C., Rabassa, J., and Mickelson, D.M., 2006, Sedimentological record of Carboniferous mountain glaciation in an exhumed paleovalley, eastern Paganzo Basin, La Rioja Province: Geological Society of America Abstracts with Programs 38 (7), 62.

Socha, B.J., Carignano, C., Rabassa, J., Mickelson, D.M., 2014. Gondwana glacial paleolandscape, diamictite record of Carboniferous valley glaciation, and preglacial remnants of an ancient weathering front in northwestern Argentina. In: Rabassa, J., Ollier, C. (Eds.), Gondwana landscapes in southern South America. Springer, Dordrecht, pp. 331–363.

Sohn, Y.K., 2000. Depositional processes of submarine debris flows in the Miocene fan deltas, Pohang Basin, SE Korea with special reference to flow transformation. Journal of Sedimentary Research 70, 491–503.

Soreghan, G.S., 2004, Déjá-vu all over again: Deep-time (climate) is here to stay: Palaios 19, 1-2.

Spearing, D.A., 1974. Alluvial fan deposits. Geological Society of America Summary Sheets of Sedimentary Deposits, sheet 1.

Stanley, K.O., Surdam, R.C., 1978. Sedimentation on the front of Eocene Gilbert-type deltas, Washakie Basin, Wyoming. Journal of Sedimentary Petrology 48: 557-573.

Sterren, A.F., Martínez, M., 1996. El paleovalle de Olta (Carbonífero): paleoambientes y paleogeografía. 13º Congreso Geológico Argentino y 3º Congreso Exploración de Hidrocarburos (Buenos Aires), Actas 2, 89-103.

Syvitski, J.M., Burrell, D.C., Skei, J.M., 1987. Fjords: processes and products, New York, Springer-Verlag, 379 p.

Suwa, H., Okuda, S., Ogawa, K., 1984. Size segregation of solid particles in debris flows; part 1, accumulation of large boulders at the flow front and inverse grading by the kinetic sieving effect. Kyoto Daigaku Bosai Kenkyujo Nenpo, Disaster Prevention Research Institute Annuals 27B-1, pp. 409–423.

Tabor, N.J., Poulsen, C.J., 2008. Late Paleozoic tropical climate and atmospheric circulation: a review of paleoclimate indicators and models. Palaeogeogr. Palaeoclimatol. Palaeoecol. 268:181–92

Talling, P.J., Masson, D.G., Sumner, E.J., Malgesini, G., 2012. Subaqueous sediment density flows: Depositional processes and deposit types, Sedimentology 59, 1937–2003.

Talling, P.J., 2014. On the triggers, resulting flow types and frequencies of subaqueous sediment density flows in different settings. Marine Geology 352, 155–182.

Tanner, W.F., 1967. Ripple mark indices and their uses. Sedimentology 9, 89-104.

Thomas, G.S.P., Connell, R.J., 1985, Iceberg drop, dump, and grounding structures from Pleistocene glacio-lacustrine sediments, Scotland. Journal of Sedimentary Petrology 55 (2), 243-249.

Ufimtsev, G.F., Skovitinia, T.M., Kulchitsky, A.A., 1998. Rockfall-dammed lakes in the Baikal region: Evidence from the past and prospects for the future, Natural Hazards 18, 167–183,

Üner, S., 2014, Seismogenic structures in Quaternary lacustrine deposits of Lake Van (eastern Turkey), Geologos 20 (2), 79-87.

Van Steijn, H., 1996. Debris-flow magnitude—frequency relationships for mountainous regions of Central and Northwest Europe. Geomorphology 15, 259–273

Veevers, J.J., Powell, M., 1987. Late Paleozoic glacial episodes in Gondwanaland reflected in transgressive–regressive depositional sequences in Euramerica. Geological Society of America Bulletin 98, 475–487.

Vesely, F.F., Assine, M.L., 2006. Deglaciation sequences in the Permo-Carboniferous Itarare Group, Paraná Basin, southern Brazil: Journal of South American Earth Sciences 22, (3-4), 156-168.

Vesely, F.F., Rostirolla, S.P., Appi, C.J., Kraft, R.P., 2007, Late Paleozoic glacially related sandstone reservoirs in the Paraná Basin, Brazil: American Association of Petroleum Geologists Bulletin 91 (2), 151-160.

Vesely, F., Assine, M.L., 2014. Ice-keel scour marks in the geologic record: evidence from Carboniferous soft-sediment striated surfaces in the Paraná Basin, southern Brazil: Journal of Sedimentary Research 84, 26-39.

Vesely, F., Trzaskos, B., Kipper, F., Assine, M.L., Souza, P.A., 2015. Sedimentary record of a fluctuating ice margin from the Pennsylvanian of western Gondwana: Paraná Basin, southern Brazil: Sedimentary Geology 326, 45-63.

Visser, J.N.J., 1983. The problems of recognizing ancient sub- aqueous debris flow deposits in glacial sequences: Transactions of the Geological Society of South Africa 86, 127-135.

Wayne, W.J., 1999, The Alemania rockfall dam: a record of a mid-Holocene earthquake and catastrophic flood in northwestern Argentina, Geomorphology 27, 296-306.

Woodborne, M.W., Rogers, J., Jarman, N., 1989. The geological significance of kelp-rafted rock along the West Coast of South Africa. Geo-Marine Letters 9, 109-118.

Ziegler, A.M., Hulver, M.L., Rowley, D.B., 1997. Permian World topography and climate. In: Martini, I.P. (Ed.), Late Glacial and Postglacial Environmental Changes: Quaternary Carboniferous–Permian, and Proterozoic. Oxford University Press, Oxford, U.K., pp. 111–146.

Appendix

Malanzán Formation

Stratigraphic Columns

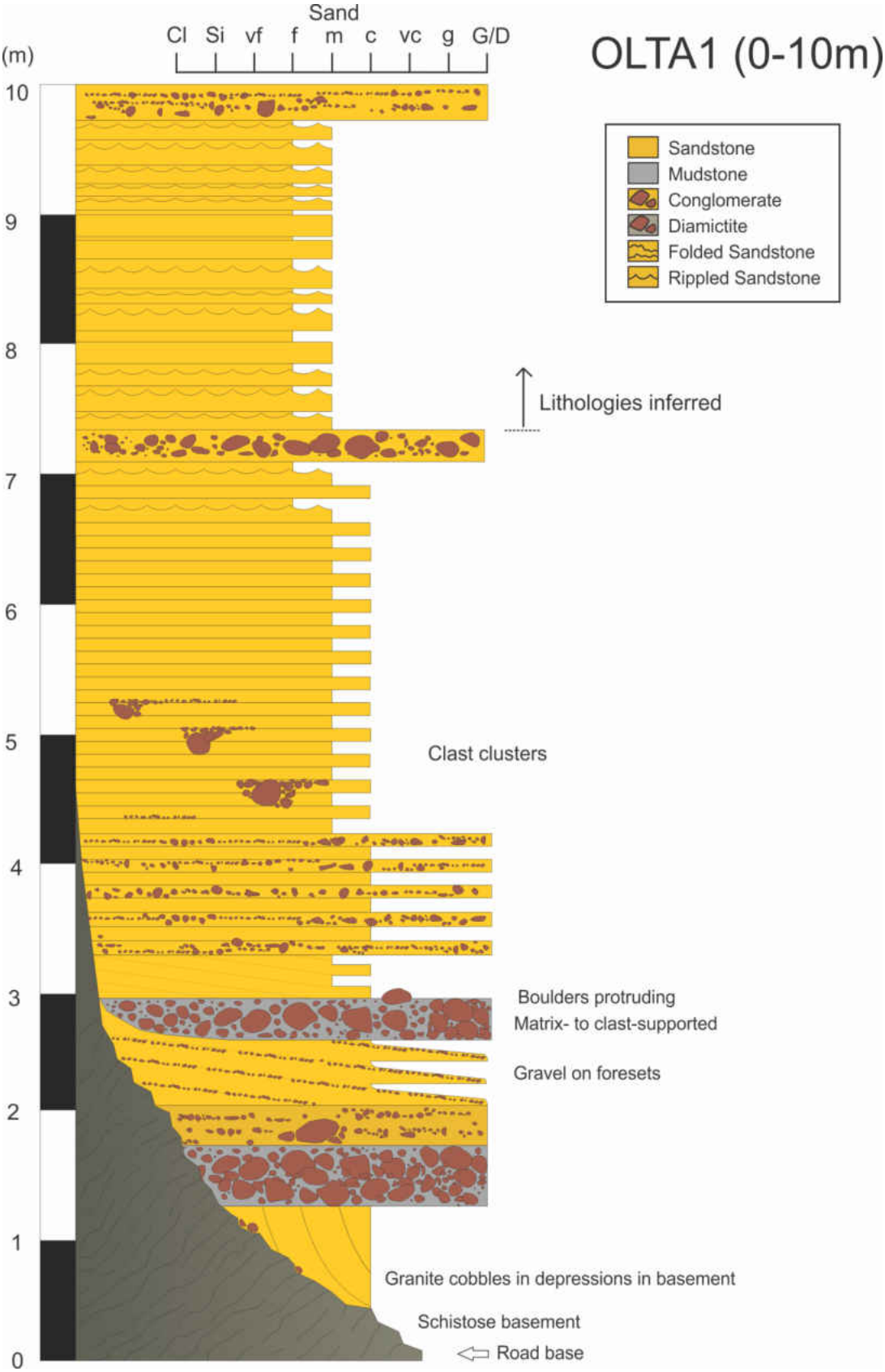
OLTA1 (0-10m)
Sand
Cl Si vf f m c vc g G/D
(m)
10
9
8
7
6
5
4
3
2
1
0
Sandstone
Mudstone
Conglomerate
Diamictite
Folded Sandstone
Rippled Sandstone
Lithologies inferred
Clast clusters
Boulders protruding
Matrix- to clast-supported
Gravel on foresets
Granite cobbles in depressions in basement
Schistose basement
Road base

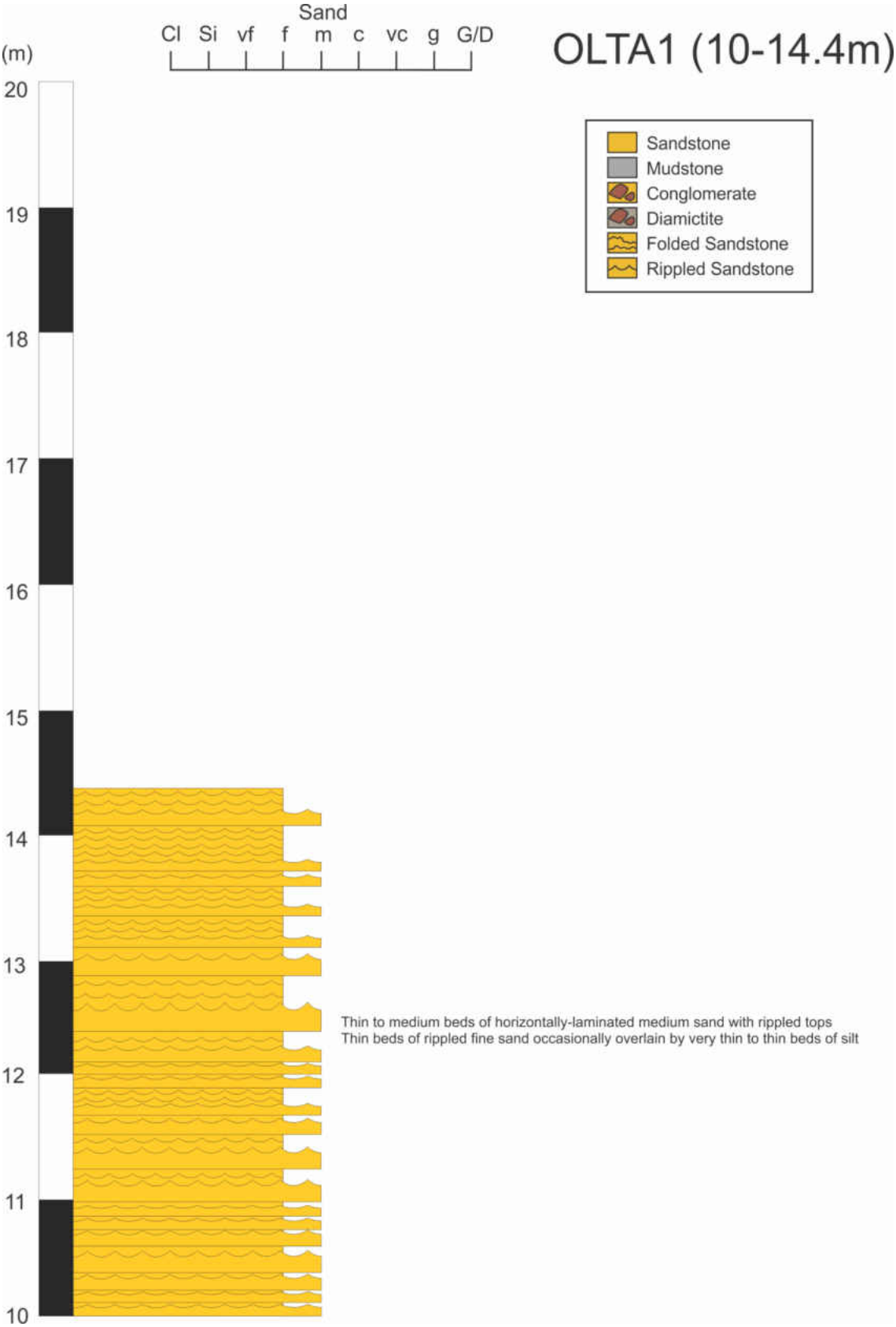
Sand
Cl Si vf f m c vc g G/D
(m)
OLTA1 (10-14.4m)
20
19
18
17
16
15
14
13
12
11
10
Sandstone
Mudstone
Conglomerate
Diamictite
Folded Sandstone
Rippled Sandstone
Thin to medium beds of horizontally-laminated medium sand with rippled tops
Thin beds of rippled fine sand occasionally overlain by very thin to thin beds of silt

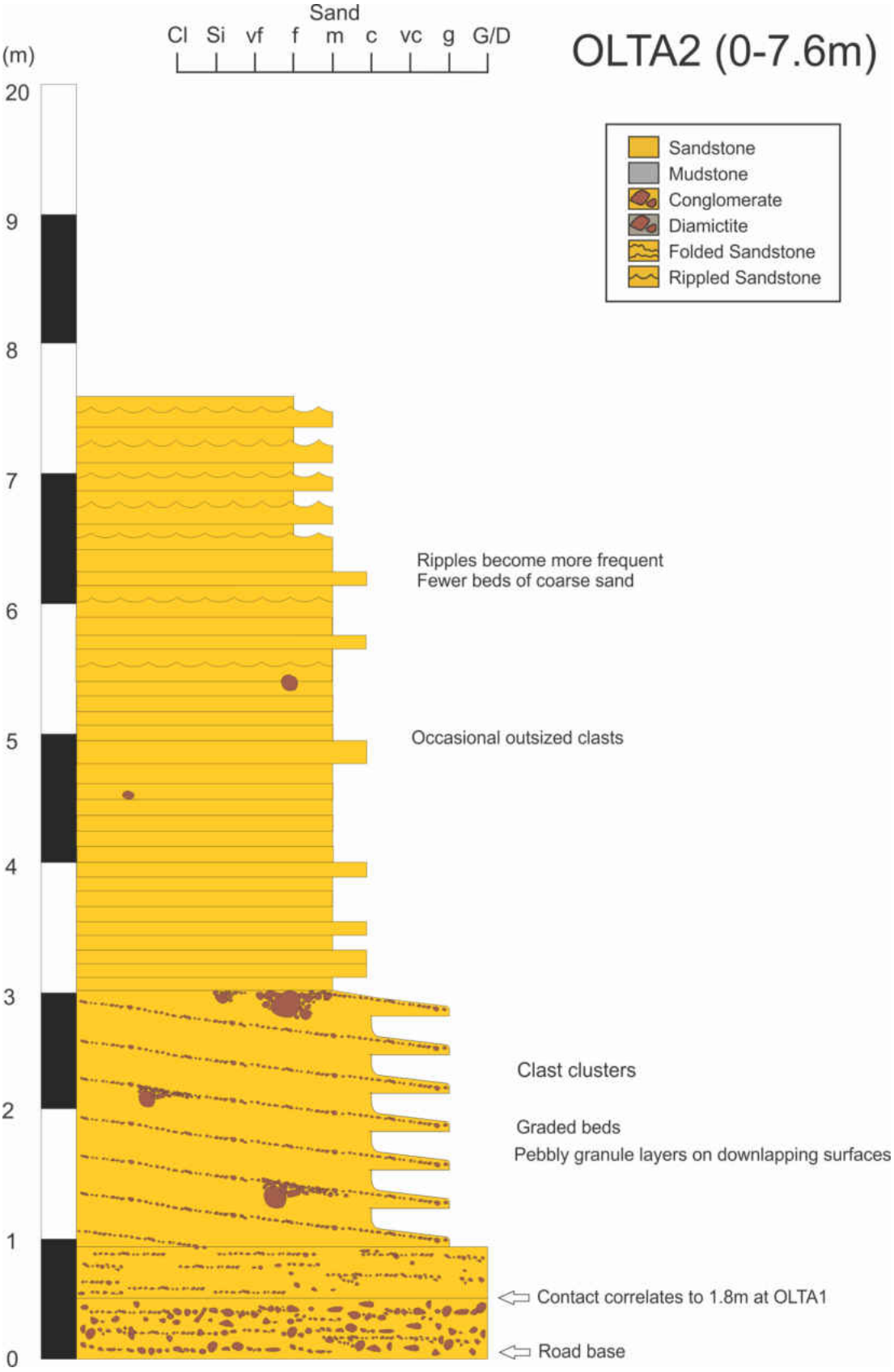
Sand
Cl Si vf f m c vc g G/D
(m)
OLTA2 (0-7.6m)
20
9
8
7
6
5
4
3
2
1
0
Sandstone
Mudstone
Conglomerate
Diamictite
Folded Sandstone
Rippled Sandstone
Ripples become more frequent
Fewer beds of coarse sand
Occasional outsized clasts
Clast clusters
Graded beds
Pebbly granule layers on downlapping surfaces
Contact correlates to 1.8m at OLTA1
Road base

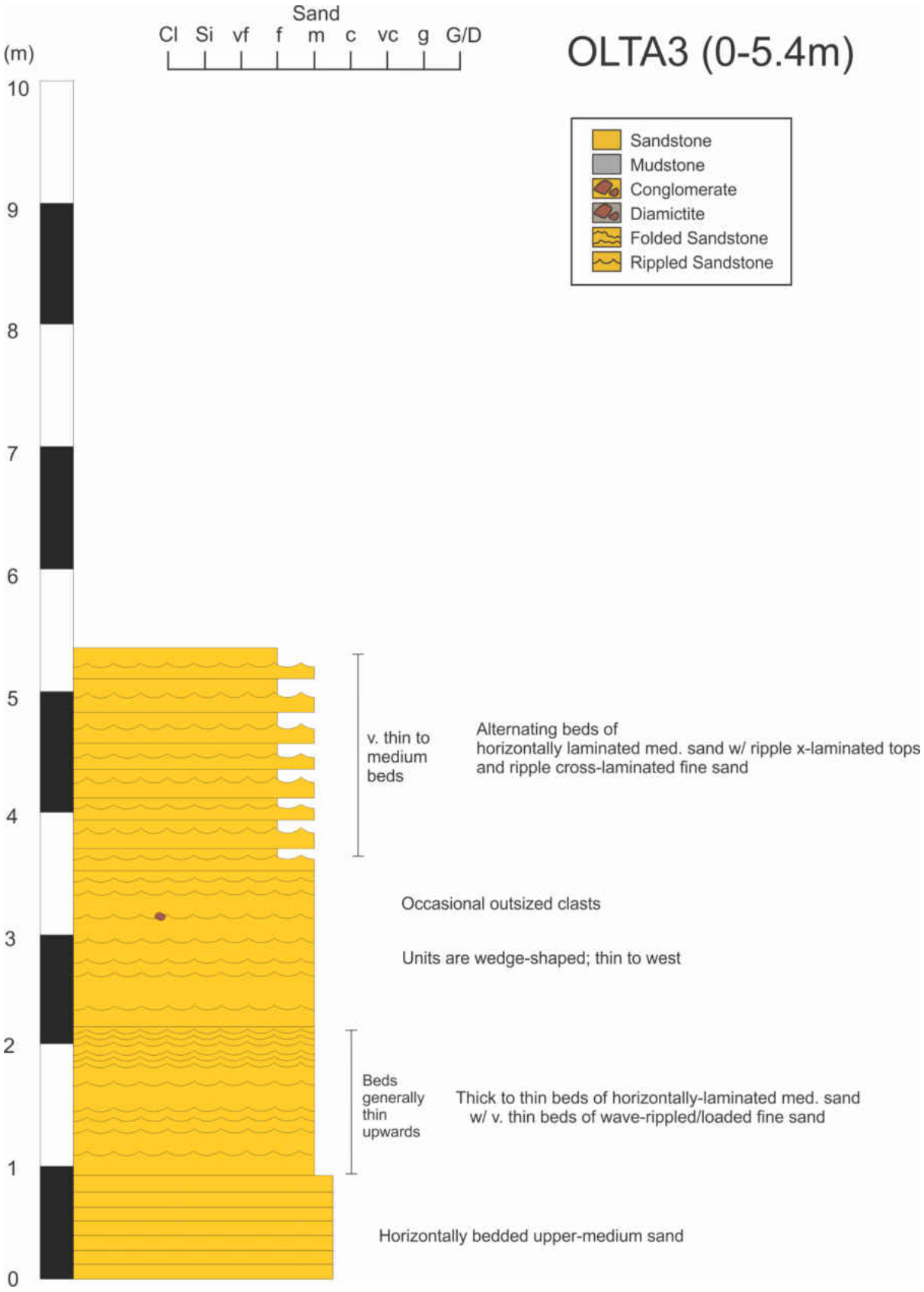
Sand
Cl Si vf f m c vc g G/D
(m)
OLTA3 (0-5.4m)
Sandstone
Mudstone
Conglomerate
Diamictite
Folded Sandstone
Rippled Sandstone
10
9
8
7
6
5
4
3
2
1
0
v. thin to medium beds
Alternating beds of horizontally laminated med. sand w/ ripple x-laminated tops and ripple cross-laminated fine sand
Occasional outsized clasts
Units are wedge-shaped; thin to west
Beds generally thin upwards
Thick to thin beds of horizontally-laminated med. sand w/ v. thin beds of wave-rippled/loaded fine sand
Horizontally bedded upper-medium sand

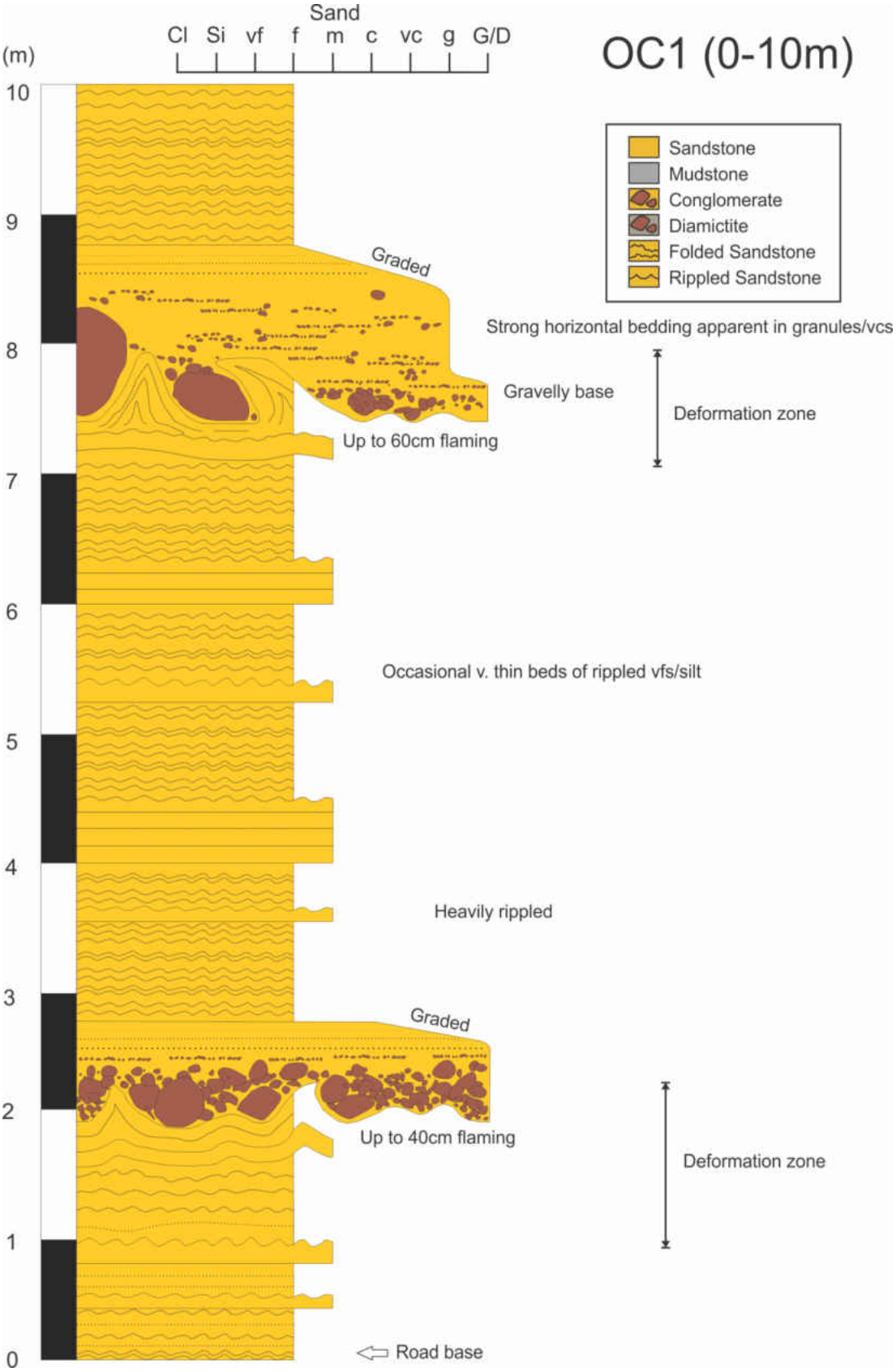
OC1 (0-10m)
Sand
Cl Si vf f m c vc g G/D
(m)
10
9
8
7
6
5
4
3
2
1
0
Sandstone
Mudstone
Conglomerate
Diamictite
Folded Sandstone
Rippled Sandstone
Graded
Gravelly base
Up to 60cm flaming
Strong horizontal bedding apparent in granules/vcs
Deformation zone
Occasional v. thin beds of rippled vfs/silt
Heavily rippled
Graded
Up to 40cm flaming
Deformation zone
Road base

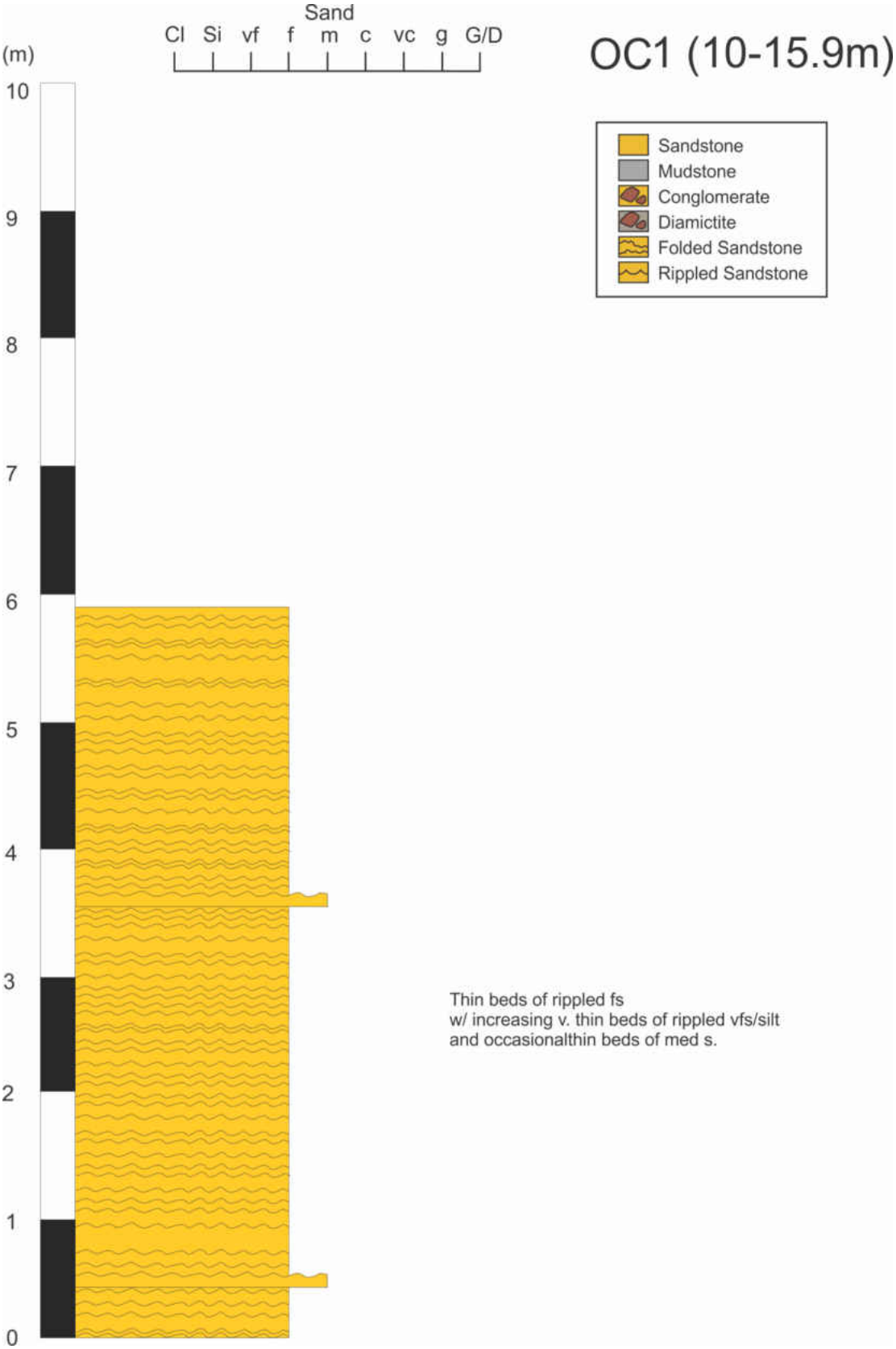
Sand
Cl Si vf f m c vc g G/D
(m)
10
9
8
7
6
5
4
3
2
1
0
OC1 (10-15.9m)
Sandstone
Mudstone
Conglomerate
Diamictite
Folded Sandstone
Rippled Sandstone
Thin beds of rippled fs
w/ increasing v. thin beds of rippled vfs/silt
and occasionalthin beds of med s.


Sand
Cl Si vf f m c vc g G/D
(m)
OC2 (0-10m)
Sandstone
Mudstone
Conglomerate
Diamictite
Folded Sandstone
Rippled Sandstone
10
9
8
7
6
5
4
3
2
1
0
Sole marks at bottom of ms
Graded
40cm schist & 50cm granite boulders
Gravelly base
Up to 40cm flaming/folding
Deformation zone
Vfs/silt recessions become more dominant
Mostly rippled fs with vfs/silt recessions
Some h-laminated ms with rippled tops

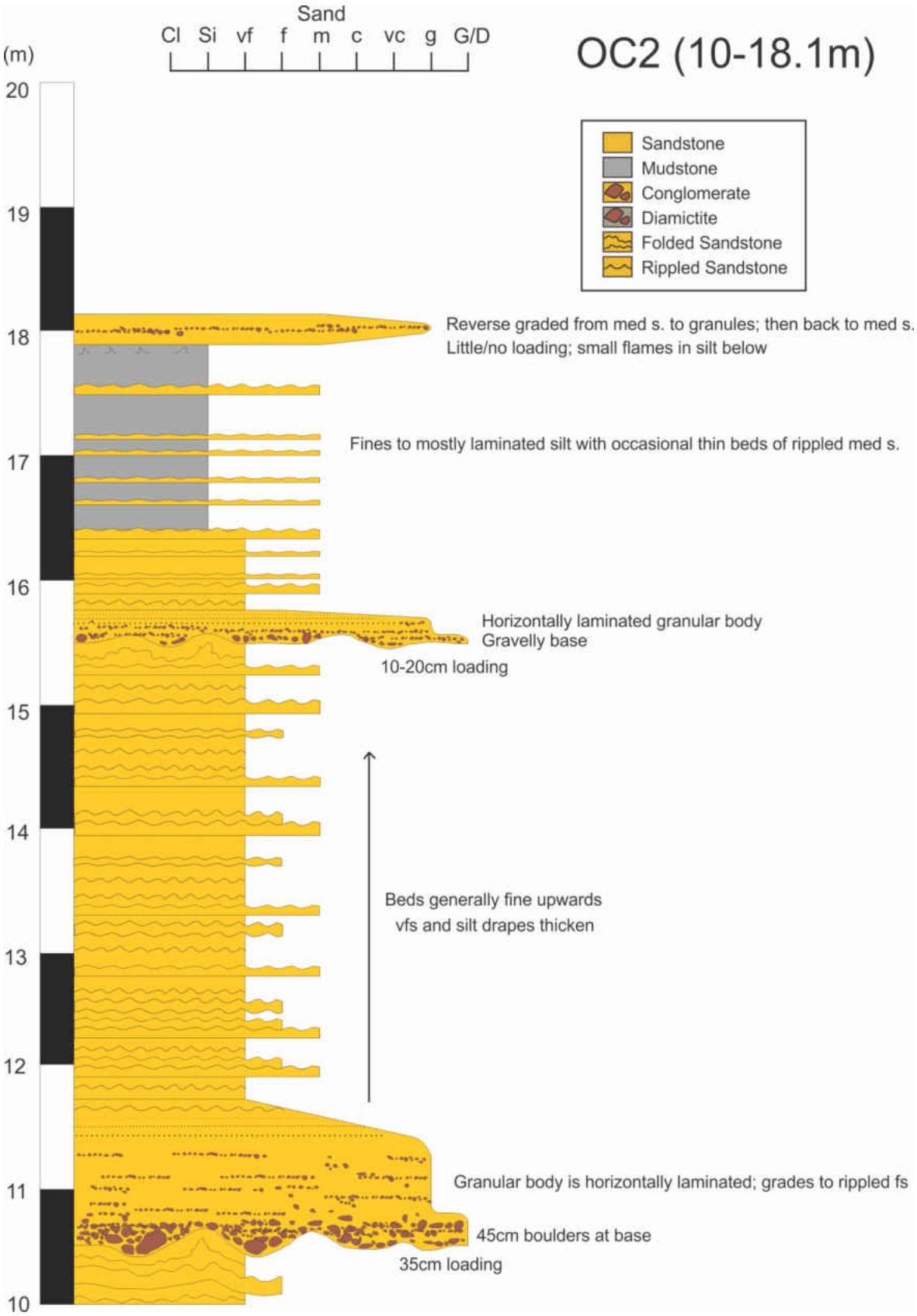
Sand
Cl Si vf f m c vc g G/D
(m)
OC2 (10-18.1m)
Sandstone
Mudstone
Conglomerate
Diamictite
Folded Sandstone
Rippled Sandstone
20
19
18
17
16
15
14
13
12
11
10
Reverse graded from med s. to granules; then back to med s.
Little/no loading; small flames in silt below
Fines to mostly laminated silt with occasional thin beds of rippled med s.
Horizontally laminated granular body
Gravelly base
10-20cm loading
Beds generally fine upwards
vfs and silt drapes thicken
Granular body is horizontally laminated; grades to rippled fs
45cm boulders at base
35cm loading

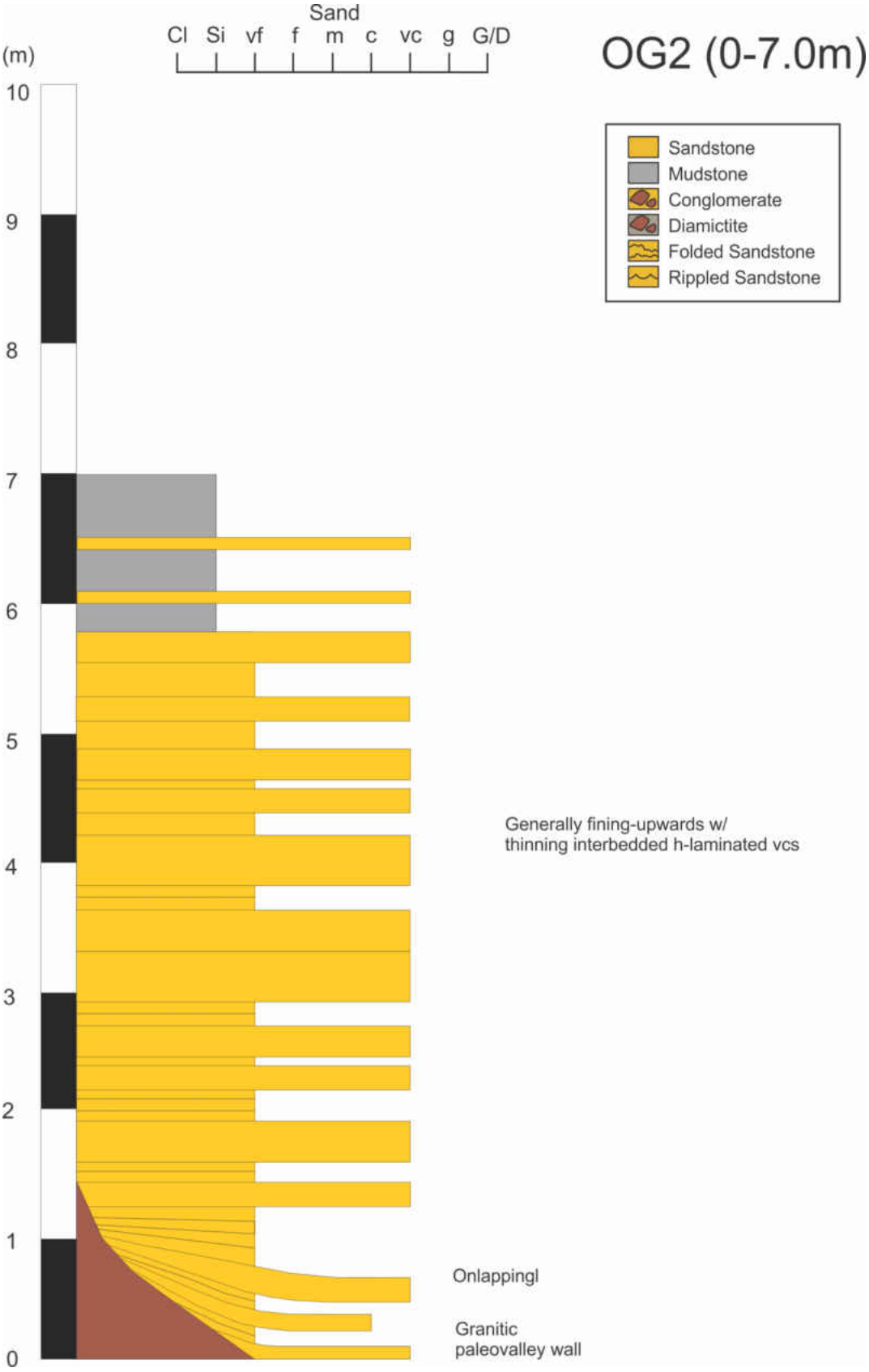
Sand
Cl Si vf f m c vc g G/D
(m)
OG2 (0-7.0m)
10
9
8
7
6
5
4
3
2
1
0
Sandstone
Mudstone
Conglomerate
Diamictite
Folded Sandstone
Rippled Sandstone
Generally fining-upwards w/
thinning interbedded h-laminated vcs
Onlappingl
Granitic
paleovalley wall

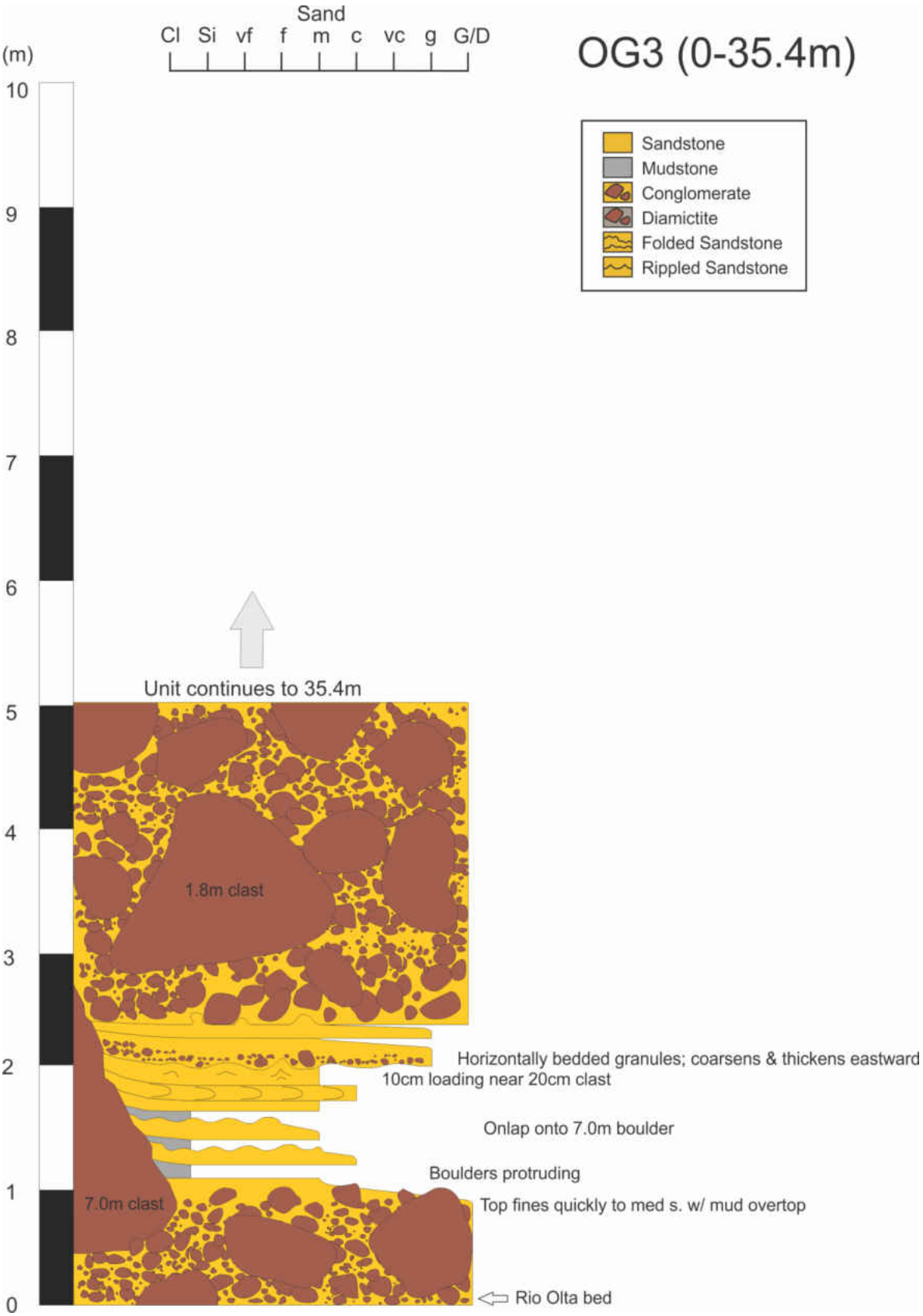
Sand
Cl Si vf f m c vc g G/D
(m)
OG3 (0-35.4m)
Sandstone
Mudstone
Conglomerate
Diamictite
Folded Sandstone
Rippled Sandstone
10
9
8
7
6
5
4
3
2
1
0
Unit continues to 35.4m
1.8m clast
Horizontally bedded granules; coarsens & thickens eastward
10cm loading near 20cm clast
Onlap onto 7.0m boulder
Boulders protruding
7.0m clast
Top fines quickly to med s. w/ mud overtop
Rio Olta bed

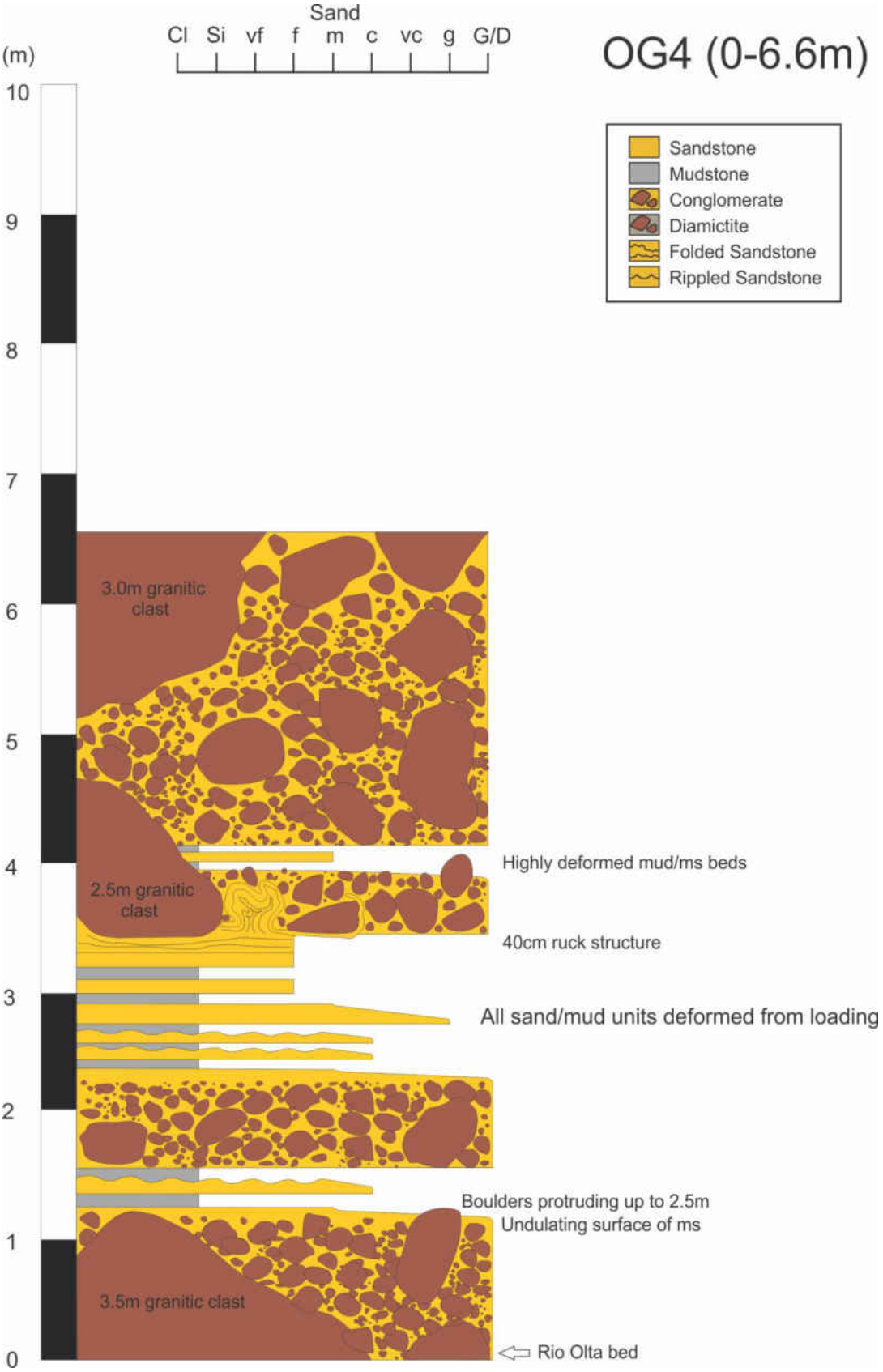
Sand
Cl Si vf f m c vc g G/D
OG4 (0-6.6m)
(m)
10
9
8
7
6
5
4
3
2
1
0
Sandstone
Mudstone
Conglomerate
Diamictite
Folded Sandstone
Rippled Sandstone
3.0m granitic clast
2.5m granitic clast
3.5m granitic clast
Highly deformed mud/ms beds
40cm ruck structure
All sand/mud units deformed from loading
Boulders protruding up to 2.5m
Undulating surface of ms
Rio Olta bed

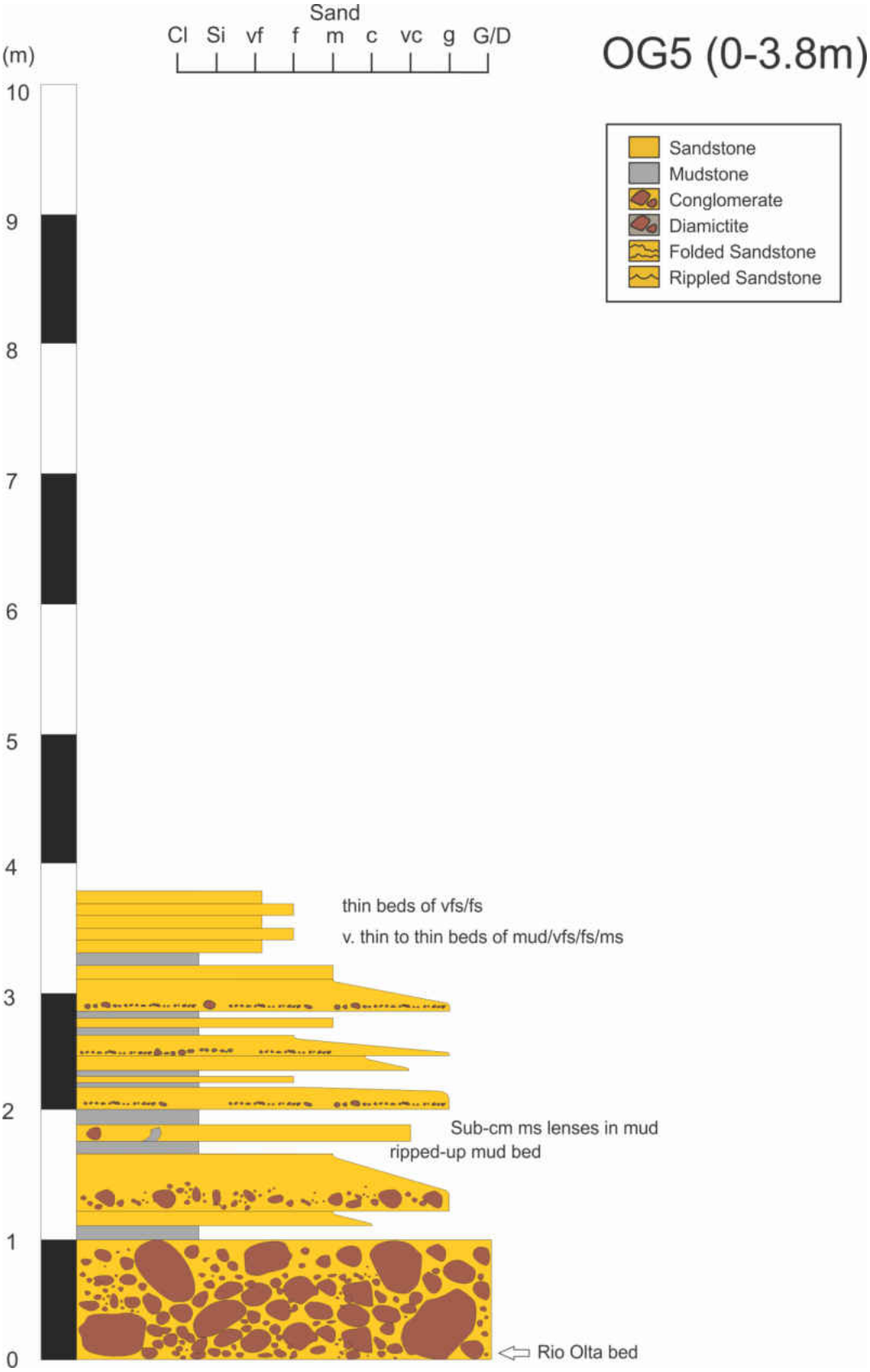
Sand
Cl Si vf f m c vc g G/D
(m)
OG5 (0-3.8m)
Sandstone
Mudstone
Conglomerate
Diamictite
Folded Sandstone
Rippled Sandstone
10
9
8
7
6
5
4
3
2
1
0
thin beds of vfs/fs
v. thin to thin beds of mud/vfs/fs/ms
Sub-cm ms lenses in mud
ripped-up mud bed
Rio Olta bed

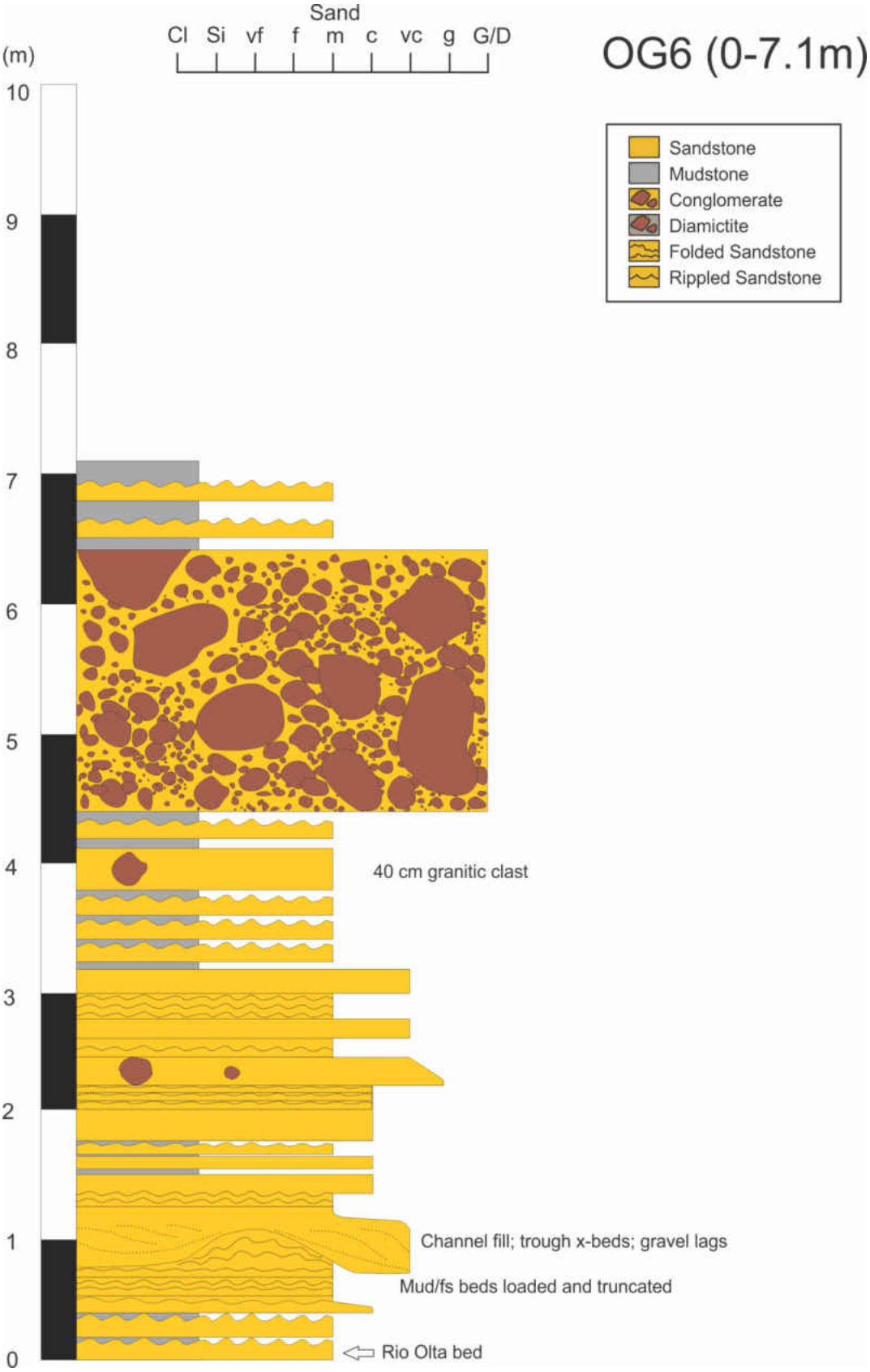
Sand
Cl Si vf f m c vc g G/D
(m)
OG6 (0-7.1m)
Sandstone
Mudstone
Conglomerate
Diamictite
Folded Sandstone
Rippled Sandstone
10
9
8
7
6
5
4
3
2
1
0
40 cm granitic clast
Channel fill; trough x-beds; gravel lags
Mud/fs beds loaded and truncated
Rio Olta bed

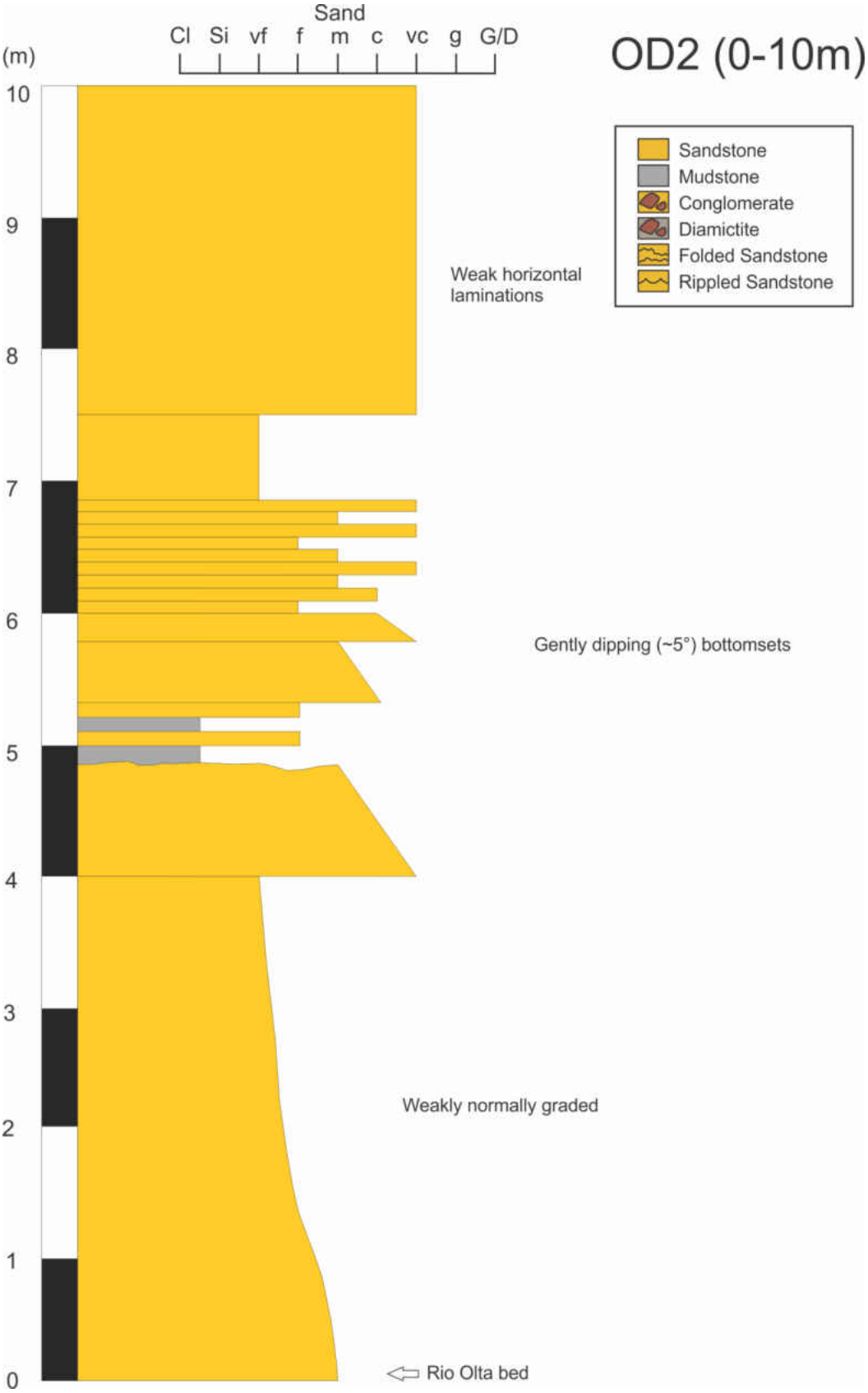
OD2 (0-10m)
Sand
Cl Si vf f m c vc g G/D
(m)
10
9
8
7
6
5
4
3
2
1
0
Sandstone
Mudstone
Conglomerate
Diamictite
Folded Sandstone
Rippled Sandstone
Weak horizontal laminations
Gently dipping (~5°) bottomsets
Weakly normally graded
Rio Olta bed

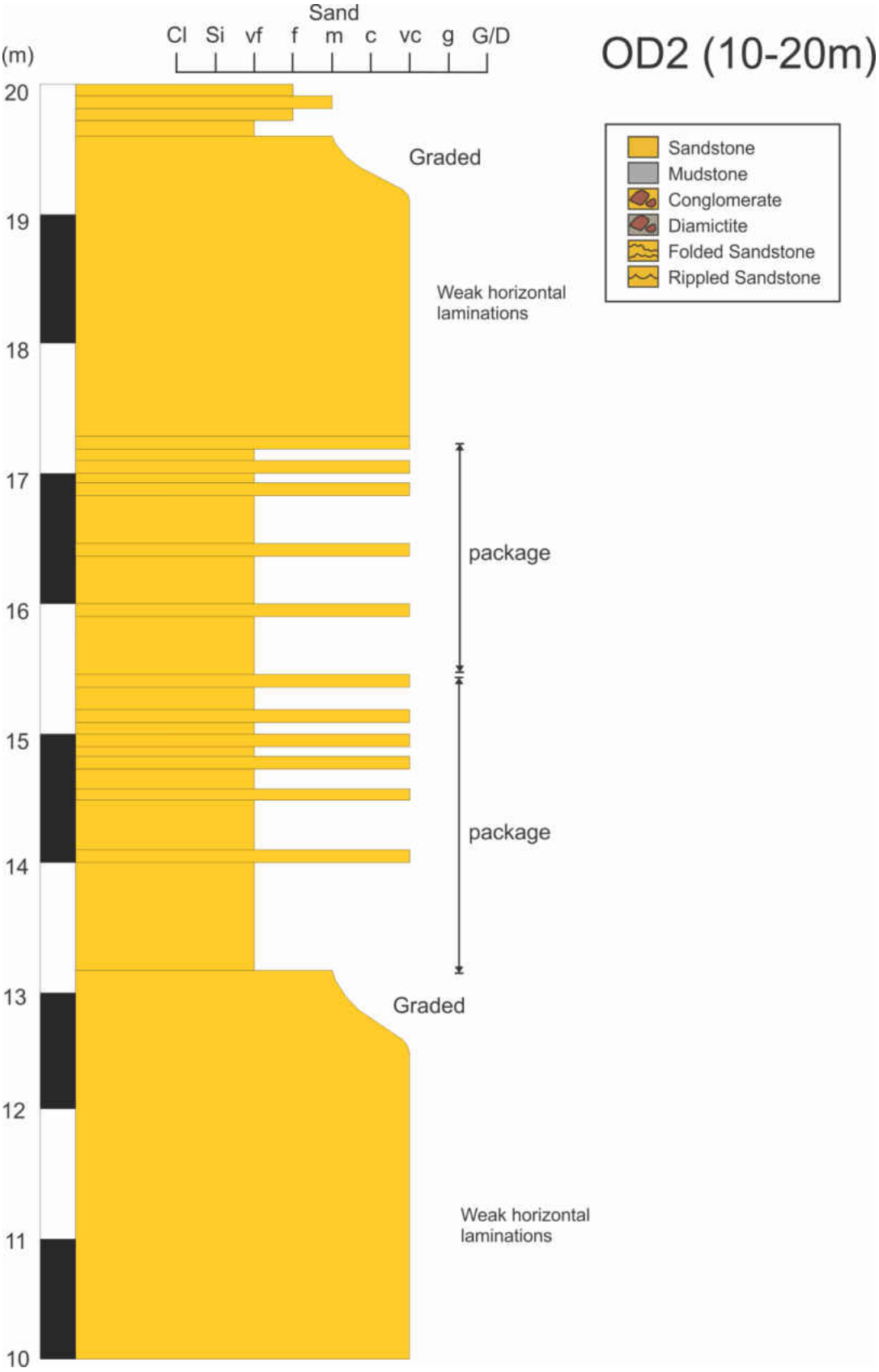
Sand
Cl Si vf f m c vc g G/D
(m)
OD2 (10-20m)
20
19
18
17
16
15
14
13
12
11
10
Graded
Weak horizontal laminations
package
package
Graded
Weak horizontal laminations
Sandstone
Mudstone
Conglomerate
Diamictite
Folded Sandstone
Rippled Sandstone

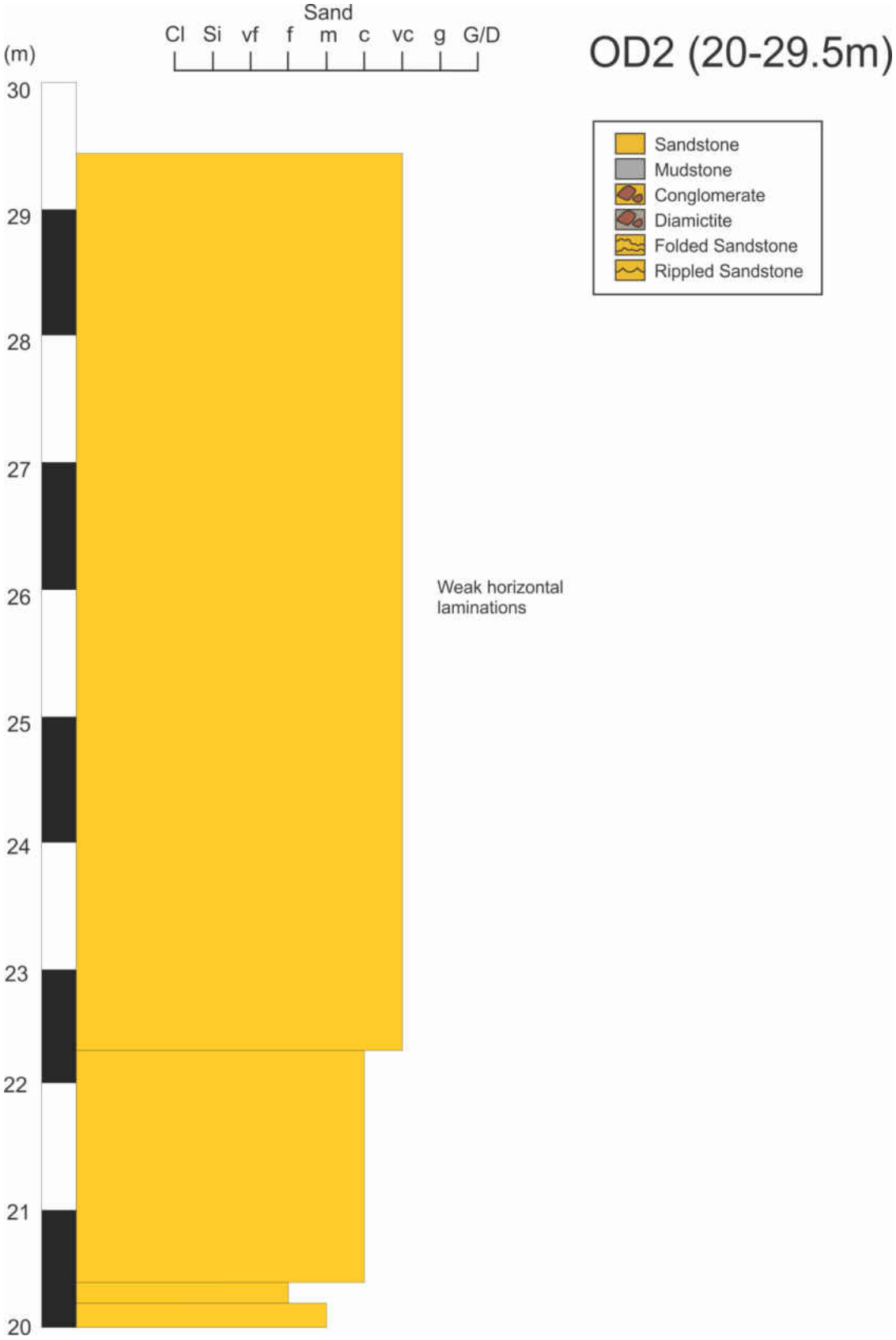
Sand
Cl Si vf f m c vc g G/D
(m)
OD2 (20-29.5m)
Sandstone
Mudstone
Conglomerate
Diamictite
Folded Sandstone
Rippled Sandstone
30
29
28
27
26
25
24
23
22
21
20
Weak horizontal laminations